学位論文

Generation of scalar, vector, tensor perturbations during cosmic inflation

(初期宇宙インフレーションにおけるスカラー・ベクトル・テンソルゆらぎの生成)

平成26年12月博士（理学）申請

東京大学大学院理学系研究科
物理学専攻

藤田智弘

Generation of scalar, vector, tensor perturbations during cosmic inflation

35-127051

Tomohiro Fujita

Department of Physics, Graduate School of Science,

the University of Tokyo

Kavli Institute for the Physics and Mathematics of the Universe

18 December, 2014

Abstract:

Inflation is widely studied as the theory describing the very early universe and now it is considered as an indispensable component of the standard model of cosmology. During inflation, cosmological perturbations are generated from the quantum fluctuations and subsequently become the seed of the cosmic structures which are currently observed. The prediction of inflation, the scale invariant spectrum of the curvature perturbation, is tested various observation, especially by the cosmic microwave background radiation (CMB) observations with great accuracy and is confirmed to be consistent.

Nevertheless, the mechanism of inflation is still unclear. The scalar perturbation which has been observed by the CMB observations puts strong constraints on a number of inflation models. But it is not sufficient to determine the correct model. Thus in the next generation of cosmology, the perturbations other than the scalar one, namely vector perturbation and tensor perturbation become increasingly important.

Although primordial vector perturbation is not intensively investigated so far, it acquires a strong motivation from recent observations. It is known for a long time that galaxies and galaxy clusters have their own magnetic fields. However, the magnetic field even in void regions is detected in 2010 by blazar observations. Since astrophysical processes are not active there, it may indicate the primordial origin of the observed magnetic fields. Indeed, if primordial magnetic field is generated in the early universe, magnetic fields in galaxies, clusters and voids can be explained in an integrated way. Thus the generation of magnetic field during inflation, or inflationary magnetogenesis, is a very interesting possibility.

It has been pointed out that the models of inflationary magnetogenesis proposed so far have problems. In this thesis, we discuss the kinetic coupling model (Ratra's model) and explore its obstacles in detail. Then we make model-independent arguments which universally constrain the possibility of inflationary magnetogenesis. In addition, we also consider the possibility that the magnetic field produced during inflation is further amplified during the subsequent inflaton oscillation phase. As a result, it turns out that the generation of magnetic field with a sufficient strength to explain the void observation is difficult mainly because of the consistency with the CMB observation.

The tensor perturbation with a primordial origin has been investigated as the primordial gravitational wave (GW) in the theoretical and observational context. However, previous works have focused on the tensor mode generated from the vacuum fluctuation and ignore the other possibilities. In this paper, we consider not only that the conventional GW but also GW produced by an alternative mechanism during inflation. That is the second order perturbation of a scalar field. If GWs from alternative sources dominate the observed primordial GW, the relation between the observation of the primordial GW

and the properties of inflation can be drastically changed. Therefore it is important to investigate the alternative scenario of the GW generation. Contrary to the previous work, we show that the GW induced by the second order perturbation of a single spectator scalar field during inflation cannot be larger than the conventional GW from the vacuum fluctuation in a very general framework, namely the action with the k-essence and the Galileon term.

Acknowledgments

I am grateful to my advisors, Hitoshi Murayama and Shinji Mukohyama. Without their helps, I could not survive the Ph.D. course. Especially, through the discussion with Shinji Mukohyama, I found one of the main topic of this thesis, the generation of magnetic field during inflation. He is always open to consider any aspect of primordial cosmology and gravitation, and we had a lot of useful discussions. I am also grateful to Shuichiro Yokoyama. Although he belongs to a different institution from mine, he kindly answers to many of my questions and is helpful in any situation of our collaboration. I would like to thank him particularly for our published works included in this thesis. I would like to express my gratitude to Jun'ichi Yokoyama. He is friendly and always gives me various perspective to research on cosmology. Without his encouragement, the study on the induced gravitational wave would not have materialized. I owe a very important debt to Masahiro Kawasaki. I could learn many important things from the discussion and collaboration with him. I would like to show my greatest appreciation to Ryo Namba. Without his persistent help, this thesis would not have been possible. I would also like to thank Daisuke Yamauchi for helpful advice and fruitful discussion. I am also grateful to students in Kavli IPMU, ICRR and RESCEU. We could help each other not only to deepen understanding of our reserch topics but also to keep our motivations. Among them, I would like to offer my special thanks to Naoyuki Takeda and Yuichiro Tada and their excellent work on numerical calculations.

Contents

INTRODUCTION

How did our universe begin? A number of works have been done to reveal the very beginning of the universe and it is known that inflation which is an era of accelerating cosmic expansion in the primordial unverse is consistent with observations [1, 2, 3]. Now the inflation theory plays a central role in the research on the primordial universe. Its key prediction is the generation of perturbations from the quantum fluctuation and it has been tested mainly by observations of cosmic microwave background radiation (CMB) [4]. Since the inflation theory provides the initial condition of the subsequent evolution of the universe, by theoretically solving the evolution and observing signals which holds information of the initial condition, one can constraint the inflation theory. Both theoretical and observational works have brought a better understanding of inflation, however, it is not sufficient to answer fundamental questions, for example, what the actual inflation mechanism is. While we have a number of models of inflation, we are lack of the discrimination capability [5, 6].

Conventional ways to access the primordial universe are based on scalar perturbation, namely the curvature perturbation (or the density perturbation) and its property. The theoretical and observational discussions on it is very mature. However, the cosmological perturbation includes not only scalar perturbation but also vector and tensor perturbations. Compared to scalar perturbation, the understanding of vector and tensor perturbations has been not yet well established. It might be because the observational result of them was limited. Recently, however, their observation or observational project are being pushed forward. Thus it is good time to develop theoretical understanding of the vector and tensor perturbation which are generated during inflation.

An interesting candidate of the vector perturbation produced in the early universe is the cosmic magnetic field. It is known for a long time that galaxies and galactic clusters have their own magnetic fields with typical strength $\sim 10^{-6}$G and it is argued that a 'seed' magnetic field is necessary to form the currently observed magnetic fields during the structure formation [7, 8, 9, 10]. In addition, it is reported recently that even in void region where astrophysical processes are not active, weak magnetic fields are detected. The lower bound on that void magnetic field is $\sim 10^{-15}$G [11, 12, 13, 14, 15, 16, 17, 18, 19]. This result supports the primordial origin of the magnetic fields in the universe because if magnetic fields are generated and fill up the entire universe in a very early epoch, they naturally evolve into both the galactic/cluster magnetic fields which are amplified during the structure formation and the void magnetic field which merely dilutes due to

the cosmic expansion so far. Therefore theoretical works on the generation of magnetic field or "magnetogenesis" aim to produce the magnetic field with 10^{-15}G at present.

In this thesis, we discuss inflationary magnetogenesis, namely the generation of primordial magnetic field during inflation. In the context of inflationary magnetogenesis, many models have been proposed so far [20, 21, 22, 23, 24, 25, 26, 27]. During inflation, large scale perturbations can be produced and hence inflation was thought to be a promising candidate of the magnetogenesis mechanism. However some critical and general obstacles are realized recently.

Among the obstacles, the backreaction problem [28] and the curvature perturbation problem [29, 30] are very important. The backreaction problem refer to the consistency between the stability of inflation and the generation of the electromagnetic fields. If one produces too much electromagnetic fields, their energy density may exceed that of inflaton and the dynamics of inflation can be significantly altered. Thus the energy density of the electromagnetic field should be much smaller than that of inflaton. The curvature perturbation problem refers to the generation of additional curvature perturbation by the produced electromagnetic fields. Since the amplitude or the non-gaussianity of the curvature perturbation is constrained by observations [31], any magnetogenesis model which predicts too much induced curvature perturbation is excluded. So far, no model overcomes these obstacles and produces the cosmic magnetic field with the sufficient strength.

In this thesis, we intensively explore the above two problems by using a specific model and in a model-independent way. First, we review the IFF (or Ratra's) model [20] and investigate the backreaction and the curvature perturbation problem in the model. It is found that the constraint from the non-linear parmeter τ_{NL} is the most stringent if the COBE normalization is used and the allowed strength of the magnetic field is far weaker than the observational lower bound. If one introduces a curvaton like mechanism and relax the COBE normalization, then the backreaction gives the strongest restriction while the allowed strength is far insufficient again [32].

Then we argue two model-independent constraints on inflationary magnetogenesis. One is derived by the backreaction problem [33] and the other is derived by the curvature perturbation problem [34]. The latter gives a tighter constraint while the former has a broader scope of application. We also discuss the post-inflation amplification of the magnetic field. We explore the model proposed in ref. [35] which is an extension of the IFF model and the electromagnetic field grow during the inflaton oscillating phase. It is found that in the model with the proposed model parameters in ref. [35], the curvature perturbation induced by the electromagnetic field is much larger than the Planck constraint and thus the model is under pressure.

In terms of tensor perturbation, the primordial gravitational wave (GW) attracts attention. In particular, the GW which generated during inflation from the vacuum fluctuation is well studied [36]. It is critically important because its power spectrum is proportional to the energy density of inflation. However, the GW from the vacuum fluctuation is not the only source of the primordial GWs. Therefore the GWs which

will be observed in the future is not necessary it. If the observed GW is dominated by that generated in an alternative way, the relationship between the property of the GW and inflation would be dramatically changed. Thus it is important to explore alternative generation mechanism of primordial GWs.

In this thesis, we consider the generation of GW from the second order perturbation of a single spectator scalar field. At the second order of perturbation, the scalar and tensor modes are coupled and hence scalar fluctuations can produce GWs. In ref. [37], the authors argued that if the sound speed of a spectator scalar field is sufficiently small during inflation, the induced GW can be larger than the GW from the vacuum fluctuation. However, we investigate the curvature perturbation induced by the spectator scalar field with a small sound speed and find that GW cannot be dominated by the alternative source because the induced curvature perturbation would be too large in that case and it is inconsistent with the CMB observation [38]. Since we work in a very general framework, our result can be interpreted that any single spectator field cannot produce a dominant GW.

The rest of this thesis is organized as follows. In sec. 2, we introduce the inflation theory and explain the standard calculation of the generation of scalar perturbation. In sec. 3, we explore inflationary magnetogenesis. First, the observaiton of cosmic magnetic fields are introduced. Second, the IFF model is reviewed and its constraints are discussed in detail. Third, the model-independent arguments are developed. Fourth, we investigate the possibility that the magnetic field produced during inflation is further amplified after inflation. The model in ref. [35] is reviewed and the induced curvature perturbations are calculated. In sec. 4, we discuss primordial GWs. First, the GW generated from the vacuum fluctuation is explained and its amplitude is computed. Second, as an alternative source of primordial GWs, the contribution of the second order perturbation of a spectator scalar field is considered. Third, we calculate the GW and curvature perturbation induced by a spectator scalar field. In sec. 5, we conclude.

INFLATIONARY COSMOLOGY

Contents

2.1   Motivation of Inflation

Cosmic inflation [1, 2, 3] is an epoch in the history of the universe in which the universe expands at an accelerating pace. The inflation theory is now considered as the standard paradigm in primordial cosmology. In the standard model of cosmology, the initial condition is assumed to be given by inflation which takes place in the very early universe. In this section, we introduce the motivation to study inflation. We have two major reasons to consider inflation. One is that inflation solves the problems of the hot big bang model. The other is that inflation can generate small density fluctuations which become the seed of cosmic structures observed today. As an additional motivation, by using the inflation theory and associated observations, we can access phenomena governed by the high energy physics whose typical energy is beyond the scope of ground-based experiments (e.g. particle accelerators).

2.1.1   The FRW universe

First of all, let us quickly introduced the flat FRW metric which represents a homogeneous and isotropic expanding universe. The FRW metric based on the *cosmological principle* which is a statement that the universe is homogeneous and isotropic on a sufficiently large scale for an observer. Current observation confirms that this principle approximately

holds on scales larger than 100Mpc. The metric satisfying the cosmological principle is given by [39]

$$ds^2 = dt^2 - a^2(t) \left[\frac{dr^2}{1 - Kr^2} + r^2 d\Omega^2 \right], \tag{2.1}$$

where t is cosmic time, $a(t)$ is the scale factor which represent the expansion of the universe, and K represents the spatial curvature. If $K = 0$, the metric is called the flat FRW.

The Einstein equations in the flat FRW metric read

$$3M_{\text{Pl}}^2 H^2 = \rho + \frac{\Lambda}{3} - \frac{3M_{\text{Pl}}^2 K}{a^2}, \tag{2.2}$$

$$\frac{\ddot{a}}{a} = -\frac{\rho + 3p}{6M_{\text{Pl}}^2} + \frac{\Lambda}{3}, \tag{2.3}$$

where $H(t) \equiv \dot{a}/a$ is the Hubble parameter which represents the expansion rate of the universe, $M_{\text{Pl}} \approx 2.43 \times 10^{18}$GeV is the reduced Planck mass, Λ, ρ and p denote the cosmological constant, the energy density and pressure, respectively. The first equation is called the Friedmann equation. From these equations one can derive

$$\dot{\rho} = -3H(\rho + p). \tag{2.4}$$

If one assumes the equation of state with a constant parameter w as

$$p = w\rho, \tag{2.5}$$

the time evolution of the energy density is solved as

$$\rho \propto a^{-3(1+w)}. \tag{2.6}$$

For a radiation component with $w = 1/3$, the density evolves as $\rho \propto a^{-4}$, while $\rho \propto a^{-3}$ for a matter component with $w = 0$. If the energy density is constant, the equation of state parameter w is -1. In the flat FRW universe, the scale factor $a(t)$ can be solved as

$$a(t) \propto t^{\frac{2}{3+3w}} \quad (w \neq -1), \qquad a(t) \propto e^{Ht} \quad (w = -1). \tag{2.7}$$

2.1.2 Problems in the hot big bang model

From the Friedmann equation, the spacial curvature K is written as

$$K = a^2 H^2 \left[\Omega(t) - 1 \right], \tag{2.8}$$

where $\Omega(t) \equiv \rho/3M_{\text{Pl}}^2 H^2$ is the dimensionless density parameter, and here the cosmological constant Λ is absorbed in ρ. Then we define the dimensionless parameter of the spatial curvature as

$$\Omega_K(t) \equiv \Omega(t) - 1 = \frac{K}{a^2 H^2}. \tag{2.9}$$

Ω_K parameterizes the deviation of ρ from the critical density $\rho_c \equiv 3M_{\text{Pl}}^2 H^2$. The present value of Ω_K has not been detected by observations and the constraint on it is imposed by the Planck satellite and other observations as [4]

$$100\Omega_K = -0.10^{+0.62}_{-0.65} \qquad (95\% CL; \text{Planck} + \text{lensing} + \text{WP} + \text{highL} + \text{BAO}). \qquad (2.10)$$

Therefore Ω_K should be small at present. However, the hot big bang model does not explain why the spatial curvature is so small. It can be shown that if the universe includes a energy component with the equation of state parameter w and the spatial curvature, Ω_K evolves as

$$\Omega_K \propto a^{1+3w}. \qquad (2.11)$$

Thus for $w > -1/3$, Ω_K increases and to match the current observation bound, its initial value must be extremely tiny. Such a initial condition looks unnatural without any mechanism which makes Ω_K small in the early universe.

The inflation model solves this problem as follows. Eq. (2.11) indicates Ω_K decreases if $w < -1/3$ and inflation is nothing but the epoch with $w < -1/3$. As we see later, slow-roll inflation gives the almost constant Hubble parameter and the scale factor which grows exponentially, $a(t) \propto e^{Ht}$. Then $\Omega_K = K/a^2 H^2$ rapidly decreases in proportional to e^{-2Ht}. Therefore if inflation lasts for a sufficient duration in the early universe, the smallness of present Ω_K is naturally explained. This can be simply understood that since the universe substantially expands during inflation, the space is stretched and the typical scale of the spacial curvature becomes much larger than the our observable scale.

The second problem is related to causality. To clarify the problem, let us introduce the particle horizon L_{ph} which represents the length scale of the causally connected region. The particle horizon is defined as the length that light can travel from $t = 0$ till t

$$L_{\text{ph}} \equiv a(t) \int_0^t \frac{dt'}{a(t')}. \qquad (2.12)$$

In the matter dominated universe ($w = 0$), the particle horizon is calculated as

$$L_{\text{ph}}(w = 0) = 3t = \frac{2}{H(t)}. \qquad (2.13)$$

On the last scattering surface on which the photons observed as cosmic microwave background radiation (CMB) are emitted, the particle horizon is $L_{\text{ph}} \sim 0.4\text{Mpc}$. Thus two photons which are separated by more than 0.4Mpc at the last scattering are causally disconnected and there is no reason to expect their temperature is almost same. However, CMB observations show that CMB photons coming from all the sky have the almost same temperature only with a tiny ($\mathcal{O}(10^{-5})$) fluctuation. This problem is call the horizon problem.

If the universe exponentially expands in the early epoch, this problem is solved because

during inflation the particle horizon is computed as

$$L_{\rm ph} = a(t_e) \int_{t_i}^{t_e} \frac{{\rm d}t'}{a(t')} \tag{2.14}$$

$$= e^N \left[2t_i + \frac{1 - e^{-N}}{H} \right] \tag{2.15}$$

$$\simeq e^N [2t_i + 1/H], \tag{2.16}$$

where t_i and t_e is the onset and the end of inflation. Here we introduce the e-fold number which is defined as

$$N \equiv \ln \left(\frac{a(t_e)}{a(t_i)} \right). \tag{2.17}$$

Therefore if inflation lasts for a sufficient duration, the causally connected region substantially expands and the horizon problem is solved.

Finally let us refer to the so-called monopole problem or unwanted relic problem. In the hot big bang model, the temperature in the very early universe is extremely high. In such a thermal bath with high temperature, some theories of particle physics predict the production of particles beyond the standard model of particle physics. Since these particles are heavy and stable, they do not disappear and the detection of them is expected. However, we do not observe these particles in the present universe. Inflation gives a simple solution to this problem. Even if such a particle is produced *before inflation*, the substantial expansion during inflation decreases the density of the particle. Therefore it is no surprise that we do not observe the heavy and stable particles. Nevertheless if such a particle is produced *after inflation*, inflation cannot solve the problem. For example, in particle physics models with the supersymmetry, this problem is serious and it is known as *gravitino problem* because gravitino often becomes the problematic particle.

2.1.3 Definition of inflation

Inflation is defined as a epoch in which the universe experiences an accelerated expansion. With the scale factor $a(t)$ and the Hubble parameter, this condition can be written in several ways as

$$\ddot{a} > 0 \quad \Longleftrightarrow \quad \frac{\rm d}{{\rm d}t} \left(\frac{1}{aH} \right) < 0 \quad \Longleftrightarrow \quad -\frac{\dot{H}}{H^2} < 1. \tag{2.18}$$

The first condition is trivial. The second condition indicates that $(aH)^{-1}$ decreases during inflation. $(aH)^{-1}$ is called the comoving Hubble radius and it represents the scale of the causal region during inflation. The third condition implies that the time variation of the Hubble parameter is small during inflation.

If the Hubble parameter is almost constant, $|\dot{H}| \ll H^2$, the scale factor is given by a exponential function of time, $a \propto e^{Ht}$ and the universe is well approximated by the de Sitter spacetime. In the Einstein theory of gravity, the above conditions are equivalent

to $w \equiv p/\rho < -1/3$. Since the physics of the big bang nucleosynthesis (BBN) and subsequent evolution of the universe is well understood and confirmed by observations, inflation have to takes place before BBN, if any. The energy scale of BBN is 10MeV and hence the energy scale of inflation is beyond 10MeV.

2.2 Mechanism of Inflation

In the previous section, we see that inflation can solve the three problems in the hot big bang scenario. In this section, we discuss how inflation takes place. To realize an accelerating expansion, the equation of state parameter w should be less than $-1/3$. Although an ordinary matter does not satisfy this condition, a scalar field with potential energy and small kinetic energy satisfies the condition. This mechanism is known as the slow-roll paradigm and the most popular mechanism of inflation. Although the cosmological constant can also be responsible for inflation, inflation never ends in that case. In slow-roll inflation, inflation ends when the scalar field starts to roll down its potential rapidly. We briefly review the slow-roll paradigm in this section.

2.2.1 Action of inflaton

The lagrangian of a scalar field is given by

$$S_\phi = \int \mathrm{d}t\mathrm{d}x^3 \sqrt{-g} \left[\frac{1}{2}\partial_\mu\phi\partial^\mu\phi - V(\phi) \right]. \tag{2.19}$$

Although the extensions of this minimal lagrangian have been intensively studied, here we consider this simple case. Then the energy momentum tensor is written as

$$T_{\mu\nu} = 2\frac{\partial\mathcal{L}_\phi}{\partial g^{\mu\nu}} - g_{\mu\nu}\mathcal{L}_\phi, \tag{2.20}$$

where $\mathcal{L}$ is the lagrangian of the scalar field. In the FRW metric, it is rewritten as

$$T_{00} = \rho = \frac{1}{2}\left[\dot\phi^2 + a^{-2}(\partial_i\phi)^2 \right] + V(\phi), \tag{2.21}$$

$$a^{-2}T_{ii} = p = \frac{1}{2}\left[\dot\phi^2 + a^{-2}(\partial_i\phi)^2 \right] - V(\phi). \tag{2.22}$$

Then the equation of state parameter is given by

$$w = \frac{p}{\rho} = \frac{\frac{1}{2}\left[\dot\phi^2 + a^{-2}(\partial_i\phi)^2 \right] - V(\phi)}{\frac{1}{2}\left[\dot\phi^2 + a^{-2}(\partial_i\phi)^2 \right] + V(\phi)}. \tag{2.23}$$

Therefore if the kinetic energy of the scalar field is negligible compared to the potential energy, $w \simeq -1$ and the exponential expansion is realized. Once inflation takes place, the scale factor becomes huge and the term with the spatial derivative of the scalar field is negligible. [1] The condition of inflation is given by

$$\dot\phi^2 \ll V(\phi). \tag{2.24}$$

This condition is called the slow-roll condition. This scalar field which is responsible fot the occurrence of inflation is called *inflaton*.

---

[1] When one discusses the onset of inflation, the spatial derivative term is also relevant.

2.2.2 The slow-roll parameters

Next, let us investigate the dynamics of slow-roll inflation. When the inflaton dominates the energy density of the universe, the Friedmann equation reads

$$3M_{\mathrm{Pl}}^2 H^2 = \frac{1}{2}\dot{\phi}^2 + V(\phi). \tag{2.25}$$

The equation of motion for the inflaton derived from the action is given by

$$\ddot{\phi} + 3H\dot{\phi} + \partial_\phi V = 0. \tag{2.26}$$

From these two equation, one can derive

$$2M_{\mathrm{Pl}}^2 \dot{H} = -\dot{\phi}^2. \tag{2.27}$$

As mentioned above, the kinetic energy of the inflaton is negligible compared to the potential energy during inflation. Then the first term in the Friedmann equation is ignored, we obtain the approximated equation as

$$3M_{\mathrm{Pl}}^2 H^2 \simeq V(\phi). \tag{2.28}$$

Using this equation, the equation of motion is also approximated as

$$3H\dot{\phi} \simeq -\partial_\phi V. \tag{2.29}$$

This is called the slow-roll equation. Using these approximated equations, the slow-roll condition, eq. (2.24), is rewritten as

$$\varepsilon \equiv \frac{M_{\mathrm{Pl}}^2}{2}\left(\frac{V'}{V}\right)^2 \ll 1. \tag{2.30}$$

This parameter ε is called the slow-roll parameter and this condition is also called the slow-roll condition. Using the slow-roll equation again, ε is recast as

$$\varepsilon \simeq \varepsilon_H \equiv -\frac{\dot{H}}{H^2}. \tag{2.31}$$

In a similar manner, the condition that the first term in the equation of motion is negligible compared to the second term, $\ddot{\phi} \ll 3H\dot{\phi}$, can be rewritten in terms of another slow-roll parameter,

$$|\eta| \ll 1, \qquad \eta \equiv M_{\mathrm{Pl}}^2 \frac{\partial_\phi^2 V}{V}. \tag{2.32}$$

Note that the slow-roll parameters, ε and η, are given in terms of the potential of inflaton. Thus a model with a potential which satisfies the slow-roll conditions can realize inflation. However, observations put tight constraints on the slow-roll parameters as we see in the next section.

2.3   Generation of Scalar Perturbation

The most important prediction of inflation is the generation of perturbations from the quantum fluctuations. In this section, we calculate the scalar perturbation produced during inflation. Technically speaking, we should take into account the metric perturbation, while for simplicity we ignore it and calculate only the perturbation of the scalar field in this section. The metric perturbation is considered and the Mukhanov-Sasaki equation is derived in sec. 4.3.2 (see eq. (4.70)).

First we introduce the conformal time,

$$d\eta = \frac{dt}{a}, \quad \eta = \int^t \frac{dt'}{a(t')}. \tag{2.33}$$

Especially in de Sitter specetime, it reads

$$\eta = -\frac{1}{aH}. \tag{2.34}$$

With the conformal time, the action of the inflaton is rewritten as

$$S_\phi = \int d\eta dx^3 \left[\frac{a^2}{2} \left(\phi'^2 - (\partial_i \phi)^2 \right) - a^4 V(\phi) \right], \tag{2.35}$$

where the prime denotes the derivative with respective to the conformal time. For concreteness, we assume the quadratic potential,

$$V(\phi) = \frac{1}{2} m^2 \phi^2. \tag{2.36}$$

Then the slow-roll conditions imply

$$\varepsilon = 2\frac{M_{\rm Pl}^2}{\phi^2} \ll 1 \quad \Longleftrightarrow \quad \phi \gg M_{\rm Pl}, \tag{2.37}$$

$$\eta = \frac{m^2}{3H^2} \ll 1 \quad \Longleftrightarrow \quad m \ll H. \tag{2.38}$$

The field value of the inflaton should be much larger than the reduced Planck mass and the mass of the inflaton should be much smaller than the Hubble parameter during inflation. With this potential, the action is now

$$S_\phi = \int d\eta dx^3 a^2 \left[\frac{1}{2} \left(\phi'^2 - (\partial_i \phi)^2 \right) - a^2 m^2 \phi^2 \right]. \tag{2.39}$$

To obtain the canonical kinetic term, we redefine the field as

$$\chi(\eta, \boldsymbol{x}) \equiv a(\eta)\phi(\eta, \boldsymbol{x}). \tag{2.40}$$

Then the action reads

$$S_\chi = \frac{1}{2} \int d\eta dx^3 \left[\chi'^2 - (\partial_i \chi)^2 + \left(\frac{a''}{a} - a^2 m^2 \right) \chi^2 \right]. \tag{2.41}$$

The equation of motion in Fourier space is given by

$$\chi_{\boldsymbol{k}}'' + \left[k^2 - \left(2 - \frac{m^2}{H^2} \right) \frac{1}{\eta^2} \right] \chi_{\boldsymbol{k}} = 0, \tag{2.42}$$

with

$$\chi(\eta, \boldsymbol{x}) = \int \frac{\mathrm{d}^3 k}{(2\pi)^3} e^{i \boldsymbol{k} \cdot \boldsymbol{x}} \chi_{\boldsymbol{k}}(\eta). \tag{2.43}$$

Now let us quantize the scalar field. The field $\chi_{\boldsymbol{k}}$ is decomposed into the mode function $u_k(\eta)$ and the creation/annihilation operators $a_{\boldsymbol{k}}, a_{\boldsymbol{k}}^\dagger$ as

$$\chi_{\boldsymbol{k}}(\eta) = a_{\boldsymbol{k}} u_k(\eta) + a_{-\boldsymbol{k}}^\dagger u_k^*(\eta), \tag{2.44}$$

where the mode function depends on the absolute value of wave number k because the equation of motion includes only k^2. The equal-time commutation relation for the canonical scalar field $\chi(\eta, \boldsymbol{x})$ and its conjugate momentum $\Pi(\eta, \boldsymbol{x}) \equiv \chi'(\eta, \boldsymbol{x})$ is given by

$$[\chi(\eta, \boldsymbol{x}), \Pi(\eta, \boldsymbol{y})] = i\delta(\boldsymbol{x} - \boldsymbol{y}), \tag{2.45}$$

$$[\chi(\eta, \boldsymbol{x}), \chi(\eta, \boldsymbol{y})] = [\Pi(\eta, \boldsymbol{x}), \Pi(\eta, \boldsymbol{y})] = 0. \tag{2.46}$$

If one imposes the usual commutation relation on the creation/annihilation operators,

$$\left[a_{\boldsymbol{k}}, a_{\boldsymbol{k}'}^\dagger \right] = (2\pi)^3 \delta(\boldsymbol{k} - \boldsymbol{k}'), \quad [a_{\boldsymbol{k}}, a_{\boldsymbol{k}'}] = \left[a_{\boldsymbol{k}}^\dagger, a_{\boldsymbol{k}'}^\dagger \right] = 0. \tag{2.47}$$

one finds that the equal-time commutators in real space read

$$[\chi(\eta, \boldsymbol{x}), \Pi(\eta, \boldsymbol{y})] = \int \frac{\mathrm{d}^3 k}{(2\pi)^3} e^{i \boldsymbol{k} \cdot (\boldsymbol{x} - \boldsymbol{y})} \left(u_k^*(\eta) u_k'(\eta) - u_k(\eta) u_k^{*'}(\eta) \right), \tag{2.48}$$

and $[\chi(\eta, \boldsymbol{x}), \chi(\eta, \boldsymbol{y})] = [\Pi(\eta, \boldsymbol{x}), \Pi(\eta, \boldsymbol{y})] = 0$. Thus the following normalization condition on the mode function $u_k(\eta)$ is required to satisfy eq. (2.45):

$$u_k^* u_k' - u_k u_k^{*'} = i. \tag{2.49}$$

Next let us consider the initial condition of the scalar field χ. In the far past, $\eta \to -\infty$, the equation of motion is approximated by $u_k''(\eta) + k^2 u_k(\eta) = 0$ and the general solution is $u_k(\eta) = C_1 e^{ik\eta} + C_2 e^{-ik\eta}$ where C_1 and C_2 are constants of integration. Then the normalization condition eq. (2.49) reads

$$2k \left(|C_1|^2 - |C_2|^2 \right) = 1. \tag{2.50}$$

However, it does not fix C_1 and C_2. Here, we fix the initial condition by assuming that the inflaton fluctuation, namely $\chi_k(\eta)$ with $k \neq 0$, is in the vacuum state in the far past. Hamiltonian of the scalar field in the far past is given by

$$\mathcal{H}(\eta \to -\infty) = \frac{1}{2} \int \frac{\mathrm{d}^3 k}{(2\pi)^3} \left(\chi_{\boldsymbol{k}}' \chi_{-\boldsymbol{k}}' + k^2 \chi_{\boldsymbol{k}} \chi_{-\boldsymbol{k}} \right) \tag{2.51}$$

When this Hamiltonian acts on the Fock vacuum state defined by $a_{\boldsymbol{k}}|0\rangle = 0$, it yields

$$\mathcal{H}(\eta \to -\infty)|0\rangle = \int \frac{\mathrm{d}^3 k}{(2\pi)^3} k^2 \Big((|C_1|^2 + |C_2|^2)(2\pi)^3 \delta(0) + 2C_1 C_2 a^\dagger_{-\boldsymbol{k}} a^\dagger_{\boldsymbol{k}} \Big). \qquad (2.52)$$

In the right hand side, the first term represents the vacuum (zero-point) energy and it is c-number, while the second term should vanish if the Hamiltonian is an eigen-operator of the vacuum. Therefore $C_1 C_2 = 0$ is required. Here we chose $C_2 = 0$ and the normalization condition fixes $C_1 = 1/\sqrt{2k}$. This initial condition is called "the Bunch-Davies vacuum" and it is obtained as,

$$u_k(\eta) \to \frac{1}{\sqrt{2k}} e^{-ik\eta}, \quad (|k\eta| \gg 1). \qquad (2.53)$$

With this initial condition, we can fully solve the equation of motion eq. (2.42) and the solution of the mode function $u_k(\eta)$ is given by the Bessel function,

$$u_k(\eta) = \frac{\sqrt{-\pi\eta}}{2} \left[J_n(-k\eta) - iY_n(-k\eta) \right], \quad n \equiv \sqrt{\frac{9}{4} - \frac{m^2}{H^2}}. \qquad (2.54)$$

On super-horizon scales, $|\eta| \ll k^{-1}$, its asymptotic form is

$$u_k(\eta) \to \frac{i\Gamma(n)}{2} \sqrt{\frac{-\eta}{\pi}} \left(\frac{2}{-k\eta} \right)^n, \quad (|k\eta| \ll 1). \qquad (2.55)$$

The root mean square of the amplitude of the scalar fluctuation can be computed as the power spectrum,

$$P_\chi = \langle 0||\chi_k|^2|0\rangle = |u_k(\eta)|^2 = \frac{\pi|\eta|}{4} \left[J_n^2(-k\eta) + Y_n^2(-k\eta) \right]. \qquad (2.56)$$

In cosmology, the dimensionless power spectrum defined as $\mathcal{P} = k^3 P / 2\pi^2$ is often used. Therefore the dimensionless power spectrum of the original scalar field $\phi = \chi/a$ is

$$\mathcal{P}_\phi(\eta, k) \simeq \left(\frac{H}{2\pi} \right)^2 \left(\frac{k}{2aH} \right)^{\frac{2m^2}{3H^2}}. \qquad (2.57)$$

So far, we work in the flat gauge in which the scale factor is independent of the position space $\boldsymbol{x}$ and calculate the perturbation of the scalar field $\delta\phi(t, \boldsymbol{x})$. However, the perturbation of the scalar field is not a gauge invariant variable and not directly compared with observations. The curvature perturbation $\zeta(\eta, k)$ is known as a useful gauge invariant variable because ζ_k is conserved on super-horizon scales $|k\eta| \ll 1$ if the universe is dominated by a single component, and ζ is directly connected to the observations. ζ is defined as the perturbation of the scale factor on the uniform density slice

$$a(t, \boldsymbol{x}) = a(t) e^{\zeta(t, \boldsymbol{x})}, \quad \text{(uniform density slice)}, \qquad (2.58)$$

where the scale factor $a(t, \boldsymbol{x})$ in the left hand side depends on $\boldsymbol{x}$, since the fluctuation of scalar field $\delta\phi(t, \boldsymbol{x})$ generated during inflation changes the duration of inflation at each local patch of the universe. For example, if a negative value of the scalar perturbation, $\delta\phi < 0$, is generated in a local patch of the universe, it takes the time $\delta t = -\delta\phi/\dot{\phi}$ for $\phi(t, \boldsymbol{x})$ to catch up the homogeneous value $\phi_0(t)$. During this extra time δt, the local universe additionally expands $a(t + \delta t) - a(t) \simeq a(t)H\delta t$. Therefore at the leading order of the perturbation, the relation between the scalar perturbation $\delta\phi$ and the curvature perturbation ζ is given by

$$\zeta(t, \boldsymbol{x}) = -\frac{H(t)}{\dot{\phi}(t)}\delta\phi(t, \boldsymbol{x}). \tag{2.59}$$

Now the power spectrum of the scalar field perturbation $\mathcal{P}_\phi$ can be translated into the power spectrum of the curvature perturbation as

$$\mathcal{P}_\zeta(k, \eta) \simeq \left(\frac{H}{\dot{\phi}}\right)^2 \left(\frac{H}{2\pi}\right)^2 \left(\frac{k}{2aH}\right)^{\frac{2m^2}{3H^2}}. \tag{2.60}$$

Using the slow-roll approximation, one can rewrite it as

$$\mathcal{P}_\zeta(k, \eta) \simeq \frac{H^2}{8\pi^2\varepsilon M_{\text{Pl}}^2} \left(\frac{k}{2aH}\right)^{\frac{2m^2}{3H^2}}. \tag{2.61}$$

The dependence on the wave number k remains while it is very weak because the power $2m^2/3H^2$ is small as we see in eq. (2.38). Therefore inflation predicts the almost scale invariant power spectrum of the curvature perturbation.

Let us compare this prediction and the observational results. The Planck satellite have reported [4]

$$\mathcal{P}_\zeta(k_0) = 2.196^{+0.051}_{-0.060} \times 10^{-9} \qquad (68\%\text{CL}; \text{Planck} + \text{WP}), \tag{2.62}$$

where $k_0 = 0.05\text{Mpc}^{-1}$ and WP denotes the polarization data of the WMAP experiment. Neglecting the weak k dependence of $\mathcal{P}_\zeta$, one obtain the slow-roll parameter ε as a function of the energy density of inflation ρ_{inf}

$$\varepsilon = \frac{1}{24\pi^2\mathcal{P}_\zeta}\frac{\rho_{\text{inf}}}{M_{\text{Pl}}^4} \approx 5.5 \times 10^{-4} \left(\frac{\rho_{\text{inf}}^{1/4}}{10^{16}\text{GeV}}\right)^4, \tag{2.63}$$

with $\rho_{\text{inf}} = 3M_{\text{Pl}}^2H^2$. This relation is known as "the COBE normalization" for the historical reason. One can also quantify the k dependence of the curvature power spectrum. The spectrum index defined as

$$n_s - 1 \equiv \frac{\text{d}\ln\mathcal{P}_\zeta}{\text{d}\ln k}, \tag{2.64}$$

indicates the scale dependence of $\mathcal{P}_\zeta$. The Planck observation puts constraint on it as [4]

$$n_s = 0.9603 \pm 0.0073 \quad (68\%\text{CL}; \text{Planck} + \text{WP}). \tag{2.65}$$

Thus the completely scale invariant spectrum, $n_s = 1$, is excluded. The red tilted ($n_s < 1$) spectrum is favored. In addition to n_s, the tensor-to-scalar ratio is also a very useful quantity to constraint inflation models. We discuss it in sec. 4.1.2. Moreover, the non-gaussianity of the curvature perturbation can be used to exclude various models of inflation [31, 40]. In spite of these constraints, an enormous number of inflation models still survive (e.g. see refs. [5, 6]). Therefore we need to explore observational signatures other than the scalar perturbation to determine the correct model of inflation.

Contents

3.1 Observation of Cosmic Magnetic Fields

In this section, we introduce observations of magnetic fields in the universe. These observations strongly motivate the theoretical research on the generation and the evolution of the cosmic magnetic fields.

3.1.1 Galactic Magnetic Fields

It has been known for a long time that galaxies and galactic clusters have their own magnetic fields [7, 8, 9, 10]. Radio synchrotron observations have revealed that the strength of the magnetic fields in galaxies are typically $10^{-6} \sim 10^{-5}$G, while stronger magnetic fields up to $\mathcal{O}(10^{-4})$G are observed in some starburst galaxies (e.g. M82, NGC4038, NGC4039) [41]. Galactic clusters also have magnetic fields with similar strength whose correlation lengthes are typically 10kpc. In our Milky Way galaxy, the strength of the magnetic field averaged over the 1kpc sphere around the Sun is about 6×10^{-6}G. The configuration of magnetic fields in galaxies have been also studied. In spiral galaxies, magnetic fields are randomly oriented in the spiral arms while more ordered magnetic fields are often observed in inter-arm regions and they are parallel to the adjacent gas spiral arms [42, 43]. They may indicate that the galactic magnetic fields co-evolve with the structure of the galaxy itself. However, the evolution of the magnetic fields in galaxies are not yet clear.

The galactic magnetic fields are widely considered to be amplified by the contraction associated with the structure formation and the plasma motion (dynamo mechanism, see ref. [44] for recent review). Nonetheless, neither adiabatic contraction nor dynamo mechanism can generate the magnetic fields from nothing. Therefore to explain the observed galactic magnetic fields, 'seed' magnetic fields should exist before its amplification mechanisms work. Accordingly, in astrophysics, seed magnetic fields are usually assumed while their origin is an outstanding problem. Since the seed magnetic fields give the initial condition of not only the galactic magnetic fields but also the galaxy structure in the light of their co-evolution, it is fundamental to find the origin of the seed magnetic fields (see refs. [45, 46, 47] for review).

Recently in ref. [48], the authors have performed a simulation which calculates the evolution of a Milky Way like galaxy taking into account magnetic fields for the first time. They set a homogeneous magnetic field with strength of 10^{-14}G as the initial seed magnetic field and follow its evolution in the ideal MHD (MagnetoHydroDynamics) approximation. They found that the magnetic fields are amplified by dynamo mechanism and the differential rotation of the galaxy, and they finally reached the strength 6μG which is consistent with the observed value. They reported that lowering or increasing the initial strength of the magnetic field by factors as large as 10^5 does not significantly change the results. This kind of simulation will be performed numerous times and will be refined. At this point, however, according to the result of ref. [48], primordial magnetic fields whose strength is larger than 10^{-19}G are required to explain the galactic magnetic fields. Thus we have a motivation to seek a mechanism which produces primordial magnetic fields at least with 10^{-19}G in the early universe.

3.1.2 Void Magnetic Fields

Recently the generation mechanism of the primordial magnetic fields in the early universe attracts much attention because there are several reports that magnetic fields are found even in void regions. Such void magnetic fields (extragalactic magnetic fields) could be detected by blazar observations [11, 12, 13, 14, 15, 16, 17, 18, 19] and it is reported that their strength is larger than $\sim 10^{-15}$G with an uncertainty of a few orders.

3.1.2.1 Detection method

The detection methodology is as follows. Observations of blazars which mainly radiate TeV scale gamma rays are used. The TeV blazars originally emit gamma rays with TeV scale energy but these gamma rays interact with extragalactic background lights (EBL) while they travel from the blazar to the earth. EBLs typically have energy of ~ 1eV and the interaction creates pairs of charged particles, namely electron and positron. Since the gamma ray from the blazar has much higher energy than the EBL photons, the pair-created charged particles travel in the same direction as the original gamma ray. Then these charged particles interact with CMB photons which fill up the entire universe. The charged particles kick the CMB photons through the inverse Compton scattering and typically give GeV scale energy to the photons. This series of process is called *electromagnetic cascade process*. It implies that all the TeV gamma rays emitted by blazars do not reach the earth but some of them produce GeV gamma rays and these GeV gamma rays reach the earth instead. Thus if a blazar radiates TeV gamma rays and we can observe them, we should also observe GeV gamma rays simultaneously.

Since H.E.S.S telescope which is a atmospheric cherenkov telescope array and sensitive to gamma rays with TeV scale energy had observed several TeV blazars, after the launch of Fermi telescope which is sensitive to GeV gamma rays, Fermi telescope tried to observe the cascaded GeV gamma rays by targeting known TeV blazars. However, Fermi telescope failed to detect GeV gamma rays from the blazars and put an upper bound on the flux of GeV gamma rays. Since the electromagnetic cascade process is described by the known physics and can be simulated with the intrinsic spectrum of the blazars reconstructed by the H.E.S.S observation, the result of Fermi telescope cannot be understood unless some phenomena reduce the cascaded GeV gamma rays.

Neronov and Vovk [11] (see also [49]) explored the possibility that magnetic fields in void regions bended the orbit of the pair-created charged particles and thus the flux of cascaded GeV gamma rays is reduced. Note that even if the magnetic field changes the direction of charged particles, the total number of GeV gamma rays which reach the earth is not necessarily decreased. A charged particle which originally heads to a slightly different direction from the earth can be directed to the earth by the void magnetic field. Therefore the magnetic fields extend and blur the image of a blazar. The gamma rays coming from a small sky area around the position of the blazar with the width of the point spread function θ_{PSF} are taken as gamma rays from the blazar in observations. Neronov and Vovk calculated how the void magnetic fields extend the blazar image of the cascaded

gamma rays θ_{ext}. If $\theta_{\text{PSF}} < \theta_{\text{ext}}$, it can be attributed to the cosmic magnetic fields which significantly decrease the gamma ray flux. In this way, the extragalactic magnetic fields can explain the observations of H.E.S.S and Fermi telescope simultaneously.

3.1.2.2 Several results

In ref. [11], they used four blazars, namely 1ES1101-232 ($z = 0.186$), 1ES0229+200 ($z = 0.14$), 1ES0347-121 ($z = 0.188$) and H2356-309 ($z = 0.165$) which were observed in the first year of the Fermi telescope operation. In the cases of two out of four blazars, the upper bound on the GeV gamma ray flux from Fermi telescope is lower than the expected flux from the H.E.S.S observation. As a result, they derived the lower bound on the strength of the void magnetic field as

$$
B_{\text{void}} \geq 3 \times 10^{-16} \text{G} \times \begin{cases} 1 & (L_B > 1\text{Mpc}) \\ \left(\frac{L_B}{1\text{Mpc}}\right)^{-1/2} & (L_B < 1\text{Mpc}) \end{cases} , \tag{3.1}
$$

where L_B is the correlation length of the void magnetic field and we will explain the reason of the last factor below. Here 1Mpc is roughly the cooling scale on which the electron/positron lose most of their energy by kicking many CMB photons through the inverse Compton scattering [15]. If the correlation length of the magnetic field, namely the size in which the magnetic field can be seen as a homogeneous field, is larger than the cooling length, the magnetic field bends the orbit of the charged particle uniformly. However, if the correlation length is shorter than the cooling length, the direction of the magnetic field changes repeatedly while a charged particle travels in a void region. Then the effect of the magnetic fields are partially cancelled out. Since the direction of magnetic fields is expected to change randomly, the deviation of the electron/positron path is modeled as random walk. The charged particles pass through $1\text{Mpc}/L_B$ different patches of correlated magnetic fields and their total effect are weaker than the entirely homogeneous case by the factor of $\sqrt{L_B/1\text{Mpc}}$. Therefore the averaged strength of the magnetic fields should be stronger than the homogeneous case by the factor of $\sqrt{1\text{Mpc}/L_B}$. Consequently, if $L_B < 1\text{Mpc}$, the lower bound on the strength of the void magnetic field is increased by $\sqrt{1\text{Mpc}/L_B}$ as eq. (3.1).

Some other groups also worked on the lower limit on the void magnetic field and obtained similar bounds. If $L_B > 1\text{Mpc}$, the lower bound is derived as 2×10^{-15}G by Tavecchio et al. [12], 5×10^{-15}G by Dolag et al. [13], 10^{-18}G by Dermer et al. [14] 2×10^{-16}G by Huan et al. [15]. In ref. [17], Neronov, Vovk and have updated the original work [11] with latest blazar observations, and obtained a new lower bound as 10^{-15}G by assuming the intrinsic flux of blazars do not vary significantly. They also reported that the lower bound is relaxed to 10^{-17}G if a possible variability of blazar flux is taken into account. Thus, although a few order of uncertainty remains, the several different groups working on the method of Noronov and Vovk obtained the consistent results and they imply the detection of non-zero void magnetic field.

In ref. [18], the authors have obtained a conservative lower bound on the void magnetic field as $10^{-20.5}$G by exploiting a different methodology from that of Neronov and Vovk. They again use simultaneous GeV-TeV observations of blazars, however, they focus on the time delay of the cascaded gamma rays. Their method does not depend on a long-term variability of blazar flux and is more reliable. On the other hand, Essey et al. [16] assumed that blazars produce not only gamma rays but also cosmic rays and the contribution from the cosmic ray dominates the cascaded (secondary) gamma rays. In that case, they obtained both lower and upper bound on the strength of the void magnetic field as

$$10^{-17}\text{G} < B_{\text{void}} < 3 \times 10^{-14}\text{G}. \tag{3.2}$$

Note that they assume $L_B = 1$Mpc.

In addition, the upper bound on the strength of primordial magnetic fields can also be obtained from the cosmic microwave background (CMB) and the large scale structure (LSS) observations. In terms of CMB, the anisotropic stress of the primordial magnetic field produces the curvature perturbation as well as the gravitational wave on super-horizon scales via gravitational effects, and they eventually generate CMB anisotropies. Regarding the matter power spectrum and the observation of LSS, the key physics is that the primordial magnetic field affects the baryon perturbation through Lorentz force after the decoupling between baryon and photon. The matter power spectrum (or the dark matter perturbation) is amplified by the induced baryon perturbation via gravitational force. In researches on these effects, resultant upper bounds on the strength of the magnetic field is typically 10^{-9}G, since the energy density of nano-Gauss magnetic field is comparable to that of the perturbation of the CMB photons at the last scattering. (see, e.g. [50, 51], and references therein) [1]. Therefore a conservative constraint on the primordial magnetic fields is given by

$$10^{-20}\text{G} \lesssim B_{\text{void}} \lesssim 10^{-9}\text{G}. \tag{3.3}$$

Nevertheless, their origin is still unknown and no successful quantitative model is established.

We also refer to refs. [53, 54, 55, 56]. In this series of works by Tashiro, Vachaspati and their collaborators, they develop the method to measure the correlators of both helical and non-helical void magnetic fields and they have reported to find $\sim 10^{-14}$G *helical* magnetic field by using the diffused gamma ray observed by the Fermi telescope. If it is confirmed by further research and it has the primordial origin, this observational result indicates that a parity violating process involves in the magnetogenesis mechanism.

Consequently, although the accurate strength of the void magnetic field is still unknown, it can be expected to be around 10^{-15}G with an uncertainty of a few orders. When one seeks the primordial generation mechanism of the cosmic magnetic field, the target strength should be $\sim 10^{-15}$G.

---

[1] Ref. [52] also reported an independent upper limit on primordial magnetic fields during big bang nucleosynthesis (BBN) as 10^{-6}G.

3.1.2.3 Effective strength of void magnetic field

By Fermi and HESS observations, there is a lower limit on the bending angle of GeV scale cascade electrons and positrons in the inter-galactic medium. However, in the literatures enumerated above, the constraint on the cosmic magnetic field is given only in terms of the correlation length of magnetic fields while theorists need the constraint in terms of the magnetic power spectrum. In this subsection, we shall generalize the constraint on the cosmic magnetic field to more general spectra. Such a generalization makes the connection between the cosmic magnetic power spectrum $\mathcal{P}_B$ and the bending angle θ.

Provided that a charged particle travels distance L in the background of a weak magnetic field $\boldsymbol{B}(\boldsymbol{r})$ from t_1 till t_2. We adopt $L = 1\text{Mpc}$ since the characteristic length scale for energy losses of charged particles due to inverse Compton scattering is around 1Mpc [15]. Then the bending angle is given by

$$\boldsymbol{\theta} \simeq \frac{\boldsymbol{v}(t_1) - \boldsymbol{v}(t_2)}{v}, \tag{3.4}$$

where $\boldsymbol{v}(t)$ is the velocity vector of the particle. Note the absolute value of the velocity vector is constant. By using the equation of motion with Lorentz force, the difference of the velocity vectors is written as

$$\boldsymbol{v}(t_2) - \boldsymbol{v}(t_1) = \int_{t_1}^{t_2} \mathrm{d}\tilde{t}\ \dot{\boldsymbol{v}}(\tilde{t}) = \frac{e}{m} \int_{t_1}^{t_2} \mathrm{d}\tilde{t}\ \boldsymbol{v}(\tilde{t}) \times \boldsymbol{B}(\tilde{t}) = \frac{e}{m} \int_0^L \mathrm{d}\boldsymbol{x} \times \boldsymbol{B}(\boldsymbol{x}), \tag{3.5}$$

where e and m are the charge and the mass of the particle, respectively, $\boldsymbol{x}(t)$ denotes the orbit of the particle and its initial value is set to $\boldsymbol{x}(t_1) = 0$. Then, we assume θ is so small that the orbit can be approximated as a straight line, $\boldsymbol{x}(t) \simeq x_1(t)\hat{\boldsymbol{e}}_1$ where $\hat{\boldsymbol{e}}_1$ is the unit vector in the direction of the axis 1. By Fourier transforming $\boldsymbol{B}(\boldsymbol{x})$, we can perform the line integral

$$\int_0^L \mathrm{d}x_1\ \hat{\boldsymbol{e}}_1 \times \boldsymbol{B}(x_1\hat{\boldsymbol{e}}_1) = \int \frac{\mathrm{d}^3 k}{(2\pi)^3} \frac{e^{ik_1 L} - 1}{ik_1}\ \hat{\boldsymbol{e}}_1 \times \tilde{\boldsymbol{B}}(\boldsymbol{k}). \tag{3.6}$$

By using these equations, we find that the variance of $\boldsymbol{\theta}$ is given by

$$\langle \boldsymbol{\theta}^2 \rangle = \left(\frac{e}{mv}\right)^2 \int \frac{\mathrm{d}^3 k \mathrm{d}^3 k'}{(2\pi)^6} \frac{\left(e^{ik_1 L} - 1\right)\left(e^{ik'_1 L} - 1\right)}{-k_1 k'_1} (\delta_{ij} - \delta_{i1}\delta_{j1})\langle \tilde{B}_i(\boldsymbol{k})\tilde{B}_j(\boldsymbol{k}')\rangle. \tag{3.7}$$

Since the divergence of magnetic field vanishes ($k_i \tilde{B}_i(\boldsymbol{k}) = 0$) and the cosmic magnetic fields are statistically isotropic and homogeneous, the square bracket in eq.(3.7) can be written as

$$\langle \tilde{B}_i(\boldsymbol{k})\tilde{B}_j(\boldsymbol{k}')\rangle = \frac{1}{2}(2\pi)^3 \delta^{(3)}\left(\boldsymbol{k} + \boldsymbol{k}'\right)\left[\left(\delta_{ij} - \frac{k_i k_j}{k^2}\right)\frac{2\pi^2}{k^3}\mathcal{P}_B(k) + i\varepsilon_{ijl}k_l H(k)\right], \tag{3.8}$$

where $\mathcal{P}_B(k)$ is the magnetic power spectrum and $H(k)$ stands for the helicity component

of magnetic fields [57]. By substituting eq.(3.8) into (3.7), we obtain

$$\langle \boldsymbol{\theta}^2 \rangle = \frac{2}{3} \left(\frac{eL}{mv} \right)^2 \int \frac{\mathrm{d}k}{k} \, \mathcal{P}_B(k) \, F(kL), \tag{3.9}$$

$$F(z) \equiv \frac{3}{2} z^{-2} \left[\cos(z) - \frac{\sin(z)}{z} + z \mathrm{Si}(z) \right] \sim \begin{cases} 1 + \mathcal{O}(z^2) & (z \ll 1) \\ \frac{3\pi}{4z} + \mathcal{O}(z^{-2}) & (z \gg 1) \end{cases}, \tag{3.10}$$

where $\mathrm{Si}(z)$ denotes the sine integral function. For $z \geq 0$, $F(z)$ satisfies

$$0 < F(z) \leq 1, \quad 0 \leq zF(z) \leq \alpha, \quad \alpha \equiv \mathrm{Max}[zF(z)] \simeq 2.48. \tag{3.11}$$

In order to find a proper definition of the effective strength of the magnetic field (including its normalization) for a given spectrum $\mathcal{P}_B(k)$, as a fiducial configuration we consider a homogeneous magnetic field whose direction is perpendicular to the particle's trajectory. Denoting the strength of the fiducial magnetic field as $B_\perp$, the bending angle is $\theta = L/R_\mathrm{L} = (eB_\perp L)/(mv)$, where R_L is the Larmor radius. On the other hand, for a statistically isotropic spectrum, the variance of the magnetic field in three-dimensions is three halves of the variance of the magnetic field projected onto the two-dimensional subspace perpendicular to the particle's trajectory. Thus, it is natural to define the effective strength of the magnetic field as

$$B_\mathrm{eff}^2 \equiv \frac{3}{2} \left(\frac{mv}{eL} \right)^2 \langle \boldsymbol{\theta}^2 \rangle. \tag{3.12}$$

In addition, one should take into account the diffusion damping of the magnetic field. Combining Faraday's law $\partial_t \boldsymbol{B} = -\boldsymbol{\nabla} \times \boldsymbol{E}$, Ampere's law $\boldsymbol{\nabla} \times \boldsymbol{B} = \boldsymbol{J}$ and Ohm's law $\boldsymbol{J} = \sigma \boldsymbol{E}$ where $\boldsymbol{J}$ is the electric current and σ is the electric conductivity, one finds the magnetic field obeys $\partial_t \boldsymbol{B} = \nabla^2 \boldsymbol{B}/\sigma$. This equation implies that even with high conductivity magnetic fields decay on small scales due to the diffusion term in the right hand side. The present typical scale of the magnetic diffusion is estimated as $k_\mathrm{diff} \simeq (1\mathrm{AU})^{-1}$ [58]. Thus the effect of the magnetic diffusion can be expressed as the cutoff in the power spectrum as

$$\mathcal{P}_B(\eta_\mathrm{now}, k) \simeq 0 \quad (\text{for } k > k_\mathrm{diff}). \tag{3.13}$$

Combining eqs. (3.9), (3.12) and (3.13), we obtain

$$B_\mathrm{eff}^2 = \int_0^{k_\mathrm{diff}} \frac{\mathrm{d}k}{k} F(kL) \, \mathcal{P}_B(k) \geq B_\mathrm{obs}^2. \tag{3.14}$$

Therefore one can take the lower bound on the void magnetic field from blazar observations (i.e. $B_\mathrm{obs} \sim 10^{-15}\mathrm{G}$) is actually the bound on this effective strength B_eff. Since B_eff is given in terms of the magnetic power spectrum, it is useful to compare theoretical predictions and observational bounds.

Now we provide intuitive understanding of B_{eff} and discuss the consistency with eq. (3.1). For this purpose, let us replace $F(kL)$ by its asymptotic forms eq. (3.10) and drop $\mathcal{O}(1)$ numerical factors to obtain the approximate formula as

$$B_{\text{eff}}^2(\eta_{\text{now}}) \sim \int_0^{1/L} \frac{\mathrm{d}k}{k} \left[\mathcal{P}_B(\eta_{\text{now}}, k) \right] + \int_{1/L}^{k_{\text{diff}}} \frac{\mathrm{d}k}{k} \left[\frac{1}{kL} \mathcal{P}_B(\eta_{\text{now}}, k) \right]. \tag{3.15}$$

Let us now think of a Fourier mode of the magnetic field. For $kL \ll 1$, the corresponding magnetic field can be treated as a homogeneous field, as far as the particle's trajectory (with the total length L) is concerned. Thus modes with $kL \ll 1$ contribute to the bending angle as if they are homogeneous fields. This explains the first term in the right hand side of (3.15). On the other hand, for $kL \gg 1$, the direction of the corresponding magnetic field randomly changes $N \sim kL$ times while the charged particle travels the total length L. If we were interested in the trajectory of the charged particle within one of short segments of the length $\sim k^{-1}$ then the magnetic field could be treated as a homogeneous field. Actually, we are interested in the total bending angle due to N segments. Because of the randomness of the direction, the total bending angle from N segments adds up to only $\sqrt{N}$ times the contribution from each segment. Therefore the contribution of modes with $kL \gg 1$ to the variance of the bending angle should acquire the weight of order $1/N \sim 1/(kL)$. This explains the second term in the right hand side of (3.15).

3.2 The Kinetic Coupling Model (Ratra's Model)

In the previous section, we see the observations of the cosmic magnetic fields and they give a strong motivation for theoretical studies on the generation of these magnetic fields in the early universe. To explore inflationary magnetogenesis with a concrete example, in this section, we introduce a model proposed by Ratra in 1991 [20]. Although a U(1) gauge field does not acquire quantum fluctuations during inflation in its minimal form due to the conformal symmetry, several ideas to extend it are proposed [21, 22, 23, 24, 25, 26, 27]. Among them, Ratra's model or the kinetic coupling model [20] is nicely simple, free of ghost instabilities [59] and well motivated by the supergravity or the string theory frame work [60, 61, 62, 63, 64, 65]. The model action is given by

$$S_A = \int \mathrm{d}\eta \mathrm{d}^3 x \sqrt{-g} \left[-\frac{1}{4} I^2(\phi) F_{\mu\nu} F^{\mu\nu} \right], \quad (F_{\mu\nu} \equiv \partial_\mu A_\nu - \partial_\nu A_\mu), \qquad (3.16)$$

where A_μ is a U(1) gauge field, ϕ is a homogeneous and dynamical scalar field which is not necessarily the inflaton and η is the conformal time.

This section is organized as follows. [2] In sec. 3.2.1, we introduce the model and briefly review its calculations and predictions. One will see that the kinetic coupling model apparently produces strong magnetic fields, however, it has some shortcomings that prevent the model from generating the magnetic field being strong enough to explain the observations. In the following two subsections, we describe these obstacles. In sec. 3.2.2 and sec. 3.2.3, the back reaction problem and the curvature perturbation problem are explained, respectively. They basically concerns that the produced electromagnetic fields during inflation may spoil the inflation dynamics which is consistent with cosmic microwave background (CMB) observations. In sec 3.2.4, these problems are quantitatively evaluated with the constraint from the Planck observation. It turns out that the magnetic field produced in the kinetic coupling model is severely limited and it cannot explain the observation of the cosmic magnetic fields, unfortunately.

3.2.1 Brief review on the model

We briefly review the kinetic coupling model [20, 59, 62, 60, 61, 63, 64, 65] in this subsection. Although it is known it can not generate the primordial magnetic field which is strong enough to be more than 10^{-15}G at present because of several obstacles as we see later, it is nicely simple and gives us the essential understanding of the problem. Moreover this model is interesting in terms of CMB observations because it can produce detectable level of non-gaussianities.

In the kinetic coupling model, the kinetic term of the U(1) gauge field is modified as $F_{\mu\nu} F^{\mu\nu} \to I^2(\phi) F_{\mu\nu} F^{\mu\nu}$ where ϕ is a homogeneous scalar field and is not necessarily inflaton. In the original work, Ratra identifies ϕ as the inflaton and considers the coupling

---

[2]This section is based on my work [32].

$I(\phi) \propto e^{\alpha\phi}$ with a constant parameter α and the inflaton potential $V(\phi)$ is also given by a exponential function of ϕ [20]. Bamba and Yokoyama assume that ϕ is a spectator field while both the coupling $I(\phi)$ and its potential $V(\phi)$ are exponential functions [62]. In both cases, it is found that the kinetic coupling function $I(\phi)$ approximately behaves as a power-law function of the conformal time in the slow-roll regime during inflation. Hereafter, therefore, we phenomenologically assume $I(\phi)$ is the power-law function of conformal time, $I \propto \eta^n$. It should be noted that the kinetic coupling may change the ϕ dynamics due to the backreaction from the gauge field and hence it may change the behavior of $I \propto \eta^n$ at certain point during inflation [66]. In that sense, the assumption of $I \propto \eta^n$ is an optimistic one for magnetogenesis. To restore the Maxwell theory after inflation, I is required to be unity at the end of inflation $\eta_{\rm f}$. Thus $I(\phi)$ is assumed to behave as

$$I(\phi) = \begin{cases} (\eta/\eta_{\rm f})^n & (\eta < \eta_{\rm f}) \\ 1 & (\eta \geq \eta_{\rm f}) \end{cases} . \tag{3.17}$$

We also assume the quasi de Sitter inflation, the Einstein gravity and the flat FLRW metric. Note that hereafter we consider only positive n to avoid the strong coupling problem. Because if n is negative and the QED coupling $e\bar{\psi}\gamma^\mu\psi A_\mu$ exists, its effective coupling constant, e/I, becomes much larger than unity during inflation. In that case, we can not calculate the behavior of A_μ without fully taking account of the interaction effects [28] (see sec. 3.3.1.1 for a further discussion).

Let us take the radiation gauge, $A_0 = \partial_i A_i = 0$, and expand the transverse part of A_i with the polarization vector $e_i^{(\lambda)}$ and the creation/annihilation operator $a_{\boldsymbol{k}}^{\dagger(\lambda)}/a_{\boldsymbol{k}}^{(\lambda)}$ as

$$A_i(\eta, \boldsymbol{x}) = \sum_{\lambda=1}^{2} \int \frac{{\rm d}^3 k}{(2\pi)^3} e^{i\boldsymbol{k}\cdot\boldsymbol{x}} e_i^{(\lambda)}(\hat{\boldsymbol{k}}) \left[a_{\boldsymbol{k}}^{(\lambda)} \mathcal{A}_k^{(\lambda)}(\eta) + a_{-\boldsymbol{k}}^{\dagger(\lambda)} \mathcal{A}_k^{(\lambda)*}(\eta) \right] , \tag{3.18}$$

where $\mathcal{A}_k^{(\lambda)}$ is the mode function of the gauge field, the hat of $\hat{\boldsymbol{k}}$ denotes the unit vector and (λ) is the polarization label. The polarization vector $e_i^{(\lambda)}$ satisfies

$$k_i e_i^{(\lambda)}(\hat{\boldsymbol{k}}) = 0, \qquad \sum_{p=1}^{2} e_i^{(\lambda)}(\hat{\boldsymbol{k}}) e_j^{(\lambda)}(-\hat{\boldsymbol{k}}) = \delta_{ij} - \frac{k_i k_j}{k^2}, \tag{3.19}$$

and the creation/annihilation operators satisfy

$$[a_{\boldsymbol{p}}^{(\lambda)}, a_{-\boldsymbol{q}}^{\dagger(\sigma)}] = (2\pi)^3 \delta(\boldsymbol{p} + \boldsymbol{q}) \delta^{\lambda\sigma}. \tag{3.20}$$

Notice the behavior of $\mathcal{A}_k$ does not depend on the polarization (λ) in this model and hence we omit the label. Then the canonical commutation relation for A_i requires the normalization condition of mode function $\mathcal{A}_k(\eta)$ as

$$I^2 \left(\mathcal{A}_k \, \partial_\eta \mathcal{A}_k^* - \mathcal{A}_k^* \, \partial_\eta \mathcal{A}_k \right) = i. \tag{3.21}$$

Using eq. (3.17), one finds that the equation of motion of the mode function during inflation is given by

$$\left[\partial_\eta^2 + k^2 - \frac{n(n-1)}{\eta^2} \right] (I\mathcal{A}_k) = 0 \,. \tag{3.22}$$

Assuming that the modes are in the Bunch-Davies vacuum on the sub-horizon scales,

$$I\mathcal{A}_k(\eta) = \frac{1}{\sqrt{2k}} e^{-ik\eta}, \qquad (-k\eta \ll 1), \tag{3.23}$$

the asymptotic solution of eq. (3.22) in the super-horizon limit is

$$|I\mathcal{A}_k(\eta)| = \frac{\Gamma(n-1/2)}{\sqrt{2\pi k}} \left(\frac{-k\eta}{2} \right)^{1-n}, \quad \left(-k\eta \ll 1, \ n > \frac{1}{2} \right), \tag{3.24}$$

where we have neglected the constant phase factor. For $0 < n < 1/2$, the asymptotic solution is different and the generated electromagnetic fields are weaker than the cases of $n > 1/2$. Hence we focus on $n > 1/2$ hereafter. In that case, one finds that $\mathcal{A}_k \propto \eta^{1-2n}$ from eq. (3.24) and the mode function of the gauge field grows on super-horizon scales. This behavior is quite distinct from that of a light scalar field or gravitons which stay almost constant on super-horizon scales. In the kinetic coupling model, the gauge field is not only produced but also significantly amplified after the horizon crossing.

At this point, we can acquire three important consequences in this model. First, the generated magnetic field is much smaller than the electric field on super-horizon scales. The power spectrum of electric and magnetic fields are given by

$$\mathcal{P}_E(\eta, k) \equiv \frac{k^3 |\partial_\eta \mathcal{A}_k|^2}{\pi^2 a^4}, \qquad \mathcal{P}_B(\eta, k) \equiv \frac{k^5 |\mathcal{A}_k|^2}{\pi^2 a^4}, \tag{3.25}$$

where two polarization modes are already summed. Then one easily sees

$$\frac{\mathcal{P}_B}{\mathcal{P}_E} \simeq |k\eta|^2 \ll 1, \qquad (|k\eta| \ll 1). \tag{3.26}$$

Since this relation originates in the definition of the electromagnetic fields and the power-law behavior of the mode function, $\mathcal{A}_k(\eta) \propto \eta^{1-2n}$, it is inevitable in this model with the setup eq. (3.17). Second, the unique model parameter n controls both the time dependence and the tilt of the electromagnetic energy spectrum. The energy contribution from each $\ln k$ mode of electric and magnetic fields can be calculated from the action eq. (3.16) ,

$$\frac{\mathrm{d}\rho_E}{\mathrm{d}\ln k} = \frac{1}{2} I^2 \mathcal{P}_E(\eta, k) = \frac{\Gamma^2(n+\frac{1}{2})}{2^{2-2n}\pi^3} H^4 (-k\eta)^{2(2-n)} \,, \tag{3.27}$$

$$\frac{\mathrm{d}\rho_B}{\mathrm{d}\ln k} = \frac{1}{2} I^2 \mathcal{P}_B(\eta, k) = \frac{\Gamma^2(n-\frac{1}{2})}{2^{4-2n}\pi^3} H^4 (-k\eta)^{2(3-n)} \,,$$

where H is Hubble parameter. The above equation tells that the electric field grows (decays) and the spectrum of the electric energy density is red-tilted (blue-tilted) for

$n > 2$ ($n < 2$). The flat spectrum can be realized in $n = 2$ case where the electric field stays constant. In the case of the magnetic field, the border of n is 3 in stead of 2.

Finally, the magnetic power spectrum at present is computed as

$$\mathcal{P}_B^{1/2}(\eta_{\text{now}}, k) = \frac{\Gamma(n - \frac{1}{2})}{2^{\frac{3}{2} - n}\pi^{\frac{3}{2}}}(a_{\text{f}}H)^{n-1}k^{3-n} \sim 10^{23n-80}\text{G} \times \left(\frac{\rho_{\text{inf}}^{1/4}}{10^{16}\text{GeV}}\right)^{n-1}\left(\frac{k}{1\text{Mpc}^{-1}}\right)^{3-n},$$
(3.28)

where ρ_{inf} is the energy density of the inflaton and a_{f} is a scale factor at the end of inflation ($a = 1$ at the present). Here we assume the instantaneous reheating and have $a_{\text{f}}^4 = \rho_\gamma/\rho_{\text{inf}}$ with ρ_γ being the present energy density of the radiation which is given by $\rho_\gamma \approx 5.7 \times 10^{-125}M_{\text{Pl}}^4$. Note that the instantaneous reheating is the most optimistic case for inflationary magnetogenesis because the magnetic energy density decays faster than the background energy density in matter dominated (inflaton oscillating) era and the present strength of the magnetic field gets smaller as the matter dominated era lasts longer. Here the produced magnetic fields are assumed not to be amplified after inflation and to decay in proportional to a^{-2} as a radiation component. After the reheating, thermally produced charged particles fill up the universe and the electric conductivity reaches $\mathcal{O}(10 - 10^2)T$, where T is the temperature of the thermal bath [21, 67, 68, 69, 70]. With such a high conductivity, it can be shown that the magnetic field decay in proportional to a^{-2} which is called *the freeze of magnetic field* [65]. On the other hand, electric fields vanish in the thermal plasma with a high conductivity and their energy is thermalized. Although one may wonder if a portion of the electric energy is transferred to the magnetic energy, it does not occur. It can be understood that the electric field is the time derivative of the vector potential and its decreasing does not imply that the amplitude of the vector potential increases. Hence eq. (3.28) is an optimistic but reasonable estimation of the present cosmic magnetic field produced in Ratra's model.

From eq. (3.28), we find that $n \gtrsim 3$ is required to make the cosmic magnetic field whose strength is more than the observational lower bound from blazars, 10^{-15}G, at Mpc scale.

3.2.2 Back reaction problem

In the previous subsection, we calculate the produced magnetic field in the model by assuming that inflation continues and the electromagnetic generation does not change regardless of the amount of the electromagnetic fields. But if the energy density of the electromagnetic field ρ_{em} becomes comparable with that of inflaton, inflation itself or the generation of electromagnetic fields must be altered. Thus for the consistency of the above calculation,

$$\rho_{\text{em}} < \rho_{\text{inf}} \tag{3.29}$$

should be satisfied. Unfortunately, however, in the parameter range where the generated magnetic field is enough strong to explain the blazar observation, namely $n \gtrsim 3$, ρ_{em}
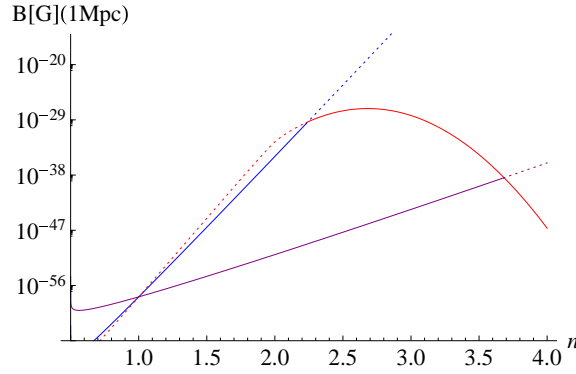
Figure 3.1 : The prediction of $\mathcal{P}_B^{1/2}(k = 1\mathrm{Mpc}^{-1})$ at present and the upper bound on that derived only by the backreaction problem. The blue and purple lines show the prediction, eq. (3.28) with $\rho_{\mathrm{inf}}^{1/4} = 10^{16}\mathrm{GeV}$ and 1GeV, respectively. The red line is the upper bound derived from the combination of eq. (3.28) and eq. (3.31) with $N_{\mathrm{tot}} = 50$. The maximum value is $\mathcal{P}_B^{1/2} \approx 7 \times 10^{-28}\mathrm{G}$ at $n \approx 2.68$.

becomes larger than ρ_{inf} [28]. This problem is called "the back reaction problem". It should be noted that in Ref. [66], the authors have investigated the possibility of the electromagnetic generation by taking into account its back reaction and the dynamics of ϕ. In their case, although the inflation still continues, the generation of the electromagnetic field is altered and fails to produce the magnetic field which is strong enough to explain the blazar observation.

From eq. (3.24), the energy density of electromagnetic field during inflation is given by

$$\rho_{\mathrm{em}}(\eta) \simeq \frac{I^2}{2} \int_{k_{\mathrm{min}}}^{aH} \frac{\mathrm{d}k}{k} \mathcal{P}_E(\eta, k) = \frac{\Gamma^2(n + \frac{1}{2})}{2^{2-2n}\pi^3} H^4 \left[\frac{(-k_{\mathrm{min}}\eta)^{2(2-n)} - 1}{2n - 4} \right], \qquad (3.30)$$

where we ignore the contribution of $\mathcal{P}_B$ and k_{min} is the wave number of the mode which crosses the horizon when $I(\eta)$ starts to behave as $(\eta/\eta_{\mathrm{f}})^n$. Because of $-k_{\mathrm{min}}\eta < 1$, $\rho_{\mathrm{em}}(\eta)$ is an increasing function of η for $n \geq 2$ while the η dependence is negligible for $n < 2$. Thus for $n \geq 2$, it is sufficient to require $\rho_{\mathrm{inf}} > \rho_{\mathrm{em}}(\eta)$ at the end of inflation for its satisfaction over the entire period of inflation. This condition puts the upper limit on ρ_{inf},

$$\frac{\rho_{\mathrm{inf}}}{M_{\mathrm{Pl}}^4} < \frac{2^{2-2n}3^2\pi^3}{\Gamma^2(n + \frac{1}{2})} D_n^{-1}(N_{\mathrm{tot}}) \qquad (n \geq 2), \qquad (3.31)$$

where $N_{\mathrm{tot}} \equiv -\ln|k_{\mathrm{min}}\eta_{\mathrm{f}}|$ and we define a new function D_n for later simplicity,

$$D_n(X) \equiv \frac{e^{(2n-4)X} - 1}{2n - 4}, \qquad \lim_{n \to 2} D_n(X) = X. \qquad (3.32)$$

Substituting eq. (3.31) into eq. (3.28), one can obtain the upper limit of the magnetic

power spectrum at present. For example, the upper limits for $n = 3$ are

$$\mathcal{P}_B^{1/2}(\eta_{\text{now}}, k, n = 3) < 1.8 \times 10^{-28}\text{G} \times \exp\left[50 - N_{\text{tot}}\right]. \tag{3.33}$$

For $n > 3$, the upper bound on $\mathcal{P}_B(\eta_{\text{now}}, k)$ is more stringent. In fig. 3.1, we plot the prediction of and the upper bound on $\mathcal{P}_B^{1/2}(k = 1\text{Mpc}^{-1})$ at present. The allowed maximum value is less than 10^{-27}G and it is far weaker than the observational lower bound. Therefore the kinetic coupling model can not generate the primordial magnetic field with sufficient strength because of the back reaction problem.

3.2.3 Curvature perturbation problem

Since the electromagnetic fields produced during inflation behave as isocurvature perturbations, they can source the adiabatic curvature perturbation on super-Hubble scales. The induced curvature perturbation has distinguishing non-gaussianities which can be large enough for detection [29, 71]. The Planck mission has given precise information about the primordial curvature perturbation and also tighter constraints on the non-linearity parameters which parameterize the non-Gaussian features of the primordial curvature perturbation. These Planck constraints can be translated into the limits on the parameters of the kinetic coupling model and inflation, and also the restrict on inflationary magnetogenesis. In this subsection, we derive the curvature perturbation induced by the electromagnetic fields in the kinetic coupling model during inflation. Then we compute its two-point, three-point, four-point correlators and their related non-linearity parameters. The observational constraints are discussed in the next subsection.

3.2.3.1 Evolution equation of ζ_{em}

The curvature perturbation $\zeta(t, \boldsymbol{x})$ is defined as the perturbation of the local scale factor $a(t, \boldsymbol{x})$ on the uniform density slice, $\zeta(t, \boldsymbol{x}) \equiv \ln\left[a(t, \boldsymbol{x})/a(t)\right]$ where t is the cosmic time. It is well known that the curvature perturbation $\zeta(t, \boldsymbol{x})$ is conserved on super-Hubble scales, if the universe is dominated by a single component. [3] However, when the universe has multiple components, $\zeta_k(t)$ can be amplified even on super-horizon scales. Indeed, the electromagnetic fields produce the curvature perturbation in addition to that generated on sub-Hubble scales. Let us derive the evolution equation of $\zeta(t, \boldsymbol{x})$. The energy continuity equation holds on super-Hubble scales [72],

$$\begin{aligned}
\dot{\rho}(t) &= -3\frac{\dot{a}(t, \boldsymbol{x})}{a(t, \boldsymbol{x})}[\rho(t) + p(t, \boldsymbol{x})] \\
&= -3\left(H(t) + \dot{\zeta}(t, \boldsymbol{x})\right)\left[\rho(t) + p(t) + \delta p_{\text{nad}}(t, \boldsymbol{x})\right],
\end{aligned} \tag{3.34}$$

---

[3]If the universe is dominated by a single component, the right hand side in eq. (3.35) is zero and the curvature perturbation is conserved on super-Hubble scales.

where the non-adiabatic pressure δp_{nad} is defined as $\delta p_{\mathrm{nad}}(t, \boldsymbol{x}) \equiv \delta p(t, \boldsymbol{x}) - \frac{\dot{p}(t)}{\dot{\rho}(t)}\delta\rho(t, \boldsymbol{x})$, in general, while $\delta p_{\mathrm{nad}}(t, \boldsymbol{x}) = \delta p(t, \boldsymbol{x})$ on the uniform density slice. By subtracting the homogeneous part of the above equation, we obtain the evolution equation of the curvature perturbation on super-Hubble scales,

$$\dot{\zeta}(t, \boldsymbol{x}) = -\frac{H(t)\delta p(t, \boldsymbol{x})}{\rho(t) + p(t)} \, . \tag{3.35}$$

In our case where the background energy density is dominated by the inflaton field and the energy density of the electromagnetic field is treated as a perturbation, we have

$$p_{\mathrm{inf}} \simeq -\left(1 - \frac{2}{3}\varepsilon\right)\rho_{\mathrm{inf}}, \quad \delta p = \frac{1}{3}\rho_{\mathrm{em}}, \tag{3.36}$$

where ε is the slow-roll parameter and indices "inf" and "em" denote the contribution from inflaton and electromagnetic fields, respectively. Hence eq. (3.35) reads

$$\dot{\zeta}^{\mathrm{em}}(t, \boldsymbol{x}) = -\frac{2H(t)}{\varepsilon\rho_{\mathrm{inf}}}\rho_{\mathrm{em}}(t, \boldsymbol{x}), \tag{3.37}$$

in the leading order of ε. Integrating it, we obtain the expression of curvature perturbation induced by electromagnetic fields as [30]

$$\zeta^{\mathrm{em}}(t, \boldsymbol{x}) = -\frac{2H}{\varepsilon\rho_{\mathrm{inf}}}\int_{t_0}^{t} dt' \rho_{\mathrm{em}}(t', \boldsymbol{x}), \tag{3.38}$$

where H, ε and ρ_{inf} are assumed to be constant during inflation and t_0 denotes an initial time when $\zeta^{\mathrm{em}}(t_0, \boldsymbol{x}) = 0$. Note that the total amplitude of the curvature perturbation is the sum of ζ^{em} and the intrinsic ζ which is generated on sub-Hubble scales usually by the inflaton perturbation. Let us assume that the electromagnetic fields are originally absent before the generation during inflation and thus all electromagnetic fields exist as perturbations, and hence we have $\rho_{\mathrm{E}} = \frac{1}{2}I^2(\eta)\boldsymbol{E}^2(\eta, \boldsymbol{x})$ and neglect the contribution of the magnetic energy (see the discussion below eq. (3.25)). By performing Fourier transformation of $\boldsymbol{E}(\eta, \boldsymbol{x})$, the electromagnetic energy density is written in the convolution of two Fourier transformed electric fields as

$$\rho_{\mathrm{em}}(\eta, \boldsymbol{k}) \simeq \frac{1}{2}I^2(\eta)\iint \frac{\mathrm{d}^3p\,\mathrm{d}^3q}{(2\pi)^3}\delta(\boldsymbol{p} + \boldsymbol{q} - \boldsymbol{k})\boldsymbol{E}(\eta, \boldsymbol{p}) \cdot \boldsymbol{E}(\eta, \boldsymbol{q}) \, . \tag{3.39}$$

By using eq. (3.18), (3.24), (3.39) and the definition of the electric field, $E_i \equiv a^{-2}\partial_\eta A_i$, eq. (3.38) reads [4]

$$\zeta^{\mathrm{em}}(\eta, \boldsymbol{k}) = \frac{c_n^2 \rho_{\mathrm{inf}}}{9\varepsilon M_{\mathrm{Pl}}^4}\iint_{k_{\min}}^{k_{\max}} \frac{\mathrm{d}^3p\,\mathrm{d}^3q}{(2\pi)^3}\,\delta(\boldsymbol{p} + \boldsymbol{q} - \boldsymbol{k})\,p^{\frac{1}{2}-n}q^{\frac{1}{2}-n}$$

$$\times \sum_{\lambda,\sigma}\varepsilon_i^{(\lambda)}(\hat{\boldsymbol{p}})\,\varepsilon_i^{(\sigma)}(\hat{\boldsymbol{q}})\left(a_{\boldsymbol{p}}^{(\lambda)} + a_{-\boldsymbol{p}}^{\dagger(\lambda)}\right)\left(a_{\boldsymbol{q}}^{(\sigma)} + a_{-\boldsymbol{q}}^{\dagger(\sigma)}\right)\int_{\eta_0}^{\eta}\mathrm{d}\tilde{\eta}\,\tilde{\eta}^{3-2n} \tag{3.40}$$

---

[4] To be precise, the constant phase of the mode function which is neglected in eq. (3.24) should be included in eq. (3.40) like $\left(a_{\boldsymbol{p}}^{(\lambda)}e^{i\xi} + a_{-\boldsymbol{p}}^{\dagger(\lambda)}e^{-i\xi}\right)$ where $e^{i\xi}$ is the constant phase factor. However, since such phase factors vanish after the calculation of the vacuum expectation value, we suppress them.

where the lower end of the time integration, $\eta_0 = -\max[p, q]^{-1}$, represents that only super-horizon modes are considered as physical modes, $k_{\max} = -\eta_f^{-1}$ is the maximum wave number exiting the horizon during inflation and we define c_n as

$$I\partial_\eta A_k(\eta) = c_n \, k^{\frac{1}{2}-n}\eta^{-n}, \quad c_n \equiv \frac{2^n\Gamma(n+\frac{1}{2})}{\sqrt{2\pi}} \,. \tag{3.41}$$

Before closing this sub-subsection, let us note that the anisotropic stress which can also source the curvature perturbation is not taken into account here. However, the contribution from the electromagnetic anisotropic stress is suppressed by slow-roll parameter ε in comparison to the contribution from the non-adiabatic pressure during inflation [30]. Thus eq. (3.38) is the leading order equation.

3.2.3.2 Calculation of 2, 3, 4-point correlators

Let us calculate two, three and four-point correlation function of the curvature perturbation in the Fourier space. At first, we consider m-point correlator,

$$\left\langle \prod_{i=1}^m \zeta^{\mathrm{em}}(\eta, \boldsymbol{k}_i) \right\rangle = \left\langle \prod_{i=1}^m \left(\frac{c_n^2 \rho_{\inf}}{9\varepsilon M_{\mathrm{Pl}}^4} \right) \iint_{k_{\min}}^{k_{\max}} \frac{\mathrm{d}^3 p_i \, \mathrm{d}^3 q_i}{(2\pi)^3} \delta(\boldsymbol{p}_i + \boldsymbol{q}_i - \boldsymbol{k}_i) p_i^{\frac{1}{2}-n} q_i^{\frac{1}{2}-n} \right.$$

$$\left. \times \sum_{\lambda_i, \sigma_i} \varepsilon_{j_i}^{(\lambda_i)}(\hat{\boldsymbol{p}}_i) \varepsilon_{j_i}^{(\sigma_i)}(\hat{\boldsymbol{q}}_i) \left(a_{\boldsymbol{p}_i}^{(\lambda_i)} + a_{-\boldsymbol{p}_i}^{\dagger(\lambda_i)} \right) \left(a_{\boldsymbol{q}_i}^{(\sigma_i)} + a_{-\boldsymbol{q}_i}^{\dagger(\sigma_i)} \right) \int_{\eta_{0,i}}^\eta \mathrm{d}\tilde{\eta}_i \, \tilde{\eta}_i^{3-2n} \right\rangle, \tag{3.42}$$

where the bracket $\langle \cdots \rangle$ denotes the vacuum expectation value and is only relevant to $a_{\boldsymbol{k}}^{(\lambda)}$ and $a_{-\boldsymbol{k}}^{\dagger(\lambda)}$. One can show $\langle m-\mathrm{point} \rangle \equiv \left\langle \prod_{i=1}^m \left(a_{\boldsymbol{p}_i}^{(\lambda_i)} + a_{-\boldsymbol{p}_i}^{\dagger(\lambda_i)} \right) \left(a_{\boldsymbol{q}_i}^{(\sigma_i)} + a_{-\boldsymbol{q}_i}^{\dagger(\sigma_i)} \right) \right\rangle$ is given by

$$\langle 2-\mathrm{point} \rangle = 2(2\pi)^6 \delta(\boldsymbol{p}_1 + \boldsymbol{q}_2)\delta(\boldsymbol{p}_2 + \boldsymbol{q}_1)\delta^{\lambda_1\sigma_2}\delta^{\lambda_2\sigma_1}, \tag{3.43}$$

$$\langle 3-\mathrm{point} \rangle = 8(2\pi)^9 \delta(\boldsymbol{p}_1 + \boldsymbol{q}_2)\delta(\boldsymbol{p}_2 + \boldsymbol{q}_3)\delta(\boldsymbol{p}_3 + \boldsymbol{q}_1)\delta^{\lambda_1\sigma_2}\delta^{\lambda_2\sigma_3}\delta^{\lambda_3\sigma_1}, \tag{3.44}$$

$$\langle 4-\mathrm{point} \rangle = 16 \left\{ (2\pi)^{12} \delta(\boldsymbol{p}_1 + \boldsymbol{q}_2)\delta(\boldsymbol{p}_2 + \boldsymbol{q}_3)\delta(\boldsymbol{p}_3 + \boldsymbol{q}_4)\delta(\boldsymbol{p}_4 + \boldsymbol{q}_1)\delta^{\lambda_1\sigma_2}\delta^{\lambda_2\sigma_3}\delta^{\lambda_3\sigma_4}\delta^{\lambda_4\sigma_1} \right.$$

$$\left. + (2 \leftrightarrow 3) + (3 \leftrightarrow 4) \right\} + (\text{disconnected terms}), \tag{3.45}$$

Since the calculation processes for $m = 2$, 3 and 4 are analogous, we illustrate only the $m = 2$ case in detail. By virtue of the delta function and the Kronecker delta in eq. (3.43), the polarization factor in eq. (3.42) reads

$$\sum_{\lambda_1, \lambda_2} \varepsilon_{j_1}^{(\lambda_1)}(\hat{\boldsymbol{p}}_1) \varepsilon_{j_1}^{(\lambda_2)}(-\hat{\boldsymbol{p}}_2) \varepsilon_{j_2}^{(\lambda_2)}(\hat{\boldsymbol{p}}_2) \varepsilon_{j_2}^{(\lambda_1)}(-\hat{\boldsymbol{p}}_1) = \left(\delta_{j_1 j_2} - (\hat{\boldsymbol{p}}_1)_{j_1}(\hat{\boldsymbol{p}}_1)_{j_2} \right) \left(\delta_{j_1 j_2} - (\hat{\boldsymbol{p}}_2)_{j_1}(\hat{\boldsymbol{p}}_2)_{j_2} \right).$$

$$\tag{3.46}$$

and the $\tilde{\eta}$ integral in eq. (3.42) reads

$$\prod_{i=1}^2 \int_{\eta_0}^\eta \mathrm{d}\tilde{\eta}_i \, \tilde{\eta}_i^{3-2n} = \left[\frac{\eta^{4-2n} - (-\max[p_1, p_2])^{2n-4}}{2n-4} \right]^2. \tag{3.47}$$

Next one can perform the q_i integrals by using $\delta(\boldsymbol{p}_i + \boldsymbol{q}_{i+1})$. In the $m = 2$ case, we obtain

$$
\langle \zeta^{\mathrm{em}}_{\boldsymbol{k}_1} \zeta^{\mathrm{em}}_{\boldsymbol{k}_2}(\eta) \rangle = 2\delta(\boldsymbol{k}_1 + \boldsymbol{k}_2) \left(\frac{c_n^2 \rho_{\mathrm{inf}}}{9\varepsilon M_{\mathrm{Pl}}^4} \right)^2 \iint_{k_{\mathrm{min}}}^{k_{\mathrm{max}}} \mathrm{d}^3 p_1 \mathrm{d}^3 p_2 \, \delta(\boldsymbol{p}_2 - \boldsymbol{p}_1 - \boldsymbol{k}_2) \, p_1^{1-2n} p_2^{1-2n}
$$
$$
\times \left(\delta_{j_1 j_2} - (\hat{\boldsymbol{p}}_1)_{j_1} (\hat{\boldsymbol{p}}_1)_{j_2} \right) \left(\delta_{j_1 j_2} - (\hat{\boldsymbol{p}}_2)_{j_1} (\hat{\boldsymbol{p}}_2)_{j_2} \right) \left[\frac{\eta^{4-2n} - (-\max[p_1, p_2])^{2n-4}}{2n - 4} \right]^2 . \quad (3.48)
$$

If $n \geq 2$, the biggest contributions of the integrals in eq. (3.48) come from the lower limit of the integration, namely $p_1 \simeq k_{\mathrm{min}}$ and $p_2 \simeq k_{\mathrm{min}}$, which we call "the pole contribution" following ref. [29]. Hereafter we concentrate on the cases where $n \geq 2$. Then eq. (3.48) can be evaluated by the pole contributions. Note the integrand has the symmetry of $\boldsymbol{p}_1 \leftrightarrow \boldsymbol{p}_2$. Even in the case of $m = 3$ and 4, the cyclic symmetry like, $\boldsymbol{p}_1 \to \boldsymbol{p}_2 \to \cdots \to \boldsymbol{p}_m \to \boldsymbol{p}_1$, exists. Thus if the p_1 pole is evaluated, the other contributions can be easily duplicated. The p_1 pole contribution in eq. (3.48) is evaluated as

$$
\langle \zeta^{\mathrm{em}}_{\boldsymbol{k}_1} \zeta^{\mathrm{em}}_{\boldsymbol{k}_2}(\eta) \rangle \big|_{p_1 \simeq k_{\mathrm{min}}} = \frac{32\pi}{3 \, k_1^3} \delta(\boldsymbol{k}_1 + \boldsymbol{k}_2) \left(\frac{c_n^2 \rho_{\mathrm{inf}}}{9\varepsilon M_{\mathrm{Pl}}^4} \right)^2 \left[\frac{(k_1/k_{\mathrm{min}})^{2n-4} - 1}{2n - 4} \right] \left[\frac{(-k_1\eta)^{4-2n} - 1}{2n - 4} \right]^2 ,
$$
$$(3.49)$$

where we use the angular integral, $\int \mathrm{d}\Omega_k \hat{k}_i \hat{k}_j = \frac{4\pi}{3} \delta_{ij}$, and assume $k_1 = k_2 \gg k_{\mathrm{min}}$. [5] Notice additional factors like $(\max[k_1, k_3]/\min[k_1, k_3])^{2n-4} \geq 1$ appear in the case of $m = 3$ and 4. Nevertheless, we conservatively ignore those factors for simplicity by assuming all reference wave numbers are close to the CMB scale, $k_i \sim k_{\mathrm{CMB}}$. Except for this point, the calculations of $m = 3, 4$ case are closely analogous to $m = 2$ case. Therefore we obtain 2, 3 and 4-point connected correlation function of the electromagnetic induced curvature perturbation at the end of inflation η_{f} as

$$
\langle \zeta^{\mathrm{em}}_{\boldsymbol{k}_1} \zeta^{\mathrm{em}}_{\boldsymbol{k}_2}(\eta_{\mathrm{f}}) \rangle = \frac{64\pi}{3 k_1^3} \delta(\boldsymbol{k}_1 + \boldsymbol{k}_2) \left(\frac{c_n^2 \rho_{\mathrm{inf}}}{9\varepsilon M_{\mathrm{Pl}}^4} \right)^2 D_n(N_{\mathrm{tot}} - N_{\mathrm{CMB}}) D_n(N_{\mathrm{CMB}})^2 , \quad (3.50)
$$

$$
\langle \zeta^{\mathrm{em}}_{\boldsymbol{k}_1} \zeta^{\mathrm{em}}_{\boldsymbol{k}_2} \zeta^{\mathrm{em}}_{\boldsymbol{k}_3}(\eta_{\mathrm{f}}) \rangle = \frac{64\pi}{3} \delta(\boldsymbol{k}_1 + \boldsymbol{k}_2 + \boldsymbol{k}_3) \left(\frac{c_n^2 \rho_{\mathrm{inf}}}{9\varepsilon M_{\mathrm{Pl}}^4} \right)^3 D_n(N_{\mathrm{tot}} - N_{\mathrm{CMB}}) D_n(N_{\mathrm{CMB}})^3
$$
$$
\times \left[\frac{1 + (\hat{\boldsymbol{k}}_1 \cdot \hat{\boldsymbol{k}}_2)^2}{(k_1 k_2)^3} + 2 \text{ perms} \right] , \quad (3.51)
$$

$$
\langle \zeta^{\mathrm{em}}_{\boldsymbol{k}_1} \zeta^{\mathrm{em}}_{\boldsymbol{k}_2} \zeta^{\mathrm{em}}_{\boldsymbol{k}_3} \zeta^{\mathrm{em}}_{\boldsymbol{k}_4}(\eta_{\mathrm{f}}) \rangle = \frac{128\pi}{3} \delta(\boldsymbol{k}_1 + \boldsymbol{k}_2 + \boldsymbol{k}_3 + \boldsymbol{k}_4) \left(\frac{c_n^2 \rho_{\mathrm{inf}}}{9\varepsilon M_{\mathrm{Pl}}^4} \right)^4 D_n(N_{\mathrm{tot}} - N_{\mathrm{CMB}}) D_n(N_{\mathrm{CMB}})^4
$$
$$
\times \left[\frac{(\hat{\boldsymbol{k}}_1 \cdot \hat{\boldsymbol{k}}_2)^2 + (\hat{\boldsymbol{k}}_1 \cdot \hat{\boldsymbol{k}}_{13})^2 + (\hat{\boldsymbol{k}}_2 \cdot \hat{\boldsymbol{k}}_{13})^2 - (\hat{\boldsymbol{k}}_1 \cdot \hat{\boldsymbol{k}}_2)(\hat{\boldsymbol{k}}_1 \cdot \hat{\boldsymbol{k}}_{13})(\hat{\boldsymbol{k}}_2 \cdot \hat{\boldsymbol{k}}_{13})}{(k_1 k_2 k_{13})^3} + 11 \text{ perms} \right] ,
$$
$$(3.52)$$

---

[5] The assumption of $k_{\mathrm{CMB}} \gg k_{\mathrm{min}}$ which corresponds to $N_{\mathrm{CMB}} < N_{\mathrm{tot}}$ means the generation of electromagnetic fields begins much *earlier* than the horizon-crossing of CMB modes. Although it may be interesting to consider the case where it begins *after* the CMB scale horizon-crossing, we focus on the former case here.

where $\boldsymbol{k}_{13} \equiv \boldsymbol{k}_1 + \boldsymbol{k}_3$, $D_n(X) \equiv (e^{(2n-4)X} - 1)/(2n - 4)$, $e^{-N_{\mathrm{CMB}}} = -k_{\mathrm{CMB}}\eta_{\mathrm{f}}$ and $e^{N_{\mathrm{tot}}-N_{\mathrm{CMB}}} = k_{\mathrm{CMB}}/k_{\mathrm{min}}$. In the limit of $n \to 2$, these results coincide with the previous works [29, 71].

When $n < 2$, the correlators of induced ζ can not be computed in the same way as eq. (3.49) because there is no pole. Then we have to calculate the correlators by brute force. But if n is not too close to 2, the results are expected to depend on neither N_{tot} nor N_{CMB}. It is because the contribution to the electric energy density from the k mode, $I^2\mathcal{P}_E(\eta, k)$, rapidly decreases on the super-horizon as $\eta^{2(2-n)}$ (see eq. (3.27)) and its contribution to generate ζ is effective only for a short interval right after its horizon-crossing. Therefore the resultant correlators are much weaker than those in $n \geq 2$ case and the motivation to constrain them is inadequate. Thus we concentrate on the cases where $n \geq 2$, hereafter.

3.2.3.3 Power spectrum and Non-gaussianities

Let us connect 2,3,4-point correlators to the observable quantities in order to compare them with the CMB observation results. Here relevant observable quantities are the power spectrum of the primordial curvature perturbations $\mathcal{P}_\zeta$, and local-type non-linearity parameters $f_{\mathrm{NL}}^{\mathrm{local}}$ and τ_{NL} which parameterize the amplitudes of the 3- and 4-point functions of the curvature perturbations in Fourier space, respectively. These are defined as

$$\langle \zeta_{\boldsymbol{k}_1} \zeta_{\boldsymbol{k}_2} \rangle = (2\pi)^3 \delta(\boldsymbol{k}_1 + \boldsymbol{k}_2) \frac{2\pi^2}{k_1^3} \mathcal{P}_\zeta \,, \tag{3.53}$$

$$\langle \zeta_{\boldsymbol{k}_1} \zeta_{\boldsymbol{k}_2} \zeta_{\boldsymbol{k}_3} \rangle = (2\pi)^3 \delta(\boldsymbol{k}_1 + \boldsymbol{k}_2 + \boldsymbol{k}_3) \, (2\pi^2 \, \mathcal{P}_\zeta)^2 \, \frac{6}{5} f_{\mathrm{NL}}^{\mathrm{local}} \frac{\sum_{i=1}^{3} k_i^3}{\prod_{i=1}^{3} k_i^3} \,, \tag{3.54}$$

$$\langle \zeta_{\boldsymbol{k}_1} \zeta_{\boldsymbol{k}_2} \zeta_{\boldsymbol{k}_3} \zeta_{\boldsymbol{k}_4} \rangle = (2\pi)^3 \delta(\boldsymbol{k}_1 + \boldsymbol{k}_2 + \boldsymbol{k}_3 + \boldsymbol{k}_4) \, (2\pi^2 \mathcal{P}_\zeta)^3 \, \tau_{\mathrm{NL}}$$
$$\times \left[\frac{1}{(k_1 k_2 k_{13})^3} + 11 \text{ perms} \right], \tag{3.55}$$

where the small deviation from scale invariant spectrum of $\mathcal{P}_\zeta$ is neglected. By substituting eq. (3.50) into eq. (3.53), one can easily obtain the induced power spectrum as

$$\mathcal{P}_\zeta^{\mathrm{em}}(k, \eta_{\mathrm{f}}) = \frac{4}{3} \left(\frac{c_n^2 \rho_{\mathrm{inf}}}{9\pi^2 \varepsilon M_{\mathrm{Pl}}^4} \right)^2 D_n(N_{\mathrm{tot}} - N_{\mathrm{CMB}}) D_n^2(N_{\mathrm{CMB}}). \tag{3.56}$$

As for $f_{\mathrm{NL}}^{\mathrm{local}}$ and τ_{NL}, however, k_i dependence of eq. (3.51) and (3.52) is different from that of eq. (3.54) and (3.55), respectively. Thus they can not be compared straightforwardly [6]. But when eq. (3.51) and (3.52) are averaged over the direction of $\hat{\boldsymbol{k}}_i$, their k_i dependence

---

[6] Planck team also investigated the bispectrum which has such non-trivial k_i dependences [31]. In order to parameterize the angular dependence of the bispectrum they introduced the Legendre Polynomial expansion [71], and they obtained the constraint on each coefficient of the expansion. The result seems to be almost comparable to the constraint on $f_{\mathrm{NL}}^{\mathrm{local}}$ and hence for simplicity we apply $f_{\mathrm{NL}}^{\mathrm{local}}$ constraint to our result.

accord with that of eq. (3.54) and (3.55), respectively. [7] Further discussion on the validity of this averaging can be found in ref. [29]. After angular averaged, eq. (3.51) and (3.52) read

$$\langle \zeta^{\rm em}_{\boldsymbol{k}_1} \zeta^{\rm em}_{\boldsymbol{k}_2} \zeta^{\rm em}_{\boldsymbol{k}_3}(\eta_{\rm f}) \rangle_{\rm ave} = \frac{2^8 \pi}{3^2} \delta(\boldsymbol{k}_1 + \boldsymbol{k}_2 + \boldsymbol{k}_3) \left(\frac{c_n^2 \rho_{\rm inf}}{9\varepsilon M_{\rm Pl}^4} \right)^3 D_n(N_{\rm tot} - N_{\rm CMB}) D_n^3(N_{\rm CMB}) \frac{\sum_{i=1}^3 k_i^3}{\prod_{i=1}^3 k_i^3}$$
(3.57)

$$\langle \zeta^{\rm em}_{\boldsymbol{k}_1} \zeta^{\rm em}_{\boldsymbol{k}_2} \zeta^{\rm em}_{\boldsymbol{k}_3} \zeta^{\rm em}_{\boldsymbol{k}_4}(\eta_{\rm f}) \rangle_{\rm ave} = \frac{2^7 \pi}{3} \delta(\boldsymbol{k}_1 + \boldsymbol{k}_2 + \boldsymbol{k}_3 + \boldsymbol{k}_4) \left(\frac{c_n^2 \rho_{\rm inf}}{9\varepsilon M_{\rm Pl}^4} \right)^4 D_n(N_{\rm tot} - N_{\rm CMB}) D_n^4(N_{\rm CMB})$$
$$\times \left[\frac{1}{(k_1 k_2 k_{13})^3} + 11 \text{ perms} \right].$$
(3.58)

Therefore we obtain electromagnetic induced local-type non-gaussianities

$$f_{\rm NL}^{\rm em} = \frac{2^2 5}{3^3} \left(\frac{c_n^2 \rho_{\rm inf}}{9\pi^2 \varepsilon M_{\rm Pl}^4} \right)^3 \mathcal{P}_\zeta^{-2} D_n(N_{\rm tot} - N_{\rm CMB}) D_n^3(N_{\rm CMB}),$$
(3.59)

$$\tau_{\rm NL}^{\rm em} = \frac{2}{3} \left(\frac{c_n^2 \rho_{\rm inf}}{9\pi^2 \varepsilon M_{\rm Pl}^4} \right)^4 \mathcal{P}_\zeta^{-3} D_n(N_{\rm tot} - N_{\rm CMB}) D_n^4(N_{\rm CMB}),$$
(3.60)

where $f_{\rm NL}^{\rm em}$ and $\tau_{\rm NL}^{\rm em}$ are $f_{\rm NL}^{\rm local}$ and $\tau_{\rm NL}$ which are induced by the electromagnetic fields, respectively. Note our three results can be written in the similar form as

$$\mathcal{P}_\zeta^{\rm em} \simeq D_n(N_{\rm tot} - N_{\rm CMB}) \, G_n^2,$$
(3.61)

$$f_{\rm NL}^{\rm em} \mathcal{P}_\zeta^2 \simeq D_n(N_{\rm tot} - N_{\rm CMB}) \, G_n^3,$$
(3.62)

$$\tau_{\rm NL}^{\rm em} \mathcal{P}_\zeta^3 \simeq D_n(N_{\rm tot} - N_{\rm CMB}) \, G_n^4,$$
(3.63)

where $G_n \equiv c_n^2 \rho_{\rm inf} D_n(N_{\rm CMB})/9\pi^2 \varepsilon M_{\rm Pl}^4$ and $\mathcal{O}(1)$ numerical factors are dropped. Then we obtain the general relationship between $f_{\rm NL}^{\rm em}$ and $\tau_{\rm NL}^{\rm em}$ in the kinetic coupling model of $n \geq 2$,

$$\tau_{\rm NL}^{\rm em} \simeq [\mathcal{P}_\zeta D_n(N_{\rm tot} - N_{\rm CMB})]^{-\frac{1}{3}} f_{\rm NL}^{{\rm em} \frac{4}{3}}.$$
(3.64)

Therefore even if $f_{\rm NL} \sim \mathcal{O}(1)$, the kinetic coupling model can produce a large $\tau_{\rm NL}$.

3.2.4 Observational constraints

In this subsection, in the light of the back reaction problem and the curvature perturbation induced by the produced electric field, we translate the Planck constraints on $\mathcal{P}_\zeta$,

---

[7]Taking angular average, one can show $(\hat{\boldsymbol{k}}_1 \cdot \hat{\boldsymbol{k}}_2)^2$ yields $1/3$ if these two unit vectors are independent. But for example, the averaged value of $(\hat{\boldsymbol{k}}_1 \cdot \hat{\boldsymbol{k}}_{13})^2$ depends on k_1 and k_3. In the limit of $k_1 = k_3$, which is the squeezed limit where the terms with $\boldsymbol{k}_{13}$ become most important, the averaged $(\hat{\boldsymbol{k}}_1 \cdot \hat{\boldsymbol{k}}_{13})^2$ is $1/2$ and averaged $(\hat{\boldsymbol{k}}_1 \cdot \hat{\boldsymbol{k}}_2)(\hat{\boldsymbol{k}}_1 \cdot \hat{\boldsymbol{k}}_{13})(\hat{\boldsymbol{k}}_2 \cdot \hat{\boldsymbol{k}}_{13})$ is $1/6$. Thus we approximate the angular averaged value of the product of vectors depending each other by that in the relevant squeezed limit.

$f_{\rm NL}^{\rm local}$ and $\tau_{\rm NL}$ [4, 31] into the constraints on the model parameters of kinetic coupling model. The following results are computed in ref. [32]. Planck collaboration reports:

$$\mathcal{P}_\zeta(k_{\rm CMB}) \approx 2.2 \times 10^{-9}\,, \tag{3.65}$$

$$f_{\rm NL}^{\rm local} \leq f_{\rm NL}^{\rm obs} \equiv 14.3 \quad (95\%\text{CL})\,, \tag{3.66}$$

$$\tau_{\rm NL} \leq \tau_{\rm NL}^{\rm obs} \equiv 2800 \quad (95\%\text{CL})\,. \tag{3.67}$$

The expressions of these observable quantities predicted in the kinetic coupling model, namely eq. (3.56), (3.59) and (3.60), include four unknown parameters $n, \varepsilon, N_{\rm tot}$ and $\rho_{\rm inf}$. Therefore, when three parameters out of four are fixed, the other one can be constrained by the observation. Note that $N_{\rm CMB}$ can be estimated as

$$N_{\rm CMB} \simeq 62 + \ln\left(\frac{\rho_{\rm inf}^{1/4}}{10^{16}\text{GeV}}\right)\,, \tag{3.68}$$

where the instantaneous reheating is assumed for simplicity. In addition, if one assume the dominant component of the power spectrum of the curvature perturbation is generated by a single slow-rolling inflaton, the curvature perturbation, $\mathcal{P}_\zeta$, is given by

$$\mathcal{P}_\zeta^{\rm inf} \equiv \frac{\rho_{\rm inf}}{24\pi^2 \varepsilon M_{\rm Pl}^4}\,, \tag{3.69}$$

and then ε can be determined by $\rho_{\rm inf}$ under eq. (3.65). However, this assumption is not mandatory because the dominant component of the curvature perturbation can be generated by the other mechanism like curvaton or modulated reheating[8]. Let us call the $\mathcal{P}_\zeta = \mathcal{P}_\zeta^{\rm inf}$ case "inflaton" case while the conservative case where $\mathcal{P}_\zeta = \mathcal{P}_\zeta^{\rm inf}$ is not assumed is called "curvaton" case although we do not specify the generation mechanism of $\mathcal{P}_\zeta$ as curvaton or any other models.

3.2.4.1 Constraint on $N_{\rm tot} - N_{\rm CMB}$

First, let us discuss the constraint on $N_{\rm tot} - N_{\rm CMB}$ with changing the parameter n. Since we assume $N_{\rm tot} > N_{\rm CMB}$ in the derivation of eq. (3.56), (3.59) and (3.60), we only consider the positive value of $N_{\rm tot} - N_{\rm CMB}$ for consistency. Combined with the restriction that $\mathcal{P}_\zeta^{\rm em}, f_{\rm NL}^{\rm local}$ and $\tau_{\rm NL}^{\rm em}$ can not exceed the observed value or upper limits, eq. (3.31), (3.56),

---

[8] Here, we neglect the non-Gaussianity generated in the curvaton or modulated reheating scenario.
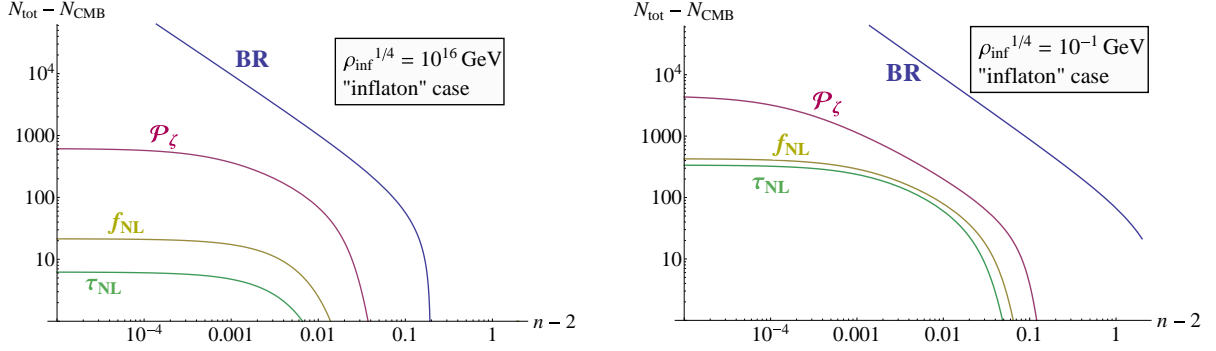
Figure 3.2 : The upper limit of $N_{\text{tot}} - N_{\text{CMB}}$ for $n \geq 2$ when inflaton generates the observed curvature perturbation. The horizontal axis is $n - 2$ and the vertical axis is $N_{\text{tot}} - N_{\text{CMB}}$. The inflation energy scale is set as $\rho_{\text{inf}}^{1/4} = 10^{16}\text{GeV}$ (left panel) or 10^{-1}GeV (right panel). The blue line denotes the upper limit of $N_{\text{tot}} - N_{\text{CMB}}$ coming from the back reaction condition, $\rho_{\text{inf}} > \rho_{\text{em}}$, while the red, yellow and green lines represent the upper limit from the induced $\mathcal{P}_\zeta$, f_{NL} and τ_{NL} from the electromagnetic field respectively. In both panels, one can see that the smaller the N_{tot} or $n - 2$ is, the milder the constraints are.

(3.59) and (3.60) can be rewritten as

$$\text{BR}: \qquad N_{\text{tot}} - N_{\text{CMB}} < \frac{1}{2n-4} \ln\left[1 + (n-2)\left(\frac{6\pi}{c_n}\right)^2 \frac{M_{\text{Pl}}^4}{\rho_{\text{inf}}}\right] - N_{\text{CMB}}, \qquad (3.70)$$

$$\mathcal{P}_\zeta: \qquad N_{\text{tot}} - N_{\text{CMB}} \leq \frac{1}{2n-4} \ln\left[1 + (n-2)\frac{3}{2}\,\mathcal{P}_\zeta\,G_n^{-2}\right], \qquad (3.71)$$

$$f_{\text{NL}}^{\text{local}}: \qquad N_{\text{tot}} - N_{\text{CMB}} \leq \frac{1}{2n-4} \ln\left[1 + (n-2)\frac{27}{10}\,f_{\text{NL}}^{\text{obs}}\,\mathcal{P}_\zeta^2\,G_n^{-3}\right], \qquad (3.72)$$

$$\tau_{\text{NL}}: \qquad N_{\text{tot}} - N_{\text{CMB}} \leq \frac{1}{2n-4} \ln\left[1 + (n-2)\frac{27}{8}\,\tau_{\text{NL}}^{\text{obs}}\,\mathcal{P}_\zeta^3\,G_n^{-4}\right], \qquad (3.73)$$

where $G_n = \frac{8}{3}c_n^2 \mathcal{P}_{\text{inf}} D_n(N_{\text{CMB}})$ by using eq. (3.69) and "BR" denotes the constraint from the back reaction problem.

In fig. 3.2, we plot the upper limit on $N_{\text{tot}} - N_{\text{CMB}}$ of the "inflaton" case with changing n. From these figures, we find that the constraint becomes more stringent as n becomes larger. It is because the generated electric field becomes stronger for larger $n > 2$ (see eq. (3.27)) and thus the induced curvature perturbation is amplified. Aside from the back reaction constraint eq. (3.70), the upper limit from m-point correlator contains the factor $\left(\frac{8}{3}c_n D_n(N_{\text{CMB}})\right)^{-m}$ in the argument of logarithm. In case with $n = 2$, it reads

$$\left(\frac{8}{3}c_n D_n(N_{\text{CMB}})\right)^{-m} \xrightarrow{n\to 2} \left(600\left(\frac{N_{\text{CMB}}}{50}\right)\right)^{-m} \qquad (m = 2, 3, 4) \qquad (3.74)$$

and it is even smaller for $n > 2$. Because of this factor, the higher m is, the more stringent the constraint is. This behavior can be seen in fig. 3.2 as the fact that the constraint of
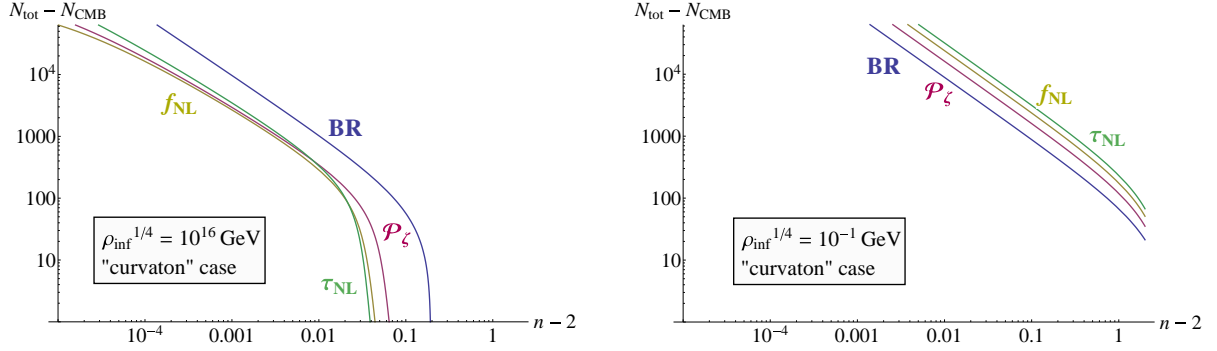
Figure 3.3 : The upper limit of $N_{\rm tot} - N_{\rm CMB}$ for $n \geq 2$ when the assumption that inflaton generates the observed curvature perturbation is relaxed. The horizontal axis is $n-2$ and the vertical axis is $N_{\rm tot} - N_{\rm CMB}$. The inflation energy scale and slow-roll parameter are set as $\rho_{\rm inf}^{1/4} = 10^{16}$GeV (left panel) or 10^{-1}GeV (right panel) and $\varepsilon = 10^{-2}$, respectively. The blue line denotes the upper limit of $N_{\rm tot} - N_{\rm CMB}$ coming from the back reaction condition, $\rho_{\rm inf} > \rho_{\rm em}$, while the red, yellow and green line represent the upper limit from the induced $\mathcal{P}_\zeta$, $f_{\rm NL}$ and $\tau_{\rm NL}$ from the electromagnetic field respectively. The back reaction constraint is unchanged from the "inflaton" case since it does not depend on ε. But one can see the other three constraints are much milder than those in fig.3.2.

$\tau_{\rm NL}$ is the tightest in the left panel. Since low $\rho_{\rm inf}$ corresponds to low $N_{\rm CMB}$ as shown in eq. (3.68), the hierarchies among the constraints derived from $\mathcal{P}_\zeta$, $f_{\rm NL}$ and $\tau_{\rm NL}$ are less significant as can be seen in the right panel of fig. 3.2 where we plot the upper limit of $N_{\rm tot} - N_{\rm CMB}$ for $\rho_{\rm inf}^{1/4} = 10^{-1}$GeV case. For $n = 2$ case, the upper limit from $\tau_{\rm NL}$ can be obtained from eq. (3.73) as

$$N_{\rm tot} - N_{\rm CMB} \;\lesssim\; 17 \times \left(\frac{N_{\rm CMB}}{50}\right)^{-4} \left(\frac{\tau_{\rm NL}^{\rm obs}}{2800}\right), \quad (n = 2, \text{ "inflaton" case}). \qquad (3.75)$$

In fig. 3.3, we plot the upper limit on $N_{\rm tot} - N_{\rm CMB}$ of the "curvaton" case by setting $\varepsilon = 10^{-2}$. In this figure, one can see that the constraint is considerably milder than the "inflaton" case. It is interesting to note that the hierarchy among the four constraint is inverted in the low $\rho_{\rm inf}$ plot (right panel). In fact, the upper bound from the back reaction problem is most stringent for $\rho_{\rm inf}^{1/4} \lesssim 10^{15}$GeV. Except for eq. (3.70), the upper limit from m-point correlator contains the factor $\mathcal{P}_\zeta^{m-1}/\mathcal{P}_{\rm inf}^m$ in the argument of logarithm. Although it reads $\mathcal{P}_\zeta^{-1}$ in the "inflaton" case, in the "curvaton" case it yields an extra factor,

$$\left(\frac{\mathcal{P}_\zeta}{\mathcal{P}_{\rm inf}}\right)^m \simeq \left(18 \times \left(\frac{\varepsilon}{0.01}\right) \left(\frac{(10^{16}\text{GeV})^4}{\rho_{\rm inf}}\right)\right)^m \qquad (m = 2, 3, 4). \qquad (3.76)$$

Therefore the constraints from higher correlator substantially relaxed especially in low $\rho_{\rm inf}$ region. At $\rho_{\rm inf}^{1/4} \simeq 10^{16}$GeV, this factor compensates the factor of eq. (3.74) and three constraints from $\mathcal{P}_\zeta$, $f_{\rm NL}$ and $\tau_{\rm NL}$ are almost degenerate (see the left panel). They are

coincident with the back reaction constraint at $\rho_{\mathrm{inf}}^{1/4} \simeq 10^{15}\mathrm{GeV}$. Thus the back reaction bound is the most stringent for $\rho_{\mathrm{inf}}^{1/4} \lesssim 10^{15}\mathrm{GeV}$.

One can understand why the "curvaton" case with $\varepsilon = 10^{-2}$ gives much milder bound than the "inflaton" case as follows. From eq. (3.61)-(3.63), one can find $\mathcal{P}_{\zeta}^{\mathrm{em}}$, $f_{\mathrm{NL}}^{\mathrm{em}}$ and $\tau_{\mathrm{NL}}^{\mathrm{em}}$ are increasing function of ρ_{inf} and decreasing function of ε. Thus one way of relaxing the upper limit is to increase ε. However ε can not vary freely in the "inflaton" case because the COBE normalization requires ε at the horizon crossing of the CMB scale modes to be as small as

$$\varepsilon = 5.5 \times 10^{-4} \left(\frac{\rho_{\mathrm{inf}}}{(10^{16}\mathrm{GeV})^4} \right). \tag{3.77}$$

Therefore the "curvaton" case does not always put milder constraint than the "inflaton" case but it does only when ε is larger than eq. (3.77).

3.2.4.2 Constraint on the inflation energy scale ρ_{inf}

If we change the set of input parameters from $\{n, \varepsilon, \rho_{\mathrm{inf}}\}$ into $\{n, \varepsilon, N_{\mathrm{tot}}\}$, we can constrain ρ_{inf} instead of $N_{\mathrm{tot}} - N_{\mathrm{CMB}}$. Although eq. (3.31) gives the upper limit of ρ_{inf} explicitly, we have to numerically calculate the bounds from $\mathcal{P}_{\zeta}$, f_{NL} and τ_{NL}. Provided that $N_{\mathrm{tot}} > \frac{3}{2}N_{\mathrm{CMB}}$, one can show that the constraints from $\mathcal{P}_{\zeta}$, f_{NL} and τ_{NL} give upper limits on ρ_{inf}.[9] Thus we adopt $N_{\mathrm{tot}} = 100, 300$ and 1000 as the fiducial values. Note the energy scale of inflation is naively restricted by the indirect observation of gravitational wave and the big bang nucleosynthesis as

$$10^{-1}\mathrm{GeV} \lesssim \rho_{\mathrm{inf}}^{1/4} \lesssim 10^{16}\mathrm{GeV}, \tag{3.78}$$

regardless of the kinetic coupling model.

In fig. 3.4, we plot the upper limits on $\rho_{\mathrm{inf}}^{1/4}$. The basic property of the constraint is unchanged from that on $N_{\mathrm{tot}} - N_{\mathrm{CMB}}$ because the origin of constraints is same. Again, one can see that the larger n is, the tighter the constraints are. τ_{NL} gives the most stringent bound in the "inflaton" case while the bound from the back reaction problem is the tightest in low energy region of the "curvaton" case. In addition, now it is clear that the lower ρ_{inf} is, the milder the constraints are. It is remarkable that $N_{\mathrm{tot}} \gtrsim 300$ is excluded in the "inflaton" case. It is consistent with the right panel of fig. 3.2. Even if $N_{\mathrm{tot}} < 300$, n and ρ_{inf} are severely restricted in the "inflaton" case. On the other hand, the constraints in the "curvaton" case are much more moderate. Especially ρ_{inf} is free from a new restriction if n is sufficiently small. Furthermore, at low energy region, the tightest constraint is given by the back reaction condition whose analytic formula is available. Since in the right hand side of eq. (3.31) the most important factor is $\exp[(2n-4)N_{\mathrm{tot}}]$,

---

[9] One can find the condition when $\mathcal{P}_{\zeta}^{\mathrm{em}}$, $f_{\mathrm{NL}}^{\mathrm{em}}$ and $\tau_{\mathrm{NL}}^{\mathrm{em}}$ are increasing function of ρ_{inf} by differentiating them with respect to ρ_{inf} and looking at their sign. It can be shown the conditions are $N_{\mathrm{tot}} > \frac{m+1}{m}N_{\mathrm{CMB}}, (m = 2, 3, 4)$ in the "inflaton" case while the conditions are far milder in the "curvaton" case.
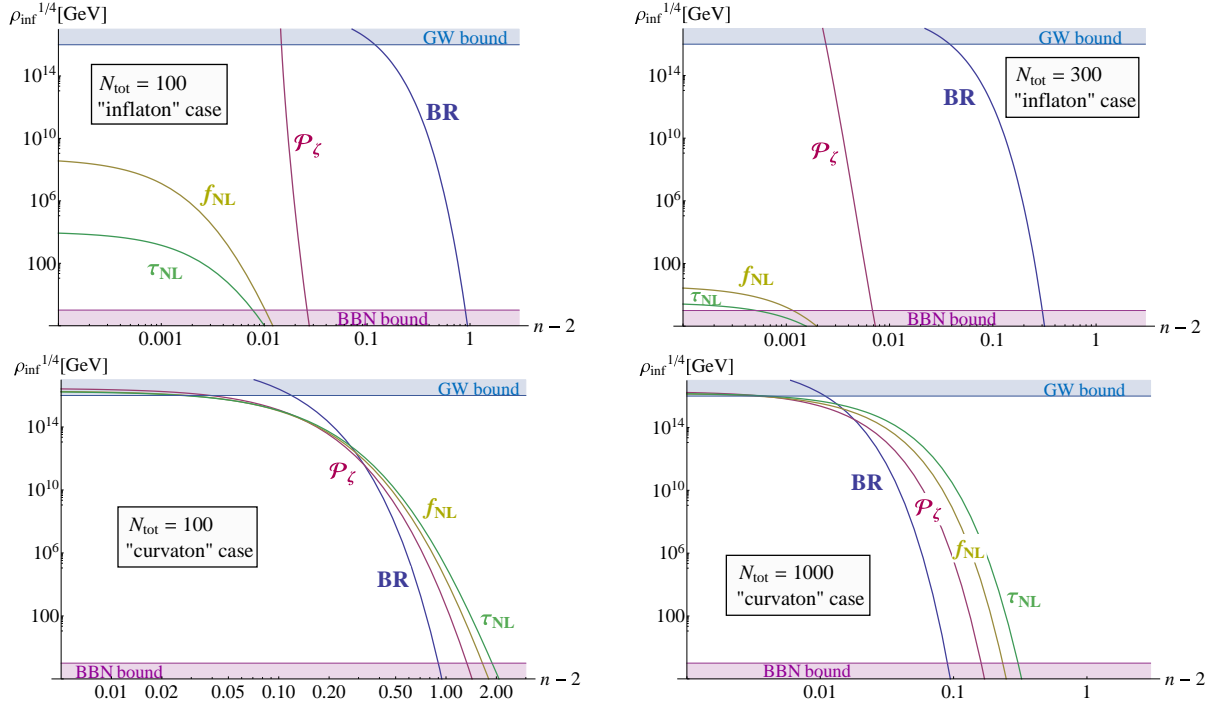
Figure 3.4 : The upper limit of $\rho_{\rm inf}^{1/4}$ for $n \geq 2$. The horizontal axis is $n-2$ and the vertical axis is $\rho_{\rm inf}^{1/4}$ [GeV]. In top two panels it is assumed that inflaton generates all observed curvature perturbation ("inflaton" case) while that assumption is relaxed and instead $\varepsilon = 10^{-2}$ is adopted in the bottom two panels ("curvaton" case). The total duration of the electromagnetic field generation is set as $N_{\rm tot} = 100$ (left panels), 300 (top right panel) or 1000 (bottom right panel). The shaded regions represent the restriction from gravitational wave (blue) and big bang nucleosynthesis (red), respectively.

eq. (3.31) can be approximated by $n - 2 \lesssim \ln(M_{\rm Pl}^4/\rho_{\rm inf})/2N_{\rm tot}$. Then the largest allowed n at $\rho_{\rm inf}^{1/4} = 10^{-1}{\rm GeV}$ is

$$n - 2 \; \lesssim \; \frac{90}{N_{\rm tot}}, \qquad (\text{``curvaton'' case}). \tag{3.79}$$

Since $N_{\rm CMB}$ is as small as ≈ 23 at such low energy scale, n can be larger than 4 in principle. However, the resultant magnetic field strength at present is depends on $\rho_{\rm inf}$ as $\mathcal{P}_B \propto \rho_{\rm inf}^{(n-1)/4}$ and thus a large n does not necessarily lead to a strong magnetic field.

3.2.4.3 Constraint on the strength of the magnetic field B

In terms of magnetogenesis, it is interesting to put the upper limit on the present strength of the magnetic field, $\mathcal{P}_B(\eta_{\rm now}, k)$. Combined with eq. (3.28), the upper limits on $\rho_{\rm inf}$ which we obtain in the previous sub-subsection by numerical calculations can be converted into the upper limits on $\mathcal{P}_B(\eta_{\rm now}, k)$. Those limits are shown in fig. 3.5.

It is known that the strength of magnetic field generated is kinetic coupling model has been already bounded above due to the back reaction problem and its present value can not exceed $10^{-32}{\rm G}$ for $N_{\rm tot} = 70$ and $k = 1{\rm Mpc}^{-1}$ [28]. But it turns out that the upper limit is $10^{-47}{\rm G}$ due to the constraint from $\tau_{\rm NL}$ in the "inflaton" case (see the top left panel of fig. 3.5). If $N_{\rm tot}$ is larger, the constraint becomes even severer. On the other hand, in the "curvaton" case, the strongest value of magnetic field in the allowed region is smaller by only a few orders of magnitude than that without the curvature perturbation constraints.

3.2.4.4 Summary of constraints

The kinetic coupling model (or IFF model) has drawn attention as both a magnetogenesis model and a generation mechanism of the curvature perturbation and non-gaussianities. Although it is known that the back reaction problem (BR) and the strong coupling problem restrict this model from generating the magnetic field which is strong enough to explain the blazar observation at present, the constraints from the curvature perturbation induced by the electromagnetic fields during inflation are not yet investigated adequately.

In this subsection, we compute the curvature power spectrum $\mathcal{P}_\zeta$ and non-linear parameters $f_{\rm NL}^{\rm local}, \tau_{\rm NL}$ of the curvature perturbation induced by the electromagnetic fields in the kinetic coupling model with $I \propto a^{-n}$ for $n \geq 2$. Recently $\mathcal{P}_\zeta, f_{\rm NL}^{\rm local}$ and $\tau_{\rm NL}$ are precisely determined or constrained by the Planck collaboration. Thus by using the Planck result, we constrain the parameters of the kinetic coupling model and inflation. We found that $\mathcal{P}_\zeta^{\rm em}, f_{\rm NL}^{\rm em}$ and $\tau_{\rm NL}^{\rm em}$ are given by the functions of four parameters $\{n, N_{\rm tot}, \rho_{\rm inf}, \varepsilon\}$ of the model and inflation (see eq. (3.56), (3.59) and (3.60)). Therefore when three parameters out of four are fixed, the other one can be constrained by the observation. Note in the case where a single slow-rolling inflaton is responsible for all the observed curvature power spectrum, which we call "inflaton" case, the slow-roll parameter ε is determined
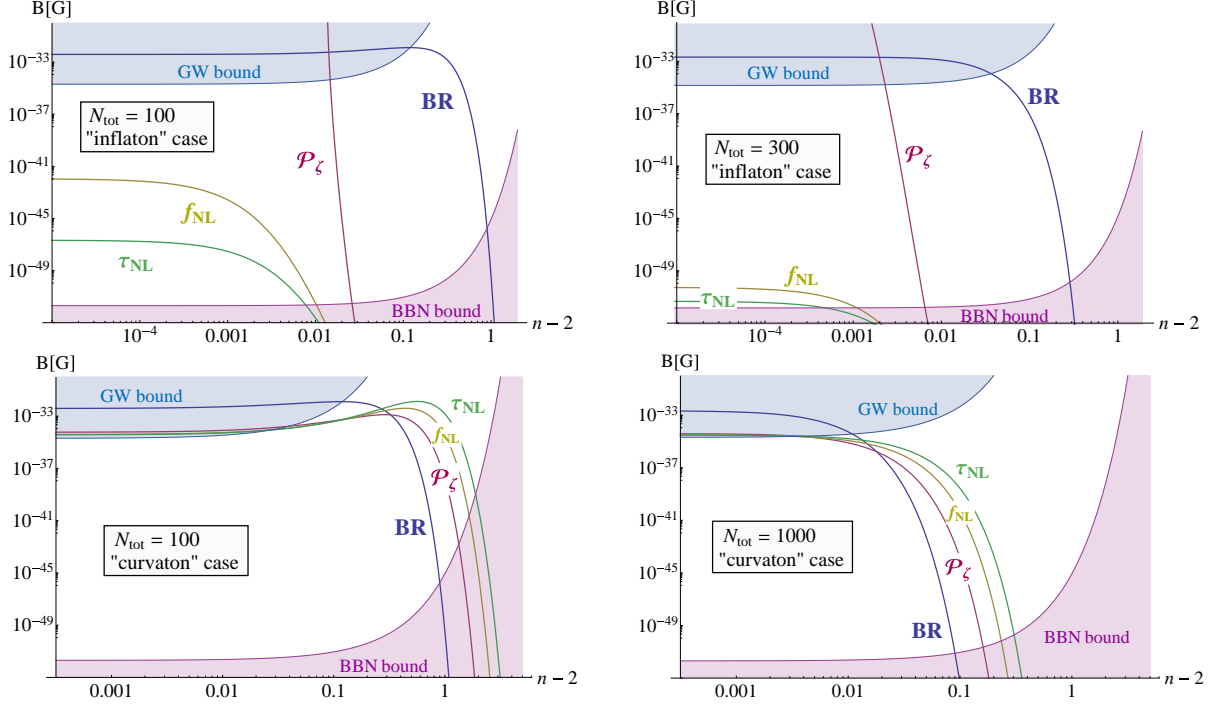
Figure 3.5 : The upper limit of the current strength of the magnetic field for $n \geq 2$. The horizontal axis is $n-2$ and the vertical axis is $\mathcal{P}_B^{1/2}(\eta_{\text{now}}, 1\text{Mpc}^{-1})$ [G]. In top two panels it is assumed that inflaton generates all observed curvature perturbation ("inflaton" case) while that assumption is relaxed and instead $\varepsilon = 10^{-2}$ is adopted in the bottom two panels ("curvaton" case). The total duration of the electromagnetic field generation is set as $N_{\text{tot}} = 100$ (left panels), 300 (top right panel) or 1000 (bottom right panel). The shaded region represent the restriction from gravitational wave (blue) and big bang nucleosynthesis (red), respectively.

by inflation energy scale ρ_{inf}. On the other hand, if the other mechanism like curvaton or modulated reheating produces observed $\mathcal{P}_\zeta$, ε can be a free parameter. For simplicity, this case is called "curvaton" case while we do not specify any model.

In order to illustrate the constraints from the BR, $\mathcal{P}_\zeta^{\mathrm{em}}$, $f_{\mathrm{NL}}^{\mathrm{em}}$ and $\tau_{\mathrm{NL}}^{\mathrm{em}}$, we show three kinds of plot which represent the upper limit of $N_{\mathrm{tot}} - N_{\mathrm{CMB}}$, ρ_{inf} and $\mathcal{P}_B^{1/2}(\eta_{\mathrm{now}}, 1\mathrm{Mpc}^{-1})$ with respect to n, respectively. The upper limits of the total e-folding number of magnetogenesis before the CMB scale exits the horizon, $N_{\mathrm{tot}} - N_{\mathrm{CMB}}$, can be expressed by analytical formula as eq. (3.70)-(3.73). The upper limits of the inflation energy density, ρ_{inf}, need numerical calculations to be obtained and can be translated to the upper limits of the present amplitude of the cosmic magnetic field at Mpc scale, $\mathcal{P}_B^{1/2}(\eta_{\mathrm{now}}, 1\mathrm{Mpc}^{-1})$. In general, all four constraints from the BR, $\mathcal{P}_\zeta^{\mathrm{em}}$, $f_{\mathrm{NL}}^{\mathrm{em}}$ and $\tau_{\mathrm{NL}}^{\mathrm{em}}$ become tighter as $n\,(\geq 2)$ is larger. It is simply because the strength of generated electromagnetic fields are amplified as $n\,(\geq 2)$ is larger.

In the "inflaton" case, interestingly, τ_{NL} gives the strongest limitation on parameters. Even for $\rho_{\mathrm{inf}}^{1/4} = 10^{-1}\mathrm{GeV}$ and $n = 2$, the constraint from τ_{NL} puts $N_{\mathrm{tot}} \lesssim 300$ and it becomes more stringent for higher ρ_{inf} or n. For $N_{\mathrm{tot}} = 100$ and $n = 2$, in turn, $\rho_{\mathrm{inf}}^{1/4} \lesssim 10^4\mathrm{GeV}$ is required and ρ_{inf} should be even lower for larger N_{tot} or n. As for the magnetic field strength, we find the upper limit from τ_{NL} is $\mathcal{P}_B^{1/2} \lesssim 10^{-47}\mathrm{G}$ at present Mpc scale for $N_{\mathrm{tot}} = 100$. It is 10^{-15} times lower than the upper limit of the conventional BR condition.

In the "curvaton" case, however, the constraints are more moderate if the free parameter ε is larger than the "inflaton" case. For clarity we fix $\varepsilon = 10^{-2}$ and show the constraints from $\mathcal{P}_\zeta^{\mathrm{em}}$, $f_{\mathrm{NL}}^{\mathrm{em}}$ and $\tau_{\mathrm{NL}}^{\mathrm{em}}$ are weaker than the BR constraint if ρ_{inf} is sufficiently small. Thus even if the induced curvature perturbation is taken into account, the resultant constraint is not dramatically changed from the conventional BR restriction in the low ρ_{inf} region. In fact, one can see in fig. 3.5 that the constraint on $\mathcal{P}_B$ at present Mpc scale becomes tighter only by $\mathcal{O}(10^{-1})$ than that given solely by the BR.

Aside from the constraints, we find the general relationship between $f_{\mathrm{NL}}^{\mathrm{em}}$ and $\tau_{\mathrm{NL}}^{\mathrm{em}}$ in eq. (3.64). According to it, even if $f_{\mathrm{NL}} \sim \mathcal{O}(1)$ which is too small to be observed by the Planck satellite, the kinetic coupling model can compatibly produce detectable $\tau_{\mathrm{NL}} \gtrsim 560$ [73]. In addition, it is expected that this model generates much higher correlators of the curvature perturbation. Thus it is also interesting to investigate the higher order correlators both in theoretical and observational sides. Furthermore, we use the averaging over the direction of $\hat{\boldsymbol{k}}_i$ for f_{NL} and τ_{NL}. It should be interesting to consider the direction dependence of τ_{NL} as well as f_{NL}.

3.3 Problems and General Constraints

In the previous section, we see that although the kinetic coupling model (Ratra's model) can generate primordial magnetic fields during inflation, the back reaction problem and the curvature perturbation problem constrain the model from producing the magnetic field which is strong enough to explain the observations. However, we have investigated only one model with a specific parameterization of an arbitrary function $I(\eta)$ (see eq. (3.17)). Thus one may wonder if in another model of inflationary magnetogenesis or even in Ratra's model with a different functional form of $I(\eta)$, it is possible to avoid these problems. In other words, at this point, it is not clear how the back reaction and the curvature perturbation problem are universal in inflationary magnetogenesis scenarios. To answer this important question, we have to investigate inflationary magnetogenesis in a model-independent way. Actually such model-independent arguments have been developed for both the back reaction problem and the curvature perturbation problem [33, 34]. According to them, the answer of the above question is yes: These problems are very general for inflationary magnetogenesis and even model-independent constraints derived from the two problems are quite stringent. In this section, we make these model-independent arguments in sec. 3.3.1 and sec. 3.3.2.

As we see in the following, upper limits on the inflation energy scale $\rho_{\rm inf}$ can be derived by the model-independent arguments. Provided that the observed void magnetic fields are totally generated during inflation, the back reaction problem requires

$$\rho_{\rm inf}^{1/4} < 6 \times 10^{11} {\rm GeV} \times \left(\frac{B_{\rm obs}}{10^{-15}G} \right)^{-2}, \tag{3.80}$$

while the curvature perturbation problem requires

$$\rho_{\rm inf}^{1/4} < 30 {\rm GeV} \left(\frac{p_B}{1 {\rm Mpc}^{-1}} \right)^{5/4} \left(\frac{B_{\rm obs}}{10^{-15} {\rm G}} \right)^{-1}, \quad (p_B \geq 1 {\rm Mpc}^{-1}), \tag{3.81}$$

where $B_{\rm obs}$ is the present strength of the void magnetic field and $p_B \simeq L_B^{-1}$ is its peak wave number. The upper bound derived from the curvature perturbation problem is much tighter than that of the back reaction problem. Eq. (3.81) is so stringent that it is very difficult to realize such a extremely low energy inflation with a viable dark matter production and baryogenesis. Note that a key assumption to derive these constraint is that the magnetic field observed today is generated during inflation and it just decays in proportional to a^{-2} after inflation. Therefore the difficulty of pure inflationary magnetogenesis might infer that the primordial magnetic field is somehow amplified after inflation. We consider this possibility in the next section. In this section, we derive the above two model-independent constraints and see that it is generally difficult to find a viable model of pure inflationary magnetogenesis.

3.3.1 Model-independent argument on the back reaction problem

In this subsection [10] , we develop a model-independent argument on the back reaction problem of inflationary magnetogenesis. Interestingly, from the argument we can derive the upper bound on the energy density of inflation. If inflation is responsible for the generation of the void magnetic fields then the inflation energy scale is bounded from above as $\rho_{\rm inf}^{1/4} < 2.5 \times 10^{-7} M_{\rm Pl} \times (B_{\rm obs}/10^{-15}{\rm G})^{-2}$ in a wide class of inflationary magnetogenesis models, where $B_{\rm obs}$ is the observed strength of cosmic magnetic fields. The tensor-to-scalar ratio is correspondingly constrained as $r < 10^{-19} \times (B_{\rm obs}/10^{-15}{\rm G})^{-8}$. Therefore, if the reported strength $B_{\rm obs} \geq 10^{-15}{\rm G}$ is confirmed and if any signatures of gravitational waves from inflation are detected in the near future, then our result indicates some tensions between inflationary magnetogenesis and observations.

3.3.1.1 Four Assumptions

To discuss the back reaction problem of inflationary magnetogenesis in a model-independent way, we make the following four assumptions.

Assumption 1: the form of kinetic term

First, we assume that the kinetic term of the photon field A_μ is of the form

$$\mathcal{L}_{\rm kin} = -\frac{1}{4} I^2(\eta) F_{\mu\nu} F^{\mu\nu}, \tag{3.82}$$

where it is understood that the time-dependence of $I(\eta)$ is due to its dependence on homogeneous, time-dependent fields present in the theory. Thus, $\mathcal{L}_{\rm kin}$ includes various interactions between the photon field and other fields [20, 61, 62, 28]. This form of coupling does not have to break either gauge or local Lorentz symmetry. In general the photon field can have additional interactions $\mathcal{L}_{\rm int}$:

$$\mathcal{L}_A = \mathcal{L}_{\rm kin} + \mathcal{L}_{\rm int}. \tag{3.83}$$

However, we let $\mathcal{L}_{\rm int}$ unspecified. Even so, under the four assumptions introduced in this sub-subsection, we can derive the upper limit on the inflation energy scale in a model independent way. Note that when $I = 1$ and $\mathcal{L}_{\rm int} = 0$, the usual Maxwell theory is restored. Note that an assumption on the form of the kinetic term is necessary to quantize the photon field and to define the kinetic energy density.

Now we can quantize the photon field in the same way as sec. 3.2.1. Let us consider the contribution of modes with $k < k_{\rm diff}$, i.e. those whose comoving length scale are longer than the cosmic diffusion length, to the kinetic energy density of the electromagnetic field

---

[10]This subsection is based on my work [33].

as [11]

$$\rho_{\text{kin}}(k_{\text{diff}}, \eta) = \frac{I^2}{2} \int_0^{k_{\text{diff}}} \frac{dk}{k} \left[\mathcal{P}_E(\eta, k) + \mathcal{P}_B(\eta, k) \right], \tag{3.84}$$

where we have defined power spectra of electric and magnetic fields as

$$\mathcal{P}_E(\eta, k) = \frac{k^3 |\mathcal{A}_k'(\eta)|^2}{\pi^2 a^4(\eta)}, \quad \mathcal{P}_B(\eta, k) = \frac{k^5 |\mathcal{A}_k(\eta)|^2}{\pi^2 a^4(\eta)}. \tag{3.85}$$

Assumption 2: Avoidance of strong coupling

The second assumption is that

$$I(\eta) \geq 1 \quad \text{for } \eta_{\text{diff}} \leq \eta, \tag{3.86}$$

where η_{diff} is the conformal time when the comoving cosimic diffusion length exits the horizon, thus defined as $k_{\text{diff}}\eta_{\text{diff}} = -1$.

This assumption essentially states that the effective coupling constants of the photon field to other fields should be always smaller than present values. For example, let us consider the interaction between the photon and a charged fermion as

$$\mathcal{L}_{\text{int}} \ni -e\bar{\psi}\gamma^\mu\psi A_\mu. \tag{3.87}$$

In order to evaluate the effective coupling constant, we should canonically normalize the fields. Let us suppose that the fermion ψ is already canonically normalized. The canonically normalized photon field is $A_\mu^c \equiv I A_\mu$. Then the interaction term is rewritten as

$$\mathcal{L}_{\text{int}} \ni -\frac{e}{I}\bar{\psi}\gamma^\mu\psi A_\mu^c. \tag{3.88}$$

It is now clear that e/I is the effective coupling constant. Therefore if $I \ll 1$, the effective coupling constant becomes large and the tree level analysis would be invalidated. In order to justify the tree level analysis, we need to assume that I is bounded from below by a positive constant I_0. For simplicity we set I_0 to be the present value of I, i.e. $I_0 = 1$.

Assumption 3: Small back reaction

The third assumption is that the kinetic energy density eq.(3.84) is smaller than that of inflaton [12],

$$\rho_{\text{kin}}(k_{\text{diff}}, \eta) < \rho_{\text{inf}} \quad \text{for } \eta_{\text{diff}} \leq \eta \leq \eta_f, \tag{3.89}$$

---

[11] It is understood that the domain of integration over k in eq.(3.84) is the same as in eq.(3.14). As a result, $\rho_{\text{kin}}(k_{\text{diff}}, \eta)$ is not the sum of all modes that exist during inflation but the sum of modes whose scales are relevant to observed cosmic magnetic fields.

[12] We are interested in modes with $k < k_{\text{diff}}$ only. One can show that these modes do not significantly contribute to the vacuum enegy part of ρ_{kin}. Validity of the effective field theory requires that the contribution of each mode ω_k to the vacuum energy must be smaller than the Planck mass scale M_{Pl}. Hence, $|\rho_{\text{vac}}(k_{\text{diff}}, \eta)| < (\text{Max}_{k \leq k_{\text{diff}}}|\omega_k|)(k_{\text{diff}}/a)^3 < M_{\text{Pl}}H^3 \ll \rho_{\text{inf}}$ for $\eta_{\text{diff}} \leq \eta \leq \eta_f$. Therefore distinction between renormalized and unrenormalized expressions is irrelevant for (3.84). One can show that such distinction is unimportant also for (3.14).

where η_f is the conformal time at the end of inflation and hereafter we ignore the time-dependence of the inflaton energy density ρ_{inf}.

This assumption is closely related to the condition for avoidance of the back reaction problem

$$|\rho_{\mathrm{kin}}(\eta) + \rho_{\mathrm{int}}(\eta)| < \rho_{\mathrm{inf}} \quad \text{for } \eta_{\mathrm{diff}} \leq \eta \leq \eta_f. \tag{3.90}$$

Note that eq.(3.89) and eq.(3.90) are different. In general, the total energy density of the photon field includes not only the kinetic energy density ρ_{kin} but also the interaction energy density ρ_{int} due to the additional interaction terms $\mathcal{L}_{\mathrm{int}}$. Also, $\rho_{\mathrm{kin}}(\eta)$ in (3.90) should be understood as $\rho_{\mathrm{kin}}(\infty, \eta)$ and thus is in general larger than $\rho_{\mathrm{kin}}(k_{\mathrm{diff}}, \eta)$ in (3.89). If the interaction energy density is non-negative ($\rho_{\mathrm{int}} \geq 0$) then eq.(3.90) requires eq.(3.89). Even if the interaction energy is negative ($\rho_{\mathrm{int}} < 0$), unless the two contributions ρ_{kin} and ρ_{int} cancel each other with a sufficiently good precision, eq.(3.90) generically requires eq.(3.89). Therefore the third assumption eq.(3.89) is mandatory unless negative ρ_{int} precisely cancels out positive ρ_{kin}.

In sec. 3.3.1.3, we confirm the necessity of the third assumption in the case of gauge and local Lorentz invariant quadratic interactions and explore the possibility of the precise cancellation between ρ_{kin} and ρ_{int}.

Assumption 4: Magnetogenesis during inflation

The fourth assumption is that all observed magnetic fields are generated during inflation. In particular, the conformal symmetry of the photon field action is broken appreciably only in the inflationary era. Since the electric conductivity of the universe increases after the completion of reheating [21, 65] and by assuming the instantaneous reheating, we have [13]

$$B_{\mathrm{eff}}^2(\eta_{\mathrm{now}}) \leq a_f^4 B_{\mathrm{eff}}^2(\eta_f), \tag{3.91}$$

where we have set $a(\eta_{\mathrm{now}}) = 1$.

By using eq.(3.86), (3.89) and the fact that B_{eff} is smaller than the usual definition of magnetic field strength ($0 < F(kL) \leq 1$), we obtain

$$B_{\mathrm{eff}}^2(\eta_{\mathrm{diff}}) < 2\rho_{\mathrm{inf}}. \tag{3.92}$$

Assuming the instantaneous reheating, we find the scale factor at the end of inflation is given by

$$a_f^4 = \frac{\rho_\gamma}{\rho_{\mathrm{inf}}} \tag{3.93}$$

where $\rho_\gamma \simeq 5.7 \times 10^{-125} M_{\mathrm{Pl}}^4 \simeq 5.2 \times 10^{-12} \mathrm{G}^2$ is the present energy density of radiation.

---

[13] With the electric conductivity σ_c, the equation of motion of the vector potential is modified as $\ddot{A}_i(t, \boldsymbol{x}) + (H + \sigma_c)\dot{A}_i(t, \boldsymbol{x}) - \partial_j^2 A_i(t, \boldsymbol{x}) = 0$ [65]. Thus with a very high conductivity, A_i becomes almost constant, the electic field vanishes and the magnetic field behaves as $B_i \propto a^{-2}$ on large scales. This phenomena is called the "freeze" of magnetic fields.

Eq.(3.91), (3.92), (3.93) and (3.14) lead to the following inequality.

$$\frac{a_{\mathrm{diff}}^4 B_{\mathrm{eff}}^2(\eta_{\mathrm{diff}})}{a_f^4 B_{\mathrm{eff}}^2(\eta_f)} < 10^{-42} \times \exp[-4(\Delta N - 35)] \left(\frac{B_{\mathrm{obs}}}{10^{-15}G}\right)^{-2}, \tag{3.94}$$

where $\Delta N \equiv \ln(a_f/a_{\mathrm{diff}})$. This inequality implies that

$$a_{\mathrm{diff}}^4 B_{\mathrm{eff}}^2(\eta_{\mathrm{diff}}) \ll a_f^4 B_{\mathrm{eff}}^2(\eta_f), \tag{3.95}$$

and thus states that the magnetic fields have to be significantly amplified during inflation to explain the observational lower limit, eq.(3.14).

3.3.1.2   Upper limit on inflation energy scale

With the four assumptions stated in the previous sub-subsection, we are now ready to derive the upper limit on the inflation energy scale. The derivation is independent of details of inflationary magnetogenesis models, the behavior of photon mode functions or the spectrum of the electromagnetic fields.

Independently from the specific functional form of the mode function $\mathcal{A}_k(\eta)$, it can be shown that

$$\begin{aligned}
|\mathcal{A}_k(\eta_f)|^2 - |\mathcal{A}_k(\eta_{\mathrm{diff}})|^2 &= \int_{\eta_{\mathrm{diff}}}^{\eta_f} \mathrm{d}\eta \, 2|\mathcal{A}_k(\eta)| \, |\mathcal{A}_k(\eta)|' \\
&\leq \int_{\eta_{\mathrm{diff}}}^{\eta_f} \frac{\mathrm{d}\eta}{k} \, 2k|\mathcal{A}_k(\eta)| \, |\mathcal{A}_k'(\eta)| \\
&\leq \int_{\eta_{\mathrm{diff}}}^{\eta_f} \frac{\mathrm{d}\eta}{k} \left(k^2|\mathcal{A}_k(\eta)|^2 + |\mathcal{A}_k'(\eta)|^2 \right), \tag{3.96}
\end{aligned}$$

where we have used the general inequalities $|z(\eta)|' \leq |z'(\eta)|$ for a complex function $z(\eta)$ and $2xy \leq x^2 + y^2$ for real numbers x and y. Multiplying the both ends of eq.(3.96) by $F(kL)k^4/\pi^2$ and integrating it over k from 0 to k_{diff}, we obtain

$$a_f^4 B_{\mathrm{eff}}^2(\eta_f) - a_{\mathrm{diff}}^4 B_{\mathrm{eff}}^2(\eta_{\mathrm{diff}}) < \frac{\alpha}{L} \int_{\eta_{\mathrm{diff}}}^{\eta_f} \mathrm{d}\eta \, a^4(\eta) \int_0^{k_{\mathrm{diff}}} \frac{\mathrm{d}k}{k} \left[\mathcal{P}_E(\eta, k) + \mathcal{P}_B(\eta, k) \right], \tag{3.97}$$

where we have used the second inequality listed in (3.11). Using the second, third and fourth assumptions as well as eq.(3.95), we obtain

$$B_{\mathrm{eff}}^2(\eta_{\mathrm{now}}) < \frac{2\alpha}{L} \rho_{\mathrm{inf}} \int_{\eta_{\mathrm{diff}}}^{\eta_f} \mathrm{d}\eta \, a^4(\eta) \simeq \frac{2\alpha}{3H_{\mathrm{inf}}L} a_f^3 \rho_{\mathrm{inf}} \tag{3.98}$$

where H_{inf} ($\simeq$ const.) is the Hubble expansion rate during inflation.

Note that $1/H_{\mathrm{inf}}$ and a_f^3, which appear in the r.h.s. of (3.98), are decreasing functions of the inflation scale. Indeed, by substituting (3.93) for a_f and using the Friedmann equation for H_{inf}, we can see that the r.h.s. of (3.98) is a decreasing function of the

inflation scale. Hence, substituting eq.(3.14) and eq.(3.93) into eq.(3.98), we finally obtain the upper limit on the inflation energy scale,

$$\rho_{\text{inf}}^{1/4} < \frac{2\alpha}{\sqrt{3}L} \rho_\gamma^{3/4} M_{\text{Pl}} B_{\text{obs}}^{-2} \approx 2.5 \times 10^{-7} M_{\text{Pl}} \times \left(\frac{B_{\text{obs}}}{10^{-15}G}\right)^{-2}. \tag{3.99}$$

Note this upper limit can become even stronger if details of reheating is taken into consideration instead of eq.(3.93). Provided that the dominant energy density behaves like matter ($\propto a^{-3}$) during reheating, the right-hand side of eq.(3.99) is multiplied by an additional factor $(\rho_{\text{reh}}/\rho_{\text{inf}})^{1/4} < 1$, where ρ_{reh} is the energy density at the end of reheating era.

Eq.(3.99) can be converted into the upper bound on the tensor-to-scalar ratio r under the slow-roll approximation,

$$r < 10^{-19} \times \left(\frac{B_{\text{obs}}}{10^{-15}G}\right)^{-8}. \tag{3.100}$$

Therefore, if all observed cosmic magnetic fields are generated during inflation, it is extremely difficult to detect any signatures of primordial gravitational waves, for example direct detections or CMB B mode polarization. Conversely, if some observations reveal that r is larger than the upper bound (3.100), it implies that inflation cannot explain the origin of cosmic magnetic fields under the four assumptions.

Now let us discuss the intuitive understanding of the reason why we obtain the upper limit on the inflation energy scale. Roughly speaking, $a^4 \mathcal{P}_B$ has to increase significantly during inflation for inflationary magnetogenesis (see eq.(3.95)). It is easy to show in the same way as eq.(3.96) that

$$\frac{1}{k}\frac{d}{d\eta}\left(a^4(\eta)\mathcal{P}_B(\eta, k)\right) \leq a^4(\eta)\left(\mathcal{P}_E(\eta, k) + \mathcal{P}_B(\eta, k)\right). \tag{3.101}$$

From the second and third assumption we know right-hand side of eq.(3.101) integrated by $\ln k$ should be smaller than $a^4 \rho_{\text{inf}}$. Thus essentially, time variation of $a^4 \mathcal{P}_B$ is bounded from above by $a^4 \rho_{\text{inf}}$. Then we can rewrite $a^4 \rho_{\text{inf}}$ by using eq.(3.93) as

$$a^4(\eta)\rho_{\text{inf}} = \rho_\gamma e^{-4N}, \quad N \equiv \sqrt{\frac{\rho_{\text{inf}}}{3M_{\text{Pl}}^2}}(t_{\text{f}} - t). \tag{3.102}$$

where N is e-folding number, t is cosmic time and t_{f} denotes the end of inlation. Therefore $a^4 \rho_{\text{inf}}$ is actually emdecreasing function of ρ_{inf} during inflation. Since lower ρ_{inf} is favored to relax the upper bound on time variation of $a^4 \mathcal{P}_B$, we obtain the upper bound on inflation energy scale.

3.3.1.3 Additional Interaction Terms

The action for the photon field consists of not only the kinetic term $\mathcal{L}_{\text{kin}}$ but also the additional interaction terms $\mathcal{L}_{\text{int}}$. As already mentioned below eq. (3.90), the third assumption

eq.(3.89) is avoidable if negative ρ_{int} precisely cancels out positive ρ_{kin}. Therefore whether such a precise cancellation is possible is a significant question. The answer we shall draw in the following discussion is that it is difficult to achieve such a cancellation. Here, it is perhaps worthwhile stressing that, as long as the four assumptions (including the third one) are satisfied, our main result eq.(3.99) holds even if ρ_{int} and ρ_{kin} precisely cancel out.

Gauge and Lorentz invariant quadratic term

In the quadratic level, the most general renormalizable interaction term which preserves gauge and local Lorentz symmetry is given by

$$\mathcal{L}_{\text{int}} = \frac{1}{8} f(\eta) \varepsilon^{\mu\nu\rho\sigma} F_{\mu\nu} F_{\rho\sigma} + \frac{1}{2} m^2(\eta) A_\mu A^\mu, \tag{3.103}$$

where $\varepsilon^{\mu\nu\rho\sigma}$ is the totally anti-symmetric tensor with $\varepsilon^{0123} = 1/\sqrt{-g}$, $f(\eta)$ is a function of homogeneous scalars. The first term is called axial coupling term [22, 25]. The second term is the effective mass term of the photon induced by expectation values of charged scalars. It stems from the kinetic term of the charged scalars, and the positivity of the time kinetic term implies the positivity of the mass squared m^2. This term spontaneously breaks the $U(1)$ gauge symmetry, and the longitudinal mode of photon field becomes a physical degree of freedom.

Actually, the axial coupling term does not contribute to the energy density of the photon field. Since the axial coupling term does not depend on the metric, its contribution to the energy momentum tensor is exactly zero. The effective mass term does contribute to ρ_{int} but the contribution is always positive because of the positivity of the mass squared. Therefore the cancellation between ρ_{int} and ρ_{kin} cannot occur.

Model with negative interaction energy

There is an existing model which gives a emnegative energy contribution from an additional interaction term. Turner and Widrow [21] proposed a model with non-minimal coupling, $\mathcal{L}_{\text{int}} \propto R A_\mu A^\mu$, where R is the Ricchi scalar. This coupling can become an effective mass term of photon with negative mass squared. However this model has three critical problems. First, the longitudinal mode of photon becomes ghost [59, 28, 74]. Second, the negative energy contribution from $\mathcal{L}_{\text{int}}$ exceeds ρ_{inf} and the back reaction spoils inflation when we require generated magnetic field is sufficient [28]. Third, this coupling explicitly breaks the gauge symmetry.

Energy conserving term

From purely phenomenological viewpoints, let us investigate the additional interaction term of the form

$$\sqrt{-g} \mathcal{L}_{\text{int}} = \frac{1}{2} a^2 J^2(\eta) V_i^2 \qquad (J^2 > 0) \tag{3.104}$$

where $J(\eta)$ is a function of homogeneous scalar fields and V_i is the photon vector mode, $A_\mu = (A_0, V_i + \partial_i S)$, $\partial_i V_i = 0$. This term is effective mass term of photon field with a

negative mass squared. Note that this term breaks both gauge invariance and Lorentz invariance. It does not yield ghost field because it contains only vector modes by breaking Lorentz symmetry and we still assume that the kinetic term of photon is given by eq. (3.82). Although it may be hard to embed such a term in a viable elementary particle theory, it is worth investigating it since we can find an interesting way to realize the cancellation between ρ_{int} and ρ_{kin}.

From eq.(3.104), the equation of motion is given by

$$\mathcal{A}_k'' + \left(k^2 - a^2 J^2\right) \mathcal{A}_k = 0. \tag{3.105}$$

Here we have assumed $I(\eta) = 1$ for simplicity, since otherwise the weak coupling effect due to $I \gg 1$ would make the interaction term irrelevant. At the same time we require the cancellation between ρ_{int} and ρ_{kin} for each mode,

$$|\mathcal{A}_k'|^2 + (k^2 - a^2 J^2)|\mathcal{A}_k|^2 = 0. \tag{3.106}$$

It is easy to show that eq.(3.105), eq.(3.106) and eq.(3.21) imply that

$$a^2 J^2(\eta) = \text{const.} \tag{3.107}$$

In other words, the coefficient of the quadratic term (3.104) should be constant.

The reason why only the interaction term with constant coefficient leads the cancellation is simple. It is the energy conservation. If there is no explicit dependence on time in the action (for example, if the time-dependence due to the scale factor $a(\eta)$ is canceled by time-evolving scalars), then the energy of the system is conserved by virtue of Noether's theorem. In the case of eq.(3.104), if $J(\eta)$ cancels the time dependence of $a(\eta)$, the photon energy (with respect to the conformal time η) is conserved. Note that the kinetic term of the photon field is originally free from $a(\eta)$. Therefore the energy density of photon does not increase even if the electromagnetic field strength increases. It is notable that, for this mechanism to work, the dynamics of the scalar fields included in $J(\eta)$ has to restore the time translation symmetry accidentally.

The above analysis implies that the magnetogenesis from inflation whose energy is larger than the constraint of eq.(3.99) may not be impossible in principle. However, in practice it is not easy to realize a model which exploits the energy conserving mechanism because the accidental symmetry restoration by the scalar field dynamics can be easily spoiled by various effects such as the back reaction of the photon field. Therefore it is fair to say that all the four assumptions (including the third one) are likely to be mandatory in a rather broad class of models and the derived upper limit on the inflation energy scale is considerably general.

3.3.1.4 Summary of subsection 3.3.1

In this subsection we have derived a universal upper limit on the inflation energy scale under the following four assumptions. (i) The kinetic term of the photon field is of the

canonical form up to a time-dependent overall factor. (ii) The effective coupling constants do not exceed present values and thus do not exhibit strong coupling. (iii) The kinetic energy of the photon field is always lower than the inflaton energy density during inflation. (iv) All observed cosmic magnetic fields are generated during inflation.

The derived constraint is eq.(3.99), $\rho_{\rm inf}^{1/4} < 2.5 \times 10^{-7} M_{\rm Pl} \times (B_{\rm obs}/10^{-15}G)^{-2}$. As a consequence, the tensor-to-scalar ratio r is bounded from above as eq.(3.100), $r < 10^{-19} \times (B_{\rm obs}/10^{-15}G)^{-8}$. We hardly expect that inflation is the origin of both cosmic magnetic fields and detectable gravitational waves if $B_{\rm obs} > 10^{-15}G$. Therefore the future detection of signatures of inflationary gravitational waves, if any, would imply tension between inflationary magnetogenesis and observations.

Although our constraint is valid in fairly broad class of inflationary magnetogenesis scenarios, we have investigated the possibility to evade it. In order to evade the constraint, at least one of the assumptions should be violated. The third assumption can be violated only if the energy density due to additional interaction terms and the kinetic energy density precisely cancel out. We have considered a possible mechanism which exploits a energy conservation law to realize the cancellation. However, it seems a challenge to build a realistic model equipped with such a mechanism.

Nonetheless, the resultant bound is expected to be useful, providing a new judgment condition. Namely, if tensor-to-scalar ratio is detected in the future, any possibilities of magnetogenesis model within our assumptions will be excluded. Alternatively, if one can derive a lower limit on inflation energy scale by different arguments for a class of models then the upper limit can be used to rule out the class of models. In this sense the upper bound we have found may be considered as an obstacle to inflationary magnetogenesis as well as an important guideline for model building.

3.3.2 Model-independent argument on the curvature perturbation problem

In this subsection [14] , we develop a model-independent argument on the curvature perturbatino problem. In inflationary magnetogenesis models, additional primordial curvature perturbations are inevitably produced from iso-curvature perturbations due to generated electromagnetic fields. We explore such induced curvature perturbations in a model independent way and derive a severe upper bound on the energy scale of inflation from the observed cosmic magnetic fields and the observed amplitude of the curvature perturbation. We show that if one requires inflation magnetogenesis is responsible for the generation of the observed magnetic fields and assumes no additional amplification after inflation, the inflation energy scale is constrained by the curvature power spectrum $\mathcal{P}_\zeta$ as

$$\mathcal{P}_\zeta^{\rm obs} > \mathcal{P}_\zeta^{\rm em} \quad \Rightarrow \quad \rho_{\rm inf}^{1/4} < 30{\rm GeV} \times \left(\frac{p_B}{1{\rm Mpc}^{-1}}\right)^{\frac{5}{4}} \left(\frac{B_{\rm obs}}{10^{-15}{\rm G}}\right)^{-1}, \tag{3.108}$$

---

[14]This subsection is based on my work [34].

where $\rho_{\rm inf}$ is the energy scale of inflation, $p_B > 1{\rm Mpc}^{-1}$ is the peak wave number of the void magnetic field and $B_{\rm obs}$ is the magnetic field strength today [34]. Therefore, without a dedicated low energy inflation model or an additional amplification of magnetic fields after inflation, inflationary magnetogenesis on Mpc scale is generally incompatible with CMB observations.

3.3.2.1 Basis of the idea

In this sub-subsection, we briefly explain our approach to obtain the model independent constraint.

Again, remember the reported lower bound for the peak strength of the magnetic field is given by [16, 17]

$$B(\eta_{\rm now}, p_B) \gtrsim 10^{-15}{\rm G} \times \begin{cases} \left(\frac{p_B}{1{\rm Mpc}^{-1}}\right)^{1/2} & (p_B > 1{\rm Mpc}^{-1}) \\ 1 & (p_B < 1{\rm Mpc}^{-1}) \end{cases}, \tag{3.109}$$

where $B(\eta_{\rm now}, k)$ denotes the void magnetic field at present in Fourier space, p_B is its peak wave number. Note that $B(\eta_{\rm now}, k)$ is assumed to have a peak at $k = p_B$ with a peak width $\Delta \ln k = \mathcal{O}(1)$ in accordance with the definite correlation length $p_B^{-1} \simeq L_B$. [15] In this subsection, we focus on the case with $p_B \geq 1{\rm Mpc}^{-1}$.

Let us discuss general properties of electromagnetic fields in the FLRW universe including the inflation era. In the FLRW universe, the Fourier transformed components of the electromagnetic fields are given in terms of the vector potential as

$$E_i(\eta, \boldsymbol{k}) = -a^{-2}\partial_\eta A_i(\eta, \boldsymbol{k}), \qquad B_i(\eta, \boldsymbol{k}) = a^{-2}i\varepsilon_{ijl}\, k_j A_l(\eta, \boldsymbol{k}), \tag{3.110}$$

in the radiation gauge. Here, a is the scale factor, k denotes wave number, η denotes conformal time and $A_i(\eta, \boldsymbol{k})$ is the vector potential in Fourier space. Note that B_i is proportional to a^{-2} and substantially decrease as the universe expands. For simple discussion about the strength of the electromagnetic fields, here we suppress the vector legs of E_i, B_i and A_i. A mathematically strict treatment including the vector legs will be shown in the following sections.

If the magnetic field is generated during inflation and it monotonically decreases by the adiabatic dilution after the inflation, the present lower bound $B(\eta_{\rm now}, p_B) \gtrsim 10^{-15}{\rm G}$ can be translated into the lower bound on the strength of the magnetic field at the end of inflation as

$$B(\eta_{\rm f}, p_B) \gtrsim 10^{-15}{\rm G} \left(\frac{a_{\rm now}}{a_{\rm f}}\right)^2 = 2 \times 10^{40}{\rm G} \left(\frac{\rho_{\rm inf}^{1/4}}{10^{15}{\rm GeV}}\right)^2, \tag{3.111}$$

where subscript f denotes the end of inflation and the instantaneous reheating is assumed for simplicity. Therefore, to explain the observational lower bound by inflationary

---

[15] A more rigorous treatment of the magnetic lower bound is discussed in sec. 3.1.2.3.

magnetogenesis, strong magnetic fields should be produced during inflation. However, the magnetic field also decreases rapidly during inflation because of the factor a^{-2}. To compensate the adiabatic dilution and produce the magnetic field effectively, the vector potential $A(\eta, p_B)$ must be amplified at least faster than a^2 as

$$A(\eta, p_B) \propto |\eta|^{-n} \quad (n > 2). \tag{3.112}$$

In such case where the vector potential evolves in time, from eq. (3.110) we can easily find that the amplitude of the electric field should be much larger than that of the magnetic field on super-horizon scales. From eqs. (3.110) and (3.112), we obtain

$$\left| \frac{E}{B} \right| = \left| \frac{n}{k\eta} \right| = n e^{N_k} \gg 1 \qquad \text{(on super-horizon scales)}, \tag{3.113}$$

where $N_k \equiv -\ln |k\eta|$ is the e-fold number measured from the end of inflation to the time at the horizon exit of the k mode. This equation means that at the end of inflation the electric field is bigger than the magnetic field whose strength is eq. (3.111) by the factor of $n e^{N_{p_B}}$. Hence it is easy to imagine that including the effect of such strong electric field into the investigation of the inflationary magnetogenesis would give a strong constraint on the scenarios.

Model-independent approach

While most previous works specify a model of magnetogenesis and fix the behavior of the vector potential $A(\eta, k)$, we assume $A(\eta, k)$ is well approximated by a power-law of η only for the last one e-fold of inflation. It should be noted that the vector potential $A(\eta)$ can be a more complicated function of η in general. In such case, the approximation of the simple power-law gets worse for considering long duration. However, in terms of obtaining a conservative constraint in model independent approach, it should be sufficient to focus on the contribution from the last one e-fold before the end of inflation and assume constant n during such short duration. We also consider only the contribution from the electromagnetic fields around the peak scale $k \sim p_B$ as shown in (3.109). Of course, in general the electromagnetic fields might have the power at the separate scales from the peak with depending on the models and they also give some contributions. Also in this respect, our constraint should be conservative, which is obtained in model independent approach. Thus, the key assumption of this argument for the vector potential is given by

$$A(\eta, k) = \left(\frac{\eta}{\eta_{\mathrm{f}}} \right)^{-n} A(\eta_{\mathrm{f}}, k), \quad \text{for} \quad e\eta_{\mathrm{f}} \leq \eta \leq \eta_{\mathrm{f}}, \ k \sim p_B, \ \text{and} \ n = \text{const.} \tag{3.114}$$

By using this assumption for the vector potential, we will calculate the curvature perturbation induced by the electric field for the last one e-folding time and obtain the constraint by requiring that the induced curvature perturbation is smaller than the observed value as eq. (3.108).

Before closing this sub-subsection, it should be noted that the constraint apparently becomes very weak when $A(\eta, p_B)$ significantly grows before $N = 1$ and $A(\eta, p_B)$ is nearly constant, $|n| \ll 1$, for the last one e-fold. However, in that case, we can obtain an even more stringent constraint by considering not last one e-fold but the time when $n \sim \mathcal{O}(1)$ before the last one e-fold. The details of this case will be discussed in last part of sec. 3.3.2.3.

3.3.2.2 Power spectrum of induced curvature perturbations

In this sub-subsection, we derive an equation that evaluates the power spectrum of the curvature perturbation induced by the electric field during inflation. As we discuss in sec. 3.2.3.1, the curvature perturbation induced by electromagnetic fields on super-horizon scales is given by (see eq. (3.38)) [30]

$$\zeta_{\boldsymbol{k}}^{\text{em}} = 2 \int dN \, \frac{\rho_{\boldsymbol{k}}^{\text{em}}}{\varepsilon \, \rho_{\text{inf}}}. \tag{3.115}$$

The energy density of the electromagnetic field in Fourier space $\rho_{\boldsymbol{k}}^{\text{em}}$ is given by

$$\rho_{\boldsymbol{k}}^{\text{em}} = \frac{1}{2} \int \frac{\mathrm{d}^3 p \, \mathrm{d}^3 q}{(2\pi)^3} \delta(\boldsymbol{p} + \boldsymbol{q} - \boldsymbol{k}) \left[\boldsymbol{E}(\eta, \boldsymbol{p}) \cdot \boldsymbol{E}(\eta, \boldsymbol{q}) + \boldsymbol{B}(\eta, \boldsymbol{p}) \cdot \boldsymbol{B}(\eta, \boldsymbol{q}) \right]. \tag{3.116}$$

Note since $\rho^{\text{em}} = (\boldsymbol{E}^2 + \boldsymbol{B}^2)/2$ in the real space, $\rho_{\boldsymbol{k}}^{\text{em}}$ is written in terms of the convolution of the electromagnetic fields. In this subsection, the kinetic term of the Maxwell theory, $\mathcal{L} = -F^{\mu\nu} F_{\mu\nu}/4$, is assumed. If one consider the kinetic coupling model where an arbitrary function of time $I(\eta)$ is multiplied, $\mathcal{L} = -I(\eta) F^{\mu\nu} F_{\mu\nu}/4$, eq. (3.116) is also multiplied by $I(\eta)$ (The relation between E and B given by eq. (3.113) still holds.). In such case, to avoid the strong coupling problem, $I(\eta)$ should be larger than unity even during inflation. Therefore, $\rho_{\boldsymbol{k}}^{\text{em}}$ is larger than eq. (3.116) and the resultant constraint becomes tighter. In other words, eq. (3.116) is a conservative estimate in view of the kinetic coupling model. Moreover, in inflationary magnetogenesis models, some interaction terms between A_μ and other fields are considered to amplify the magnetic field. In those cases, the energy density of the interaction terms also contribute to source ζ (see sec. 3.3.1.3). Nonetheless they can be conservatively ignored.

In FLRW universe, when electromagnetic fields do not have helical component, the power spectra of the electromagnetic fields are respectively defined as [16]

$$\langle E_i(\eta, \boldsymbol{k}) E_j(\eta, \boldsymbol{k}') \rangle \equiv (2\pi)^3 \delta(\boldsymbol{k} + \boldsymbol{k}') \frac{1}{2} \left[\delta_{ij} - \hat{k}_i \hat{k}_j \right] \frac{2\pi^2}{k^3} \mathcal{P}_E(\eta, k), \tag{3.117}$$

$$\langle B_i(\eta, \boldsymbol{k}) B_j(\eta, \boldsymbol{k}') \rangle \equiv (2\pi)^3 \delta(\boldsymbol{k} + \boldsymbol{k}') \frac{1}{2} \left[\delta_{ij} - \hat{k}_i \hat{k}_j \right] \frac{2\pi^2}{k^3} \mathcal{P}_B(\eta, k), \tag{3.118}$$

---

[16]We consider the non-helical case where the parity is not violated. The extension to the helical case is straightforward [26].

where $\langle\cdots\rangle$ denotes the vacuum expectation value. The gauge field (or the vector potential) $A_i(\eta, \boldsymbol{x})$ is quantized in the same way as eq. (3.18). First, substituting eq. (3.116) into eq. (3.115), we obtain

$$\langle\zeta_{\boldsymbol{k}}^{\mathrm{em}}\zeta_{\boldsymbol{k}'}^{\mathrm{em}}\rangle = \int \mathrm{d}N\mathrm{d}N' \frac{1}{\varepsilon\,\rho_{\mathrm{inf}}}\frac{1}{\varepsilon\,\rho_{\mathrm{inf}}}\int \frac{\mathrm{d}^3p\,\mathrm{d}^3q\mathrm{d}^3p'\,\mathrm{d}^3q'}{(2\pi)^6}\delta(\boldsymbol{p}+\boldsymbol{q}-\boldsymbol{k})\delta(\boldsymbol{p}'+\boldsymbol{q}'-\boldsymbol{k}')$$
$$\times \langle(\boldsymbol{E_p}\cdot\boldsymbol{E_q}+\boldsymbol{B_p}\cdot\boldsymbol{B_q})\,(\boldsymbol{E_{p'}}\cdot\boldsymbol{E_{q'}}+\boldsymbol{B_{p'}}\cdot\boldsymbol{B_{q'}})\rangle. \quad (3.119)$$

Here, 4-point correlation functions of the electromagnetic fields appear. Then the 4-point correlation function of $\boldsymbol{E}$ can be computed as

$$\langle\boldsymbol{E_p}\cdot\boldsymbol{E_q}\ \boldsymbol{E_{p'}}\cdot\boldsymbol{E_{q'}}\rangle = a^{-4}(\eta)a^{-4}(\eta')\sum_{\lambda,\sigma,\lambda',\sigma'}\varepsilon_i^{(\lambda)}(\hat{\boldsymbol{p}})\varepsilon_i^{(\sigma)}(\hat{\boldsymbol{q}})\varepsilon_j^{(\lambda')}(\hat{\boldsymbol{p}}')\varepsilon_j^{(\sigma')}(\hat{\boldsymbol{q}}')$$
$$\times \partial_\eta\mathcal{A}_p(\eta)\partial_\eta\mathcal{A}_q(\eta)\partial_{\eta'}\mathcal{A}_{p'}(\eta')\partial_{\eta'}\mathcal{A}_{q'}(\eta')$$
$$\times \left\langle\left(a_{\boldsymbol{p}}^{(\lambda)}+a_{-\boldsymbol{p}}^{\dagger(\lambda)}\right)\left(a_{\boldsymbol{q}}^{(\sigma)}+a_{-\boldsymbol{q}}^{\dagger(\sigma)}\right)\left(a_{\boldsymbol{p}'}^{(\lambda')}+a_{-\boldsymbol{p}'}^{\dagger(\lambda')}\right)\left(a_{\boldsymbol{q}'}^{(\sigma')}+a_{-\boldsymbol{q}'}^{\dagger(\sigma')}\right)\right\rangle. \quad (3.120)$$

Since the bracket of the annihilation/creation operators yields $2(2\pi)^6\delta(\boldsymbol{p}+\boldsymbol{q}')\delta(\boldsymbol{p}'+\boldsymbol{q})\delta^{\lambda\sigma'}\delta^{\lambda'\sigma}$ [32], performing the q and q' integrals by using the delta functions, one obtains

$$\int \frac{\mathrm{d}^3q\,\mathrm{d}^3q'}{(2\pi)^6}\,\langle\boldsymbol{E_p}\cdot\boldsymbol{E_q}\ \boldsymbol{E_{p'}}\cdot\boldsymbol{E_{q'}}\rangle$$
$$= 2a^{-4}(\eta)a^{-4}(\eta')\partial_\eta\mathcal{A}_p(\eta)\partial_\eta\mathcal{A}_{p'}^*(\eta)\partial_{\eta'}\mathcal{A}_{p'}(\eta')\partial_{\eta'}\mathcal{A}_p^*(\eta')\left[1+(\hat{\boldsymbol{p}}\cdot\hat{\boldsymbol{p}}')^2\right]. \quad (3.121)$$

Repeating similar calculations, one can show

$$\int \frac{\mathrm{d}^3q\,\mathrm{d}^3q'}{(2\pi)^6}\,\langle\boldsymbol{E_p}\cdot\boldsymbol{E_q}\ \boldsymbol{B_{p'}}\cdot\boldsymbol{B_{q'}}\rangle$$
$$= 4a^{-4}(\eta)a^{-4}(\eta')\partial_\eta\mathcal{A}_p(\eta)\partial_\eta\mathcal{A}_{p'}^*(\eta)\,\mathcal{A}_{p'}(\eta')\mathcal{A}_p^*(\eta')\left[\boldsymbol{p}\cdot\boldsymbol{p}'\right]^2, \quad (3.122)$$
$$\int \frac{\mathrm{d}^3q\,\mathrm{d}^3q'}{(2\pi)^6}\,\langle\boldsymbol{B_p}\cdot\boldsymbol{B_q}\ \boldsymbol{B_{p'}}\cdot\boldsymbol{B_{q'}}\rangle$$
$$= 2a^{-4}(\eta)a^{-4}(\eta')\mathcal{A}_p(\eta)\mathcal{A}_{p'}^*(\eta)\mathcal{A}_{p'}(\eta')\mathcal{A}_p^*(\eta')\,p^2p'^2\left[1+(\hat{\boldsymbol{p}}\cdot\hat{\boldsymbol{p}}')^2\right]. \quad (3.123)$$

As we discussed in sec. 3.3.2.1, the magnetic field is far smaller than the electric field on super-horizon. Thus we neglect the contributions that include $\boldsymbol{B}$, namely eqs. (3.122) and (3.123), and focus on eq. (3.121). Note that this procedure underestimates eq. (3.119). Substituting eq. (3.121) into eq. (3.119), we obtain

$$\langle\zeta_{\boldsymbol{k}}^{\mathrm{em}}\zeta_{\boldsymbol{k}'}^{\mathrm{em}}\rangle > 2\delta(\boldsymbol{k}+\boldsymbol{k}')\int \mathrm{d}N\mathrm{d}N'\frac{1}{\varepsilon\,\rho_{\mathrm{inf}}}\frac{1}{\varepsilon\,\rho_{\mathrm{inf}}}\int \mathrm{d}^3p\,\mathrm{d}^3p'\delta(\boldsymbol{p}-\boldsymbol{p}'-\boldsymbol{k})$$
$$\frac{\partial_\eta\mathcal{A}_p(\eta)\partial_\eta\mathcal{A}_{p'}^*(\eta)}{a^4(\eta)}\frac{\partial_{\eta'}\mathcal{A}_{p'}(\eta')\partial_{\eta'}\mathcal{A}_p^*(\eta')}{a^4(\eta')}\left[1+(\hat{\boldsymbol{p}}\cdot\hat{\boldsymbol{p}}')^2\right]. \quad (3.124)$$

By using the definition of the curvature power spectrum eq. (3.53), eq. (3.124) can be rewritten in terms of the induced power spectrum $\mathcal{P}_\zeta^{\mathrm{em}}$ as

$$\mathcal{P}_\zeta^{\mathrm{em}}(k) > \frac{k^3}{2^3\pi^5} \int \mathrm{d}N\mathrm{d}N' \frac{1}{\varepsilon\,\rho_{\mathrm{inf}}} \frac{1}{\varepsilon\,\rho_{\mathrm{inf}}} \int \mathrm{d}^3p\,\mathrm{d}^3p'\delta(\boldsymbol{p}-\boldsymbol{p}'-\boldsymbol{k})$$
$$\frac{\partial_\eta\mathcal{A}_p(\eta)\partial_\eta\mathcal{A}_{p'}^*(\eta)}{a^4(\eta)} \frac{\partial_{\eta'}\mathcal{A}_{p'}(\eta')\partial_{\eta'}\mathcal{A}_p^*(\eta')}{a^4(\eta')} \left[1+(\hat{\boldsymbol{p}}\cdot\hat{\boldsymbol{p}}')^2\right]. \quad (3.125)$$

This expression is a general result.

Since we consider the case where the electromagnetic fields has a peak strength at $p_B \geq 1\mathrm{Mpc}^{-1}$ that is much smaller than the Planck pivot scale $k = 0.05\mathrm{Mpc}^{-1}$, the delta function $\delta(\boldsymbol{p}-\boldsymbol{p}'-\boldsymbol{k})$ in the integration in terms of $\boldsymbol{p}$ and $\boldsymbol{p}'$ can be approximated by $\delta(\boldsymbol{p}-\boldsymbol{p}')$. Performing the p' integral with $\delta(\boldsymbol{p}-\boldsymbol{p}')$, eq. (3.125) reads

$$\mathcal{P}_\zeta^{\mathrm{em}}(k) > \frac{k^3}{2^2\pi^5} \int \mathrm{d}N\mathrm{d}N'\frac{1}{\varepsilon\,\rho_{\mathrm{inf}}} \frac{1}{\varepsilon\,\rho_{\mathrm{inf}}} \int^k \mathrm{d}^3p\frac{|\partial_\eta\mathcal{A}_p(\eta)|^2}{a^4(\eta)} \frac{|\partial_{\eta'}\mathcal{A}_p(\eta')|^2}{a^4(\eta')}. \quad (3.126)$$

By using eq. (3.25), we finally obtain

$$\mathcal{P}_\zeta^{\mathrm{em}}(k) > \frac{k^3}{4\pi} \int \mathrm{d}N\mathrm{d}N'\frac{1}{\varepsilon\,\rho_{\mathrm{inf}}(\eta)} \frac{1}{\varepsilon\,\rho_{\mathrm{inf}}(\eta')} \int^k \frac{\mathrm{d}^3p}{p^6}\,\mathcal{P}_E(\eta,p)\,\mathcal{P}_E(\eta',p). \quad (3.127)$$

In the following discussion, we investigate the constraint on the inflationary magnetogenesis based on the above expression with the observed lower bound for the magnetic field given by eq. (3.109).

3.3.2.3 Model independent constraint

In this sub-subsection, we discuss the condition that the induced curvature power spectrum eq. (3.127) does not exceed the observed value. That condition leads to a general and critical constraint on the inflationary magnetogenesis scenarios.

To evaluate eq. (3.127), we adopt the strategy outlined in sec. 3.3.2.1. In eq. (3.127), the interval of the N integral should be performed from the end of inflation to the time when the electric field is produced. In the standard inflationary magnetogenesis models, the electric field is initially produced when the scale of interest exits the horizon and evolves until the end of inflation. Then the integration interval should be $N = [0, \ln|k\eta_{\mathrm{f}}|^{-1}]$ where k is the scale of interest and $N = \ln|k\eta_{\mathrm{f}}|^{-1}$ denotes a time at the exit of the horizon. However, the time dependence of the electric field from the initial time to the end of inflation is quite dependent on what model is considered. Hence, as we have discussed in sec. 3.3.2.1, to obtain the conservative constraint in a model independent way, we consider only the integration during last 1 e-folds $N = [0, 1]$ and assume that the vector potential $\mathcal{A}_k(\eta)$ is a simple power-law during that period. Moreover, we consider that the power spectrum of the electric field has a peak at a wavenumber p_B which is

related to the observed magnetic fields as shown in eq. (3.109). That is, we assume the mode function $\mathcal{A}_k(\eta)$ as

$$\mathcal{A}_k(\eta) = \left(\frac{\eta}{\eta_{\rm f}}\right)^{-n} \mathcal{A}_k(\eta_{\rm f}), \qquad (e\,\eta_{\rm f} \leq \eta \leq \eta_{\rm f},\ k \sim p_B), \tag{3.128}$$

and by substituting this into eq (3.25) we can relate the time dependent power spectrum of the electric field to that of the magnetic field at the end of inflation as

$$\mathcal{P}_E(\eta, k) = \frac{n^2}{k^2\eta^2}\mathcal{P}_B(\eta, k) = \frac{n^2}{k^2\eta^2}\left(\frac{\eta}{\eta_{\rm f}}\right)^{4-2n} \mathcal{P}_B(\eta_{\rm f}, k), \quad (e\,\eta_{\rm f} \leq \eta \leq \eta_{\rm f},\ k \sim p_B). \tag{3.129}$$

To connect the magnetic field at the end of inflation, $\eta_{\rm f}$, and the present value, we assume that no amplification of the magnetic field occurs and hence it dilutes adiabatically after inflation, $\mathcal{P}_B \propto a^{-4}$. As we discussed above eq. (3.13), the magnetic fields on small scales vanish until today due to the dissipation effect. However, such dissipation scale is about 1 AU which is much smaller than the scale of interest here and then the adiabatic dilution should be valid [58]. For simplicity, we also assume the instantaneous reheating.[17] Then $\mathcal{P}_B(\eta_{\rm f}, k)$ is directly connected with the present $\mathcal{P}_B(\eta_{\rm now}, k)$ as

$$\mathcal{P}_B(\eta_{\rm f}, k) = \frac{\rho_{\rm inf}}{\rho_\gamma}\mathcal{P}_B(\eta_{\rm now}, k), \tag{3.130}$$

where $\rho_\gamma \approx 5.2 \times 10^{-12}{\rm G}^2$ is the present energy density of radiation. The lower bound for the strength of the magnetic field given by eq. (3.109) is rewritten in terms of the power spectrum as

$$\mathcal{P}_B(\eta_{\rm now}, k) \gtrsim \mathcal{P}_B^{\rm obs}(p_B) \equiv 10^{-30}{\rm G}^2 \left(\frac{p_B}{1{\rm Mpc}^{-1}}\right), \qquad \text{for } k \sim p_B \geq 1{\rm Mpc}^{-1}. \tag{3.131}$$

Substituting eqs. (3.129), (3.130) and (3.131) into eq. (3.127), the p integral in eq. (3.127) reads

$$\int \frac{{\rm d}^3 p}{p^6}\,\mathcal{P}_E(\eta, p)\,\mathcal{P}_E(\eta', p) = \left(\frac{\rho_{\rm inf}}{\rho_\gamma}\right)^2 \frac{n^4}{\eta^2\eta'^2}\left(\frac{\eta}{\eta_{\rm f}}\right)^{4-2n}\left(\frac{\eta'}{\eta_{\rm f}}\right)^{4-2n} \int \frac{{\rm d}^3 p}{p^{10}}\,\mathcal{P}_B^2(\eta_{\rm now}, p)$$
$$\gtrsim 4\pi\left(\frac{\rho_{\rm inf}}{\rho_\gamma}\right)^2 \frac{n^4}{\eta^2\eta'^2}\left(\frac{\eta}{\eta_{\rm f}}\right)^{4-2n}\left(\frac{\eta'}{\eta_{\rm f}}\right)^{4-2n} \left(\mathcal{P}_B^{\rm obs}(p_B)\right)^2 \frac{p_B^{-7}}{7}, \tag{3.132}$$

where $e\eta_{\rm f} \leq \eta,\ \eta' \leq \eta_{\rm f}$. In the second line of the above equation, an inequality comes from the assumption that $\mathcal{P}_B(\eta_{\rm now}, p) \simeq$ constant in p for $p \sim p_B$ and $\mathcal{P}_B(\eta_{\rm now}, p) \simeq 0$ for $p \gg p_B$ and $p \ll p_B$ while it may have a finite value (see the discussion below eq. (3.109)).

---

[17]In sec. 3.3.2.4 we relax this assumption for the reheating stage and show that the similar constraint on the reheating energy scale $\rho_{\rm reh}$ can be obtained.

Then, as we have discussed in sec. 3.3.2.1, N integral within $N = [0, 1]$ in eq. (3.127) can be calculated as

$$\eta_{\mathrm{f}}^{2n-4} \int_0^1 \mathrm{d}N \, \frac{\eta^{2-2n}}{\varepsilon \, \rho_{\mathrm{inf}}} > \rho_{\mathrm{inf}}^{-1} \eta_{\mathrm{f}}^{2n-4} \int_{\eta_{\mathrm{f}}}^{e \, \eta_{\mathrm{f}}} \mathrm{d}\eta \, \eta^{1-2n} = \rho_{\mathrm{inf}}^{-1} \eta_{\mathrm{f}}^{-2} \frac{1 - e^{2-2n}}{2n - 2}, \tag{3.133}$$

where an inequality comes from the fact that we have used $0 < \varepsilon \le 1$ and $\mathrm{d}N = -aH\mathrm{d}\eta \simeq \frac{1}{1-\varepsilon}\mathrm{d}\ln\eta > \mathrm{d}\ln\eta$.[18] We have also assumed that the energy density of the inflaton ρ_{inf} does not significantly vary for the last 1 e-fold. Thus, we can obtain the conservative lower bound for the power spectrum of the curvature perturbations induced from the electromagnetic fields during inflation as

$$\mathcal{P}_\zeta^{\mathrm{em}}(k) > \frac{1}{7} \left[n^2 \frac{1 - e^{2-2n}}{2n - 2} \right]^2 \left(\frac{k}{p_B} \right)^3 e^{4N_B} \left(\frac{\mathcal{P}_B^{\mathrm{obs}}}{\rho_\gamma} \right)^2, \tag{3.134}$$

where we define $|p_B\eta_{\mathrm{f}}|^{-1} = e^{N_B}$ and N_B is the e-folding number measured between the end of inflation and a time when the p_B mode exits the horizon during inflation. N_B can be written in terms of the energy density of the inflaton ρ_{inf} and p_B as [75, 76]

$$N_B \ge 58.8 - \ln \left(\frac{p_B}{H_0} \right) + \ln \left(\frac{\rho_{\mathrm{inf}}^{1/4}}{10^{15}\mathrm{GeV}} \right), \tag{3.135}$$

where $H_0^{-1} = 4.4\mathrm{Gpc}$ is the present horizon scale and we have assumed the instantaneous reheating, and then we have

$$\mathcal{P}_\zeta^{\mathrm{em}}(k) > \frac{e^{4\times 58.8}}{7} \left[n^2 \frac{1 - e^{2-2n}}{2n - 2} \right]^2 \left(\frac{k}{p_B} \right)^3 \left(\frac{H_0}{p_B} \right)^4 \left(\frac{\mathcal{P}_B^{\mathrm{obs}}}{\rho_\gamma} \right)^2 \left(\frac{\rho_{\mathrm{inf}}^{1/4}}{10^{15}\mathrm{GeV}} \right)^4. \tag{3.136}$$

Finally, by requiring that the induced curvature perturbations given by the above expression should not exceed the observed power spectrum $\mathcal{P}_\zeta^{\mathrm{obs}}(k) = 2.2 \times 10^{-9}$ at the Planck pivot scale $k^{-1} = 20\mathrm{Mpc}$ [40], we can obtain the upper bound on the inflationary energy scale as

$$\rho_{\mathrm{inf}}^{1/4} < 30\mathrm{GeV} \left(n^2 \frac{1 - e^{2-2n}}{2n - 2} \right)^{-1/2} \left(\frac{p_B}{1\mathrm{Mpc}^{-1}} \right)^{5/4} \left(\frac{B_{\mathrm{obs}}}{10^{-15}\mathrm{G}} \right)^{-1}. \tag{3.137}$$

Here, we use B_{obs} given by $\mathcal{P}_B^{\mathrm{obs}} = B_{\mathrm{obs}}^2(p_B/1\mathrm{Mpc}^{-1})$ for $p_B \ge 1\mathrm{Mpc}^{-1}$ which is the strength of the magnetic field measured by blazar observations, as shown in sec. 3.3.2.1. The result eq. (3.137) depends on the parameter n in the factor $f(n)$ defined by

$$f(n) \equiv \left(n^2 \frac{1 - e^{2-2n}}{2n - 2} \right)^{-1/2}. \tag{3.138}$$

$f(n)$ is plotted in fig.3.6 as a function of n. In this figure, one can see $f(n) \le 1$ for $|n| \ge 1$. Therefore $f(n)$ can be roughly replaced by 1 in eq. (3.137) in the case of $|n| \ge 1$ and we obtain

---

[18] The factor $(1 - e^{2-2n})/(2n - 2)$ in eq. (3.133) should be replaced by 1 for $n = 1$.
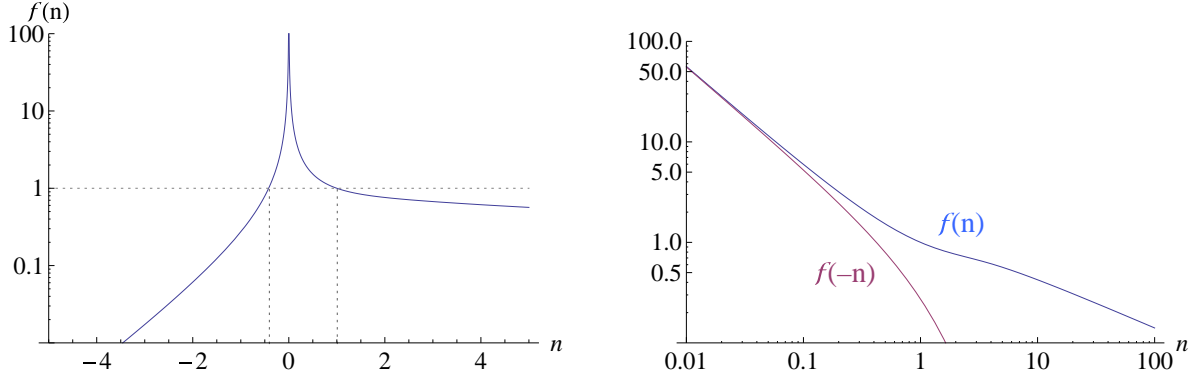
Figure 3.6 : The behavior of $f(n)$ defined in eq. (3.138). The left panel is the log plot while the right panel is the log-log plot. It is shown that $f(n) = 1$ for $n = 1$ and $n \approx -0.42$. One can easily see that $f(n) \leq 1$ for $|n| \geq 1$ and $f(n) \gg 1$ only for $|n| \ll 1$.

$$\rho_{\rm inf}^{1/4} < 30{\rm GeV} \left(\frac{p_B}{1{\rm Mpc}^{-1}} \right)^{5/4} \left(\frac{B_{\rm obs}}{10^{-15}{\rm G}} \right)^{-1}, \qquad (|n| \geq 1). \tag{3.139}$$

This is a main conclusion of this subsection.

As for the case with $|n| \ll 1$, namely $\mathcal{A}_p \simeq$ const, the constraint eq. (3.137) seems to be relaxed because the electric field, $E \propto \partial_\eta \mathcal{A}_p$, becomes very small. Nevertheless, for $|n| \ll 1$, we can obtain a tighter constraint than eq. (3.139) by the following argument. This argument is based on the discussion that in order to achieve effective inflationary magnetogenesis there must exist a time when $n \sim \mathcal{O}(1)$ during inflation even if $|n| \ll 1$ for the last one e-fold, as we have mentioned in the last part of sec. 3.3.2.1.

For the last 1 e-folding time of inflation, the magnetic power spectrum behaves as $\mathcal{P}_B \propto a^{2n-4}$ (see eqs. (3.25) and (3.114)). Thus $\mathcal{P}_B$ decreases in proportion to a^{-4} for $|n| \ll 1$, in other words, $\mathcal{P}_B$ becomes much larger as goes back in time during inflation. On the other hand, to realize the effective production of the magnetic field during inflation, $\mathcal{P}_B$ must significantly increase and hence n should reach $\mathcal{O}(1)$ at some e-folding time N_c. Let us estimate the induced $\mathcal{P}_\zeta^{\rm em}$ generated within $N = [N_c, N_c + 1]$ by assuming that $\mathcal{A}_k(\eta)$ is well approximated as

$$\mathcal{A}_k(\eta) = \left(\frac{\eta}{\eta_c} \right)^{-n} \mathcal{A}_k(\eta_c), \qquad (e\,\eta_c \leq \eta \leq \eta_c, \ k \sim p_B), \tag{3.140}$$

where $\eta_c \equiv e^{N_c}\eta_{\rm f}$. In such case, the p integral in eq. (3.127) reads

$$\int \frac{{\rm d}^3 p}{p^6} \mathcal{P}_E(p, N)\,\mathcal{P}_E(p, N')$$
$$= \left(\frac{\rho_{\rm inf}}{\rho_\gamma} \right)^2 \frac{n^4}{\eta^2 \eta'^2} \left(\frac{\eta}{\eta_c} \right)^{4-2n} \left(\frac{\eta'}{\eta_c} \right)^{4-2n} \int \frac{{\rm d}^3 p}{p^{10}} e^{8N_c} \mathcal{P}_B^2(p, \eta_{\rm now})$$
$$\gtrsim 4\pi \left(\frac{\rho_{\rm inf}}{\rho_\gamma} \right)^2 \frac{n^4}{\eta^2 \eta'^2} \left(\frac{\eta}{\eta_c} \right)^{4-2n} \left(\frac{\eta'}{\eta_c} \right)^{4-2n} \left(e^{4N_c} \mathcal{P}_B^{\rm obs}(p_B) \right)^2 \frac{p_B^{-7}}{7}. \tag{3.141}$$

This equation looks similar to eq. (3.132). However, note that since $\mathcal{P}_B \propto a^{-4}$ for $N = [0, N_c]$, the required strength of the magnetic field becomes large as $\mathcal{P}_B(p_B, \eta_c) = e^{4N_c}\mathcal{P}_B(p_B, \eta_f)$ at N_c. The time integration in eq. (3.127) is given by

$$\eta_c^{2n-4} \int_{N_c}^{N_c+1} \mathrm{d}N \eta^{2-2n} = \eta_c^{2n-4} \int_{\eta_c}^{e\,\eta_c} \mathrm{d}\eta\, \eta^{1-2n} = \eta_c^{-2} \frac{1 - e^{2-2n}}{2n - 2}. \tag{3.142}$$

In addition, the slow-roll parameter ε is much smaller than unity because N_c is taken to be a some time during inflation. Thus, $\mathcal{P}_\zeta^{\mathrm{em}}(k, \eta_c)$ is bounded as

$$\mathcal{P}_\zeta^{\mathrm{em}}(k, \eta_c) > \frac{1}{7} \left[n^2 \frac{1 - e^{2-2n}}{2n - 2} \right]^2 \left(\frac{k}{p_B} \right)^3 \left(\frac{\mathcal{P}_B^{\mathrm{obs}}}{\rho_\gamma} \right)^2 e^{4N_B} \times \left(\frac{e^{4N_c}}{\varepsilon^2} \right), \tag{3.143}$$

where we use $e^{4N_c}/(p_B\eta_c)^4 = e^{4N_B}$. Note that except for the last factor, $e^{4N_c}/\varepsilon^2 \gg 1$, this equation is same as eq. (3.134). As a result, the constraint on $\rho_{\mathrm{inf}}^{1/4}$ becomes tighter by $\sqrt{\varepsilon}e^{-N_c}$ than eq. (3.139) in cases where $|n| \ll 1$ for the last one e-fold of inflation, as

$$\rho_{\mathrm{inf}}^{1/4} < 30\mathrm{GeV} \left(\frac{p_B}{1\mathrm{Mpc}^{-1}} \right)^{5/4} \left(\frac{B_{\mathrm{obs}}}{10^{-15}\mathrm{G}} \right)^{-1} \sqrt{\varepsilon}e^{-N_c}, \qquad (|n| \ll 1). \tag{3.144}$$

The reason why the stronger constraint is obtained can be understood as follows. If the vector potential $\mathcal{A}_p$ stops growing and becomes constant during inflation ($n \sim 0$), the electric field becomes negligible. But, at the same time, the magnetic field begins to rapidly decrease, $B \propto a^{-2}$. To achieve the sufficient magnetic production, much stronger magnetic field should be generated before $\mathcal{A}_p$ stops. Therefore the induced curvature perturbation that are generated right before $\mathcal{A}_p$ stops is larger than the case with $|n| \geq 1$. [19]

Consequently, we conclude that eq. (3.139) holds as a conservative and general constraint on inflationary magnetogenesis for any n:

$$\rho_{\mathrm{inf}}^{1/4} < 30\mathrm{GeV} \left(\frac{p_B}{1\mathrm{Mpc}^{-1}} \right)^{5/4} \left(\frac{B_{\mathrm{obs}}}{10^{-15}\mathrm{G}} \right)^{-1}, \quad (p_B \geq 1\mathrm{Mpc}^{-1}). \tag{3.145}$$

3.3.2.4 Non instantaneous reheating case

In this sub-subsection, we relax the assumption of the instantaneous reheating. First, it is useful to introduce the reheating parameter [77, 78]:

$$R \equiv \left(\frac{a_{\mathrm{f}}}{a_{\mathrm{reh}}} \right) \left(\frac{\rho_{\mathrm{inf}}}{\rho_{\mathrm{reh}}} \right)^{1/4} = \left(\frac{a_{\mathrm{reh}}}{a_{\mathrm{f}}} \right)^{\frac{1-3\bar{w}}{4}} = \left(\frac{\rho_{\mathrm{reh}}}{\rho_{\mathrm{inf}}} \right)^{\frac{1-3\bar{w}}{12(1+\bar{w})}}, \tag{3.146}$$

---

[19] On the other hand, right before $\mathcal{A}_p$ stops, the physical wave length of the mode p is smaller than that at the end of inflation. Thus the hierarchy between the electric field and the magnetic field is milder (see eq. (3.113)). Although this effect somewhat weakens the constraint, the bound on ρ_{inf} becomes tighter than eq. (3.139), as a result.

where subscript "reh" denotes the end of reheating (thermalization) and $\bar{w}$ is the effective equation of state parameter that is the averaged w over the intermediate era between the end of inflation and the end of thermalization. When the assumption of the instantaneous reheating is relaxed, two equations in sec. 3.3.2.3 are modified. One is eq. (3.130) which should be modified as

$$\mathcal{P}_B(p, \eta_{\rm f}) = R^{-4} \frac{\rho_{\rm inf}}{\rho_\gamma} \mathcal{P}_B(p, \eta_{\rm now}). \tag{3.147}$$

The other is eq. (3.135) and it is changed as

$$N_B = 58.8 - \ln\left(\frac{p_B}{H_0}\right) + \ln\left(\frac{\rho_{\rm inf}^{1/4}}{10^{15}{\rm GeV}}\right) + \ln R. \tag{3.148}$$

Therefore the generalization to non-instantaneous reheating cases can be taken into account by multiplying the right hand side of eq. (3.145) by R. If $\bar{w} > 1/3$ and $R > 1$, the constraint on $\rho_{\rm inf}$ becomes milder because the dominant component of the energy density decays faster than the magnetic fields.

Nevertheless, it is important that $\rho_{\rm reh}^{1/4}$ can not be bigger than the upper bound on $\rho_{\rm inf}^{1/4}$ of the instantaneous reheating case, namely eq. (3.145). Since eq. (3.146) reads $\rho_{\rm reh}^{1/4} = R^{\frac{3(1+\bar{w})}{1-3\bar{w}}} \rho_{\rm inf}^{1/4}$, $\rho_{\rm reh}^{1/4}$ can not exceed $R^{\frac{4}{1-3\bar{w}}} \times$ (r.h.s of eq. (3.145)). On the other hand, $\rho_{\rm reh}$ is smaller than $\rho_{\rm inf}$, by definition. Except for $\bar{w} = 1/3$, the constraint on $\rho_{\rm reh}^{1/4}$ can be written as

$$\rho_{\rm reh}^{1/4} < \begin{cases} R^{\frac{4}{1-3\bar{w}}} \times 30\gamma{\rm GeV} & (\bar{w} > 1/3, \ R^{\frac{4}{1-3\bar{w}}} < 1) \\ \rho_{\rm inf}^{1/4} < R \times 30\gamma{\rm GeV} & (\bar{w} < 1/3, \ R < 1) \end{cases}, \tag{3.149}$$

where $\gamma \equiv \left(\frac{p_B}{1{\rm Mpc}^{-1}}\right)^{5/4} \left(\frac{B_{\rm obs}}{10^{-15}{\rm G}}\right)^{-1}$. Therefore the reheating (thermalization) energy scale $\rho_{\rm reh}$ is maximized in the instantaneous reheating where $R = 1$ and $\rho_{\rm inf} = \rho_{\rm reh}$.

3.3.2.5 Summary of subsection 3.3.2

In this subsection, we show that inflationary magnetogenesis is generally constrained as eq. (3.145) by requiring that the curvature perturbation induced by the electric field during inflation should be smaller than the Planck observation value: $\mathcal{P}_\zeta^{\rm obs}(k) = 2.2 \times 10^{-9}$. We emphasize that our argument is model independent as we outlined in sec. 3.3.2.1. The main result eq. (3.145) indicates that inflationary magnetogenesis is under pressure in several ways.

First, it is known that the reheating (thermalization) energy scale is bounded as $\rho_{\rm reh}^{1/4} \gtrsim 10{\rm MeV}$ in order to achieve a successful BBN [79]. Therefore even if eq. (3.145) is almost saturated, for example $\rho_{\rm inf}^{1/4} \sim 10{\rm GeV}$, the reheating should be quickly completed.

Second, the generation of the observed curvature perturbation is in danger. Eq. (3.145) can be translated as

$$H_{\rm inf} < 2 \times 10^{-7}{\rm eV} \left(\frac{p_B}{1{\rm Mpc}^{-1}}\right)^{5/2} \left(\frac{B_{\rm obs}}{10^{-15}{\rm G}}\right)^{-2}, \tag{3.150}$$

where $H_{\rm inf}$ is the Hubble parameter during inflation. For a scalar field to acquire a perturbation during inflation, its mass should be smaller than $H_{\rm inf}$. Thus inflaton field or a spectator field which is responsible to produce $\mathcal{P}_\zeta^{\rm obs}$ must be extremely light during inflation. During reheating era, however, it has to quickly decay into the standard model particles to cause the BBN properly. Furthermore, in the case of single slow roll inflation, eq.(3.150) and the COBE normalization indicate an extreme slow-roll $\varepsilon < 4 \times 10^{-62}$ which demands a dedicated inflation model. It is interesting to note that eq.(3.150) corresponds to the very small tensor-to-scalar ratio, $r < 7 \times 10^{-61}$. Hence a detection of background gravitational waves in the future excludes inflationary magnetogenesis. [20]

Third, in such a low reheating temperature, thermal production of the dark matter or the baryon number seems hopeless. Since 30GeV is accessible by particle accelerators, effects beyond the standard model have been severely restricted. To realize the dark matter production and baryogenesis, a non-thermal mechanism like the direct decay of inflaton should be considered.

In spite of these negative implications, since we have the observational evidence of the magnetic fields in the universe and we are lack of a plausible magnetogenesis model, the inflationary origin of the magnetic field is still an appealing idea. It should be noted that we assume no amplification of the magnetic fields after inflation to derive eq. (3.145). Thus our result might imply that inflationary magnetogenesis need an additional amplification or a non-adiabatic dilution of magnetic fields after inflation. If the magnetic field generated during inflation is amplified by some mechanism like preheating process [23] or the inverse cascade the constraint is alleviated.

Another possible way out from our constraint is to produce a large amplitude of the vector potential before the horizon crossing. It is known that, in the so-called strong coupling regime of the kinetic coupling model, the electric field is not much stronger than the magnetic field and the backreaction and curvature perturbation problems are evaded (if loop effects are neglected) [28]. This is because the vector potential $\mathcal{A}_k$ is almost constant on super-horizon ($n \simeq 0$ in our language). The magnetic field is produced since $\mathcal{A}_k$ has a large amplitude at the horizon crossing due to the small kinetic function. However, as discussed below eq. (3.116), such a model suffers from the strong coupling problem and reliable calculations are difficult to be done. If a large amplitude of a static vector potential is realized without the strong coupling or one can take into account the loop effects in some non-perturbative way, sufficient magnetogenesis might be achieved.

---

[20]See ref. [76] in which our model-independent constraint is followed up in the light of the BICEP2 result [80].

3.4   Post-Inflationary Amplification in IFF Model

In the earlier sections, we review a conventional model of inflationary magnetogenesis, namely the kinetic coupling model, and find that the model cannot generate primordial magnetic field which is strong enough to explain the observations. We also derive model-independent constraints on inflationary magnetogenesis based on the back reaction problem and the curvature perturbation problem. Now we know that it is considerably difficult to generate primordial magnetic fields with the sufficient strength only during inflation.

Therefore, we seek the possibility to amplify the magnetic fields after inflation in this section. It should be noted that we consider only the cases where primordial magnetic fields are generated during inflation and an amplification mechanism works in addition to that. Hence this possibility is still classified as inflationary magnetogenesis.

In this section, we examine the possibility that an amplification of the magnetic fields occurs between the end of inflation and reheating in the framework of the kinetic coupling model. Since $I(\eta)$ in the kinetic coupling model can continue to vary even after inflation if I is driven by a spectator scalar field which is not inflaton, the magnetic field can be amplified after inflation. Indeed, in ref. [35], Kobayashi proposed a behavior of the kinetic function $I(\eta)$ with which the magnetic field is substantially amplified after the end of inflation. Since he claimed the primordial magnetic field with the strength 10^{-15}G on Mpc scale can be generated in his model, it deserves scrutiny here.

Unfortunately, however, this model is under pressure by the curvature perturbation problem as we will see in sec. 3.4.2 and sec. 3.4.3. The curvature perturbation problem described in sec. 3.2.3 and sec. 3.3.2 refers to the curvature perturbation induced by the electromagnetic fields *during inflation*. On the other hand, the electromagnetic fields reach their maximum value *during the inflaton oscillating phase* in Kobayashi's model and hence we should calculate the curvature perturbation produced in the period. The calculation can be done in a similar manner because the only difference is the background evolution. With the proposed model parameters given in ref. [35], it is found that the non-linear parameter f_{NL} of the induced curvature perturbation is larger than the observational upper bound by the factor of $\mathcal{O}(10^4)$. Therefore the generation of the 10^{-15}G magnetic field on Mpc scale in this model with the proposed parameters is inconsistent with the CMB observation.

3.4.1   Brief review on the model

In ref. [35], the author has shown primordial magnetic fields can be significantly amplified after inflation. He considered the kinetic coupling model (see sec. 3.2 for a review on the

original work), and the following behavior of the kinetic function I.

$$I(a) = \begin{cases} I_1(a/a_1)^{-s} & (a_{\text{IR}} < a < a_1) \\ I_1 & (a_1 < a < a_2) \\ I_1(a/a_2)^{-n} & (a_2 < a < a_3) \\ I_1(a_3/a_2)^{-n} \equiv I_f & (a_3 < a) \end{cases} , \tag{3.151}$$

where inflation ends at $a = a_e$ between a_1 and a_2, namely $a_1 < a_{\text{e}} < a_2$. This behavior is shown in fig. 3.7. This rather complicated behavior looks artificial, while we consider it as a toy model and do not discuss how to realize it.

The mode function of the vector potential $\mathcal{A}_k(\eta)$ can be solved with the Bunch-Davies initial condition, eq. (3.23). Before I stops at $a = a_1$, $\mathcal{A}_k$ on super-horizon is given by

$$I A_k = \frac{\Gamma(s - 1/2)}{\sqrt{2\pi k}} \left(\frac{2a H_{\text{inf}}}{k} \right)^{s-1}, \qquad (|k\eta| \ll 1, \ a < a_1). \tag{3.152}$$

Since the power spectrum of electric and magnetic fields are defined as eq. (3.25), the power spectra during inflation are obtained as

$$I^2 \mathcal{P}_B(a < a_1) = \frac{8\Gamma^2(s - 1/2)}{\pi^3} H_{\text{inf}}^4 \left(\frac{2a H_{\text{inf}}}{k} \right)^{2(s-3)},$$

$$I^2 \mathcal{P}_E(a < a_1) = \frac{8\Gamma^2(s + 1/2)}{\pi^3} H_{\text{inf}}^4 \left(\frac{2a H_{\text{inf}}}{k} \right)^{2(s-2)}. \tag{3.153}$$

Next, I stops varying at $a = a_1$. When I is constant, the mode function behaves as a plane wave, $I A_k = C_+ e^{-ik\eta} + C_- e^{ik\eta}$, and the power spectra decay as a usual radiation component, $\mathcal{P}_E, \mathcal{P}_B \propto a^{-4}$. Thus it is easily shown

$$\mathcal{P}_B = 4s^2 \left(\frac{a_1}{a} \right)^4 \mathcal{P}_B(a_1), \quad \mathcal{P}_E = \left(\frac{a_1}{a} \right)^4 \mathcal{P}_E(a_1), \quad (a_1 < a < a_2), \tag{3.154}$$
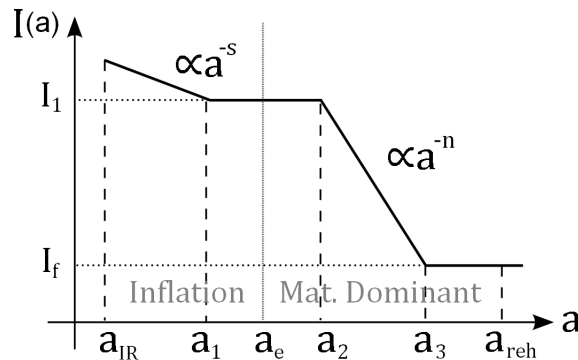

Figure 3.7 : The behavior of $I(a)$ given in eq. (3.151). $a_{\text{IR}}, a_{\text{e}}$ and a_{reh} denote the scale factor at the onset of magnetogenesis, the end of inflation and at reheating, respectively.

where the $4s^2$ factor in $\mathcal{P}_B$ comes from the junction condition at $a = a_1$.

At $a = a_2$, I begins to vary again. Note that for $a_e < a < a_{\rm reh}$, the inflaton is oscillating and the evolution of the scale factor a is assumed to be the one in the matter dominated (MD) universe,

$$\eta = \frac{2}{aH} \propto a^{\frac{1}{2}} \quad \Longrightarrow \quad I \propto a^{-n} \propto \eta^{-2n}. \tag{3.155}$$

Then the mode function for a super-horizon mode is given by

$$A_k = D_1 + D_2 \eta^{4n+1}, \quad (|k\eta| \ll 1, \ a_2 < a < a_3), \tag{3.156}$$

where D_1 and D_2 are constant which are determined by the junction condition at a_2. One can show that the power spectra for super horizon modes are given by

$$I^2 \mathcal{P}_B(a) = \left(\frac{4s - 2}{4n + 1}\right)^2 I^2 \left(\frac{a_1}{a}\right)^4 \left(\frac{a}{a_2}\right)^{4n} \left(\frac{a_1 H_{\rm inf}}{aH}\right)^2 \mathcal{P}_B(a_1) \propto a^{2n-3},$$

$$I^2 \mathcal{P}_E(a) = I^2 \left(\frac{a_1}{a}\right)^4 \left(\frac{a}{a_2}\right)^{4n} \mathcal{P}_E(a_1) \propto a^{2n-4}, \qquad (|k\eta| \ll 1, \ a_2 < a < a_3). \tag{3.157}$$

Here we assume that the oscillation phase lasts sufficiently long,

$$\left(\frac{a}{a_2}\right)^{2n} \frac{a_1 H_{\rm inf}}{aH} = \left(\frac{a}{a_2}\right)^{2n} \frac{a_1}{a_e} \sqrt{\frac{a}{a_e}} \gg 1, \tag{3.158}$$

and the growing part of $\mathcal{A}_k$ (the second term in eq. (3.156)) is dominant. In this period, although inflation has already ended, the magnetic field can be rapidly amplified due to the varying I. Thus a post-inflationary amplification is realized in the kinetic coupling model.

One also sees in eq. (3.157) that the magnetic field grows faster than the electric field by $a^{1/2}$ in this period. This is because of the behavior of the conformal time. For $\mathcal{A}_k \propto \eta^m$, the ratio between the magnetic and the electric power spectrum is obtained as

$$\frac{\mathcal{P}_B}{\mathcal{P}_E} = \frac{k^2 |\mathcal{A}_k|^2}{|\partial_\eta \mathcal{A}_k|^2} = \frac{k^2 \eta^2}{m^2} \propto \begin{cases} a^{-2} & \text{(inflation)} \\ a & \text{(MD)} \end{cases}. \tag{3.159}$$

Therefore the hierarchy between $\mathcal{P}_B$ and $\mathcal{P}_E$ is being relaxed during MD era. [21]

Finally, I reaches its final value I_f and stops varying at a_3. Again, the plane wave, $\mathcal{A}_k(\eta) = \tilde{C}_+ e^{-ik\eta} + \tilde{C}_- e^{ik\eta}$, is the solution and the junction condition fixes the coefficients $\tilde{C}_\pm$. One can show that the resultant power spectra are

$$I^2 \mathcal{P}_B(a) = (4s - 2)^2 I_f^2 \left(\frac{a_1}{a}\right)^4 \left(\frac{a_3}{a_2}\right)^{4n} \left(\frac{a_1 H_{\rm inf}}{aH}\right)^2 \mathcal{P}_B(a_1) \propto a^{-3},$$

$$I^2 \mathcal{P}_E(a) = I_f^2 \left(\frac{a_1}{a}\right)^4 \left(\frac{a_3}{a_2}\right)^{4n} \mathcal{P}_E(a_1) \propto a^{-4}, \qquad (|k\eta| \ll 1, \ a_3 < a < a_{\rm reh}). \tag{3.160}$$

---

[21] If the equation of state parameter is w, this ratio reads $\mathcal{P}_B/\mathcal{P}_E \propto a^{1+3w}$. Thus during the radiation dominant era ($w = 1/3$), for example, this ratio increases more rapidly, $\mathcal{P}_B/\mathcal{P}_E \propto a^2$.

Here $\mathcal{P}_B$ is proportional to not a^{-4} but a^{-3} because the plane wave on super-horizon scales is approximated as

$$\frac{\sin^2[k(\eta - \eta_3)]}{a^4} \simeq \frac{k^2\eta^2}{a^4} \propto a^{-3}, \qquad \text{(MD)}. \tag{3.161}$$

Using $I_1/I_f = (a_3/a_2)^n$ and considering the vector potential is freezed after reheating (see the discussion below eq. (3.28)), one obtains the magnetic power spectrum for $a > a_{\text{reh}}$ as

$$\mathcal{P}_B(a > a_{\text{reh}}) = \frac{128\Gamma^2(s+1/2)}{\pi^3} \left(\frac{a_1}{a}\right)^4 \left(\frac{a_3}{a_2}\right)^{2n} \left(\frac{a_1 H_{\text{inf}}}{a_{\text{reh}} H_{\text{reh}}}\right)^2 \left(\frac{2a H_{\text{inf}}}{k}\right)^{2(s-3)} H_{\text{inf}}^4. \tag{3.162}$$

This is the main result in ref. [35].

In ref. [35], the author discussed the case with following parameters as an example.

$$H_{\text{inf}} = 10^{-6} M_{\text{Pl}} \simeq 10^{12}\text{GeV}, \quad H_{\text{reh}} = 10^{-21}\text{GeV} \ (T_{\text{reh}} \simeq 50\text{MeV}), \tag{3.163}$$

$$s = \frac{5}{2}, \quad n = 6, \tag{3.164}$$

$$a_{\text{IR}} H_{\text{inf}} = 10^{-6}\text{Mpc}^{-1}, \quad a_1 H_{\text{inf}} = 10^4\text{Mpc}^{-1}, \tag{3.165}$$

$$\frac{a_3}{a_2} = 1.4 \times 10^6, \quad \frac{a_{\text{reh}}}{a_3} = 10, \tag{3.166}$$

which correspond to $H_2 \simeq 10^{-10}\text{GeV}$ and $H_3 \simeq 10^{-20}\text{GeV}$. These parameters give $\mathcal{P}_B \sim 10^{-15}\text{G}$ on Mpc scale without the backreaction problem [22],

$$\frac{\rho_{\text{EM}}(a_1)}{3M_{\text{Pl}}^2 H_1^2} \sim 10^{-3}, \quad \frac{\rho_{\text{EM}}(a_3)}{3M_{\text{Pl}}^2 H_3^2} \sim 10^{-1}. \tag{3.167}$$

However, the curvature perturbation problem was not considered there. If the amplitude or the non-gaussianities of the curvature perturbation induced by the generated electromagnetic fields exceed the observed value or the observational upper bound, the model is excluded. Therefore the induced curvature perturbation should be explored.

3.4.2   The induced curvature perturbation

In this subsection, we calculate the amplitude and the non-gaussianity of the curvature perturbation induced by the generated electric field in the model discussed in ref. [35] with the parameter shown in the previous section.

---

[22]For $a_{\text{e}} < a \leq a_3$, inflation has already ended and it is not a problem if the electromagnetic fields dominate the universe. However, since the electromagnetic fields grow due to the varying I which is driven by not inflaton but a spectator field, the energy density of the spectator field is expected to be larger than the electromagnetic field. Otherwise its dynamics would be significantly affected by the electromagnetic fields.

3.4.2.1 The electric energy density

From eq. (3.153) and eq. (3.160) (or eq. (4.14) in ref. [35]), we see that when $a_3 < a < a_{\text{reh}}$, the electric power spectrum for the super-horizon modes $k \ll a_1 H_{\text{inf}}$ is

$$\mathcal{P}_E \simeq \frac{k^4 \Gamma^2(s + \frac{1}{2})}{2\pi^3 I_f^2 a^4} \left(\frac{a_3}{a_2}\right)^{2n} \left(\frac{2a_1 H_{\text{inf}}}{k}\right)^{2s}. \tag{3.168}$$

Substituting

$$s = \frac{5}{2}, \quad n = 6, \tag{3.169}$$

one finds

$$\mathcal{P}_E \simeq \frac{2^6}{\pi^3 I_f^2} \left(\frac{a_3}{a_2}\right)^{12} (a_1 H_{\text{inf}})^5 \frac{k^{-1}}{a_{\text{reh}}^4} \left(\frac{a_{\text{reh}}}{a}\right)^4. \tag{3.170}$$

Then we also use

$$\frac{a_3}{a_2} = 1.4 \times 10^6, \quad a_1 H_{\text{inf}} = 10^4 \text{Mpc}^{-1}, \quad a_{\text{reh}}^2 \approx 3 \times 10^{-63} \frac{M_{\text{Pl}}}{H_{\text{reh}}}, \tag{3.171}$$

with $H_{\text{reh}} = 10^{-21} \text{GeV}$ and obtain

$$\mathcal{P}_E \approx 3.7 \times 10^{-13} \text{GeV}^4 I_f^{-2} \left(\frac{k^{-1}}{\text{Mpc}}\right) \left(\frac{a_{\text{reh}}}{a}\right)^4. \tag{3.172}$$

Remembering $\rho_E(k) = \frac{I^2}{2} \mathcal{P}_E(k)$ and $I(\eta) = I_f$ for $a > a_3$, the electric energy spectrum is given by

$$\rho_E(k) \approx 2 \times 10^{-13} \text{GeV}^4 \left(\frac{k^{-1}}{\text{Mpc}}\right) \left(\frac{a_{\text{reh}}}{a}\right)^4, \quad (k < a_1 H_{\text{inf}}, \ a_3 < a < a_{\text{reh}}). \tag{3.173}$$

Since $k_{\text{IR}} \simeq 10^{-6} \text{Mpc}^{-1}$, $\rho_E(k_{\text{IR}})$ reaches $2 \times 10^{-7} \text{GeV}^4$ at reheating. On the other hand, the total energy density is

$$\rho_{\text{tot}} = 3 M_{\text{Pl}}^2 H_{\text{reh}}^2 \left(\frac{a_{\text{reh}}}{a}\right)^3 \approx 2 \times 10^{-5} \text{GeV}^4 \left(\frac{a_{\text{reh}}}{a}\right)^3. \tag{3.174}$$

Thus the large scale electric field accounts for $\approx 1\%$ of the total energy density of the universe at a_{reh} and even $\approx 10\%$ at $a_3 = a_{\text{reh}}/10$. Such a large amount of isocurvature perturbation on large scale causes the curvature perturbation problem.

3.4.2.2 The curvature perturbation induced by the electric field

It has been well known that the curvature perturbation is constant on super-horizon scales if any isocurvature component does not exist as we see in eq. (3.35). However, we now have a considerable isocurvature component and hence the curvature perturbation can grow even on super-horizon scales.

Substituting the non-adiabatic pressure $\delta p = \rho^{\text{em}}/3$ and the background behavior $\dot{p}/\dot{\rho} \simeq 9H^2/4m^2 \ll 1$ for the oscillating inflaton [23] into eq. (3.35) and performing the time integration, we obtain the curvature perturbations induced from the electromagnetic field as

$$\zeta_{\boldsymbol{k}}^{\text{em}} \simeq \frac{1}{3} \int dt \, \frac{H \rho_{\boldsymbol{k}}^{\text{em}}}{\rho_{\text{tot}}}. \tag{3.175}$$

The energy density of the electromagnetic field in Fourier space $\rho_{\boldsymbol{k}}^{\text{em}}$ is given by

$$\rho_{\boldsymbol{k}}^{\text{em}} = \frac{I^2}{2} \int \frac{\mathrm{d}^3 p \, \mathrm{d}^3 q}{(2\pi)^3} \delta(\boldsymbol{p} + \boldsymbol{q} - \boldsymbol{k}) \left[\boldsymbol{E}(\eta, \boldsymbol{p}) \cdot \boldsymbol{E}(\eta, \boldsymbol{q}) + \boldsymbol{B}(\eta, \boldsymbol{p}) \cdot \boldsymbol{B}(\eta, \boldsymbol{q}) \right]. \tag{3.176}$$

Note since $\rho^{\text{em}} \propto (\boldsymbol{E}^2 + \boldsymbol{B}^2)$ in the real space, $\rho_{\boldsymbol{k}}^{\text{em}}$ is written in terms of the convolution of the electromagnetic fields. Ignoring the subdominant contribution from the magnetic fields, and remembering the super-horizon electric field is written as

$$E_i(\boldsymbol{k}) = a^{-2} \partial_\eta \mathcal{A}_k(\eta) \sum_{\lambda=1}^{2} \varepsilon_i^{(\lambda)}(\hat{\boldsymbol{k}}) \left[a_{\boldsymbol{k}}^{(\lambda)} + a_{-\boldsymbol{k}}^{\dagger(\lambda)} \right], \tag{3.177}$$

where $\varepsilon_i^{(\lambda)}$ is the polarization vector and $a_{\boldsymbol{k}}$ is the annihilation operator, we obtain

$$\begin{aligned}
\zeta_{\boldsymbol{k}}^{\text{em}} \simeq &\frac{1}{6} \int dt \, H(t) \int \frac{\mathrm{d}^3 p \, \mathrm{d}^3 q}{(2\pi)^3} \delta(\boldsymbol{p} + \boldsymbol{q} - \boldsymbol{k}) \frac{I^2 \partial_\eta \mathcal{A}_p \partial_\eta \mathcal{A}_q}{a^4 \rho_{\text{tot}}} \\
&\times \sum_{\lambda, \sigma} \varepsilon_i^{(\lambda)}(\hat{\boldsymbol{p}}) \, \varepsilon_i^{(\sigma)}(\hat{\boldsymbol{q}}) \left(a_{\boldsymbol{p}}^{(\lambda)} + a_{-\boldsymbol{p}}^{\dagger(\lambda)} \right) \left(a_{\boldsymbol{q}}^{(\sigma)} + a_{-\boldsymbol{q}}^{\dagger(\sigma)} \right),
\end{aligned} \tag{3.178}$$

where we use the fact that the mode function $\mathcal{A}_k$ is a real number up to a constant phase on super-horizon scales.

---

[23] Approximating the oscillationg inflaton by $\phi = \phi_i (a/a_i)^{-3/2} \cos(mt)$ where a_i denotes a certain time after the onset of the oscillation, ϕ_i is the field value at the time and m is the mass of the inflaton, and taking the one cycle average, one can show $\dot{p}/\dot{\rho} \simeq 9H^2/4m^2 \ll 1$.

3.4.2.3   The calculation of the curvature power spectrum

From eq. (3.178), it can be shown that the power spectrum of the induced curvature perturbation is given by

$$
(2\pi)^3\delta(\boldsymbol{k}_1 - \boldsymbol{k}_2)\frac{2\pi^2}{k_1^3}\mathcal{P}_\zeta^{\mathrm{em}}(k_1) = \left\langle \zeta_{\boldsymbol{k}_1}^{\mathrm{em}}\zeta_{\boldsymbol{k}_2}^{\mathrm{em}*}\right\rangle
$$

$$
\simeq \frac{1}{36}\int \mathrm{d}\tilde{t}\mathrm{d}t' H(\tilde{t})H(t')\int \frac{\mathrm{d}^3p_1\mathrm{d}^3q_1\mathrm{d}^3p_2\mathrm{d}^3q_2}{(2\pi)^6}\delta(\boldsymbol{p}_1 + \boldsymbol{q}_1 - \boldsymbol{k}_1)\delta(\boldsymbol{p}_2 + \boldsymbol{q}_2 - \boldsymbol{k}_2)
$$

$$
\times \frac{I^2\partial_{\eta_1}\mathcal{A}_{p_1}\partial_{\eta_1}\mathcal{A}_{q_1}}{a^4\rho_{\mathrm{tot}}}(\tilde{t})\frac{I^2\partial_{\eta_2}\mathcal{A}_{p_2}\partial_{\eta_2}\mathcal{A}_{q_2}}{a^4\rho_{\mathrm{tot}}}(t')
$$

$$
\times \sum_{\lambda,\sigma}\varepsilon_{j_1}^{(\lambda_1)}(\hat{\boldsymbol{p}}_1)\varepsilon_{j_1}^{(\sigma_1)}(\hat{\boldsymbol{q}}_1)\varepsilon_{j_2}^{(\lambda_2)*}(\hat{\boldsymbol{p}}_2)\varepsilon_{j_2}^{(\sigma_2)*}(\hat{\boldsymbol{q}}_2)
$$

$$
\times \left\langle \left(a_{\boldsymbol{p}_1}^{(\lambda_1)} + a_{-\boldsymbol{p}_1}^{\dagger(\lambda_1)}\right)\left(a_{\boldsymbol{q}_1}^{(\sigma_1)} + a_{-\boldsymbol{q}_1}^{\dagger(\sigma_1)}\right)\left(a_{\boldsymbol{p}_2}^{(\lambda_2)\dagger} + a_{-\boldsymbol{p}_2}^{(\lambda_2)}\right)\left(a_{\boldsymbol{q}_2}^{(\sigma_2)\dagger} + a_{-\boldsymbol{q}_2}^{(\sigma_2)}\right)\right\rangle
$$

$$
= \frac{2}{36}\delta(\boldsymbol{k}_1 - \boldsymbol{k}_2)\int \mathrm{d}\tilde{t}\mathrm{d}t' H(\tilde{t})H(t')\int \mathrm{d}^3p_1\mathrm{d}^3p_2\,\delta(\boldsymbol{p}_1 + \boldsymbol{p}_2 - \boldsymbol{k}_1)
$$

$$
\times \frac{I^2\partial_{\eta_1}\mathcal{A}_{p_1}\partial_{\eta_1}\mathcal{A}_{p_2}}{a^4\rho_{\mathrm{tot}}}(\tilde{t})\frac{I^2\partial_{\eta_2}\mathcal{A}_{p_2}\partial_{\eta_2}\mathcal{A}_{p_1}}{a^4\rho_{\mathrm{tot}}}(t')\left(\delta_{j_1j_2} - (\hat{\boldsymbol{p}}_1)_{j_1}(\hat{\boldsymbol{p}}_1)_{j_2}\right)\left(\delta_{j_1j_2} - (\hat{\boldsymbol{p}}_2)_{j_1}(\hat{\boldsymbol{p}}_2)_{j_2}\right).
$$

$$(3.179)$$

For simplicity, let us focus on the generation of the curvature perturbation only when $a_3 < a < a_{\mathrm{reh}}$ and only for $k_{\mathrm{IR}} < k < a_1 H_{\mathrm{inf}}$. Note that this treatment underestimates the induced curvature perturbation and hence the resultant constraint is conservative. Eq. (3.173) can be rewritten as

$$
a^{-2}I\partial_\eta\mathcal{A}_k = \sqrt{2\pi^2 k^{-3}\rho_E(k)} \simeq 2\times 10^{-6}k^{-2}\left(\frac{a_{\mathrm{reh}}}{a}\right)^2\mathrm{GeV}^2\mathrm{Mpc}^{-\frac{1}{2}}. \tag{3.180}
$$

With eq. (3.174), one also finds

$$
H\frac{I^2\partial_{\eta_1}\mathcal{A}_{p_1}\partial_{\eta_1}\mathcal{A}_{p_2}}{a^4\rho_{\mathrm{tot}}}(t) \approx 2\times 10^{-7}H_{\mathrm{reh}}\left(\frac{t}{t_3}\right)^{-\frac{5}{3}}(p_1p_2)^{-2}\mathrm{Mpc}^{-1}. \tag{3.181}
$$

The time integral with $t = [t_3, t_{\mathrm{reh}}]$ yields

$$
\int_{t_3}^{t_{\mathrm{reh}}}\mathrm{d}\tilde{t}\,H\frac{I^2\partial_{\eta_1}\mathcal{A}_{p_1}\partial_{\eta_1}\mathcal{A}_{p_2}}{a^4\rho_{\mathrm{tot}}}(\tilde{t})
$$

$$
\approx 2\times 10^{-7}\left[\left(\frac{t_{\mathrm{reh}}}{t_3}\right)^{\frac{2}{3}} - 1\right](p_1p_2)^{-2}\mathrm{Mpc}^{-1},
$$

$$
\approx 2\times 10^{-6}(p_1p_2)^{-2}\mathrm{Mpc}^{-1}. \tag{3.182}
$$

Then we obtain

$$
\mathcal{P}_\zeta^{\mathrm{em}}(k) \gtrsim \frac{k^3(2\times 10^{-6})^2}{(2\pi)^3 2\pi^2 18}\mathrm{Mpc}^{-2}\int \mathrm{d}^3p_1\mathrm{d}^3p_2\,\delta(\boldsymbol{p}_1 + \boldsymbol{p}_2 - \boldsymbol{k}_1)\frac{1 - (\hat{\boldsymbol{p}_1}\cdot\hat{\boldsymbol{p}_2})^2}{p_1^4 p_2^4}. \tag{3.183}
$$

This momentum integral can be evaluated by focusing on the identical two pole contributions from $p_1 \sim k_{\mathrm{IR}}$ and $p_2 \sim k_{\mathrm{IR}}$ as

$$
\int \mathrm{d}^3 p_1 \mathrm{d}^3 p_2 \, \delta(\boldsymbol{p_1} + \boldsymbol{p_2} - \boldsymbol{k_1}) \frac{1 - (\hat{\boldsymbol{p_1}} \cdot \hat{\boldsymbol{p_2}})^2}{p_1^4 p_2^4}
$$
$$
\simeq \frac{2}{k^4} \int_{k_{\mathrm{IR}}} \mathrm{d}^3 p \frac{1 - (\hat{\boldsymbol{p}} \cdot \hat{\boldsymbol{k}})^2}{p^4}
$$
$$
= \frac{4\pi}{k^4} \int_{k_{\mathrm{IR}}} \frac{\mathrm{d}p}{p^2} \int_{-1}^{1} \mathrm{d}(\cos\theta) \left[1 - \cos^2\theta \right]
$$
$$
= \frac{16\pi}{3k^4} \int_{k_{\mathrm{IR}}} \frac{\mathrm{d}p}{p^2} \simeq \frac{16\pi}{3k^4 k_{\mathrm{IR}}}, \tag{3.184}
$$

where we use $k_{\mathrm{IR}} \ll k$. Thus finally we obtain

$$
\mathcal{P}_\zeta^{\mathrm{em}} \gtrsim 4 \times 10^{-7} \left(\frac{0.002 \mathrm{Mpc}^{-1}}{k_{\mathrm{CMB}}} \right) \left(\frac{10^{-6} \mathrm{Mpc}^{-1}}{k_{\mathrm{IR}}} \right). \tag{3.185}
$$

This value is larger than the Planck observation result [40], $\mathcal{P}_\zeta^{\mathrm{obs}} \approx 2.2 \times 10^{-9}$, and hence the model in ref. [35] with his choice of parameters is excluded.

With the parameters given in eq. (3.166), the electric power spectrum $\mathcal{P}_E(k)$ has a peak at $k = k_{\mathrm{IR}}$ which is a far larger scale than the CMB scale, $k_{\mathrm{IR}} \ll k_{\mathrm{CMB}}$. However, the electric mode at the large scale contributes to induce the curvature perturbation at the CMB scale because the electric energy density is given by the squared of the electric field $\rho_E \propto \boldsymbol{E}^2$, it becomes the convolution in the Fourier space and it contributes to different scales.

3.4.3 Calculation of f_{NL}

Next, let us compute the bispectrum of the curvature perturbation induced by the electric field when $a_3 < a < a_{\mathrm{reh}}$ and for $k_{\mathrm{IR}} < k < a_1 H_{\mathrm{inf}}$. From eq. (3.178), the three-point correlation function of the induced curvature perturbation in Fourier space is given by

$$
\langle \zeta^{\mathrm{em}}(\boldsymbol{k_1}) \zeta^{\mathrm{em}}(\boldsymbol{k_2}) \zeta^{\mathrm{em}}(\boldsymbol{k_3}) \rangle (t_{\mathrm{reh}}) \gtrsim \left\langle \prod_{i=1}^{3} \frac{1}{6} \int_{t_3}^{t_{\mathrm{reh}}} dt_i H(t_i) \int_{k_{\mathrm{IR}}}^{a_1 H_{\mathrm{inf}}} \frac{\mathrm{d}^3 p_i \, \mathrm{d}^3 q_i}{(2\pi)^3} \delta(\boldsymbol{p_i} + \boldsymbol{q_i} - \boldsymbol{k_i}) \right.
$$
$$
\left. \times \frac{I^2 \partial_{\eta_i} \mathcal{A}_{p_i} \partial_{\eta_i} \mathcal{A}_{q_i}}{a^4 \rho_{\mathrm{tot}}} (t_i) \sum_{\lambda_i, \sigma_i} \varepsilon_{j_i}^{(\lambda_i)}(\hat{\boldsymbol{p}}_i) \varepsilon_{j_i}^{(\sigma_i)}(\hat{\boldsymbol{q}}_i) \left(a_{\boldsymbol{p_i}}^{(\lambda_i)} + a_{-\boldsymbol{p_i}}^{\dagger(\lambda_i)} \right) \left(a_{\boldsymbol{q_i}}^{(\sigma_i)} + a_{-\boldsymbol{q_i}}^{\dagger(\sigma_i)} \right) \right\rangle, \tag{3.186}
$$

where the inequality sign represents that the r.h.s underestimates the bispectrum because of the limited time and momentum integrals. It can be shown that the expectation value of the creation/annihilation operators yield

$$
\left\langle \prod_{i=1}^{3} \left(a_{\boldsymbol{p_i}}^{(\lambda_i)} + a_{-\boldsymbol{p_i}}^{\dagger(\lambda_i)} \right) \left(a_{\boldsymbol{q_i}}^{(\sigma_i)} + a_{-\boldsymbol{q_i}}^{\dagger(\sigma_i)} \right) \right\rangle
$$
$$
= 8(2\pi)^9 \delta(\boldsymbol{p_1} + \boldsymbol{q_2}) \delta(\boldsymbol{p_2} + \boldsymbol{q_3}) \delta(\boldsymbol{p_3} + \boldsymbol{q_1}) \delta^{\lambda_1 \sigma_2} \delta^{\lambda_2 \sigma_3} \delta^{\lambda_3 \sigma_1}. \tag{3.187}
$$

Using these delta functions and the Kronecker deltas, one finds that eq. (3.186) reads,

$$
\langle \zeta^{\rm em}(\boldsymbol{k}_1)\zeta^{\rm em}(\boldsymbol{k}_2)\zeta^{\rm em}(\boldsymbol{k}_3)\rangle (t_{\rm reh}) \gtrsim 6^{-3} \int_{t_3}^{t_{\rm reh}} dt_1 dt_2 dt_3
$$

$$
\times \int_{k_{\rm IR}}^{a_1 H_{\rm inf}} d^3p_1 d^3p_2 d^3p_3 \delta(\boldsymbol{p}_1 - \boldsymbol{p}_3 - \boldsymbol{k}_1)\delta(\boldsymbol{p}_2 - \boldsymbol{p}_1 - \boldsymbol{k}_2)\delta(\boldsymbol{p}_3 - \boldsymbol{p}_2 - \boldsymbol{k}_3)
$$

$$
\times H \frac{I^2 \partial_{\eta_1}\mathcal{A}_{p_1} \partial_{\eta_1}\mathcal{A}_{p_3}}{a^4 \rho_{\rm tot}}(t_1) H \frac{I^2 \partial_{\eta_2}\mathcal{A}_{p_2}\partial_{\eta_2}\mathcal{A}_{p_1}}{a^4 \rho_{\rm tot}}(t_2) H \frac{I^2 \partial_{\eta_3}\mathcal{A}_{p_3}\partial_{\eta_3}\mathcal{A}_{p_2}}{a^4 \rho_{\rm tot}}(t_3)
$$

$$
\times \left(\delta_{li} - (\hat{\boldsymbol{p}}_1)_l(\hat{\boldsymbol{p}}_1)_i\right)\left(\delta_{ij} - (\hat{\boldsymbol{p}}_2)_i(\hat{\boldsymbol{p}}_2)_j\right)\left(\delta_{jl} - (\hat{\boldsymbol{p}}_3)_j(\hat{\boldsymbol{p}}_3)_l\right). \quad (3.188)
$$

The time integrations can be performed in the same way as the two-point function, eq. (3.182), and then we obtain

$$
\langle \zeta^{\rm em}(\boldsymbol{k}_1)\zeta^{\rm em}(\boldsymbol{k}_2)\zeta^{\rm em}(\boldsymbol{k}_3)\rangle (t_{\rm reh}) \gtrsim \left(\frac{10^{-6}}{3}\right)^3 {\rm Mpc}^{-3} \int_{k_{\rm IR}}^{a_1 H_{\rm inf}} \frac{d^3p_1 d^3p_2 d^3p_3}{p_1^4 p_2^4 p_3^4}\delta(\boldsymbol{p}_1 - \boldsymbol{p}_3 - \boldsymbol{k}_1)
$$

$$
\times \delta(\boldsymbol{p}_2 - \boldsymbol{p}_1 - \boldsymbol{k}_2)\delta(\boldsymbol{p}_3 - \boldsymbol{p}_2 - \boldsymbol{k}_3)\left(\delta_{li} - (\hat{\boldsymbol{p}}_1)_l(\hat{\boldsymbol{p}}_1)_i\right)\left(\delta_{ij} - (\hat{\boldsymbol{p}}_2)_i(\hat{\boldsymbol{p}}_2)_j\right)\left(\delta_{jl} - (\hat{\boldsymbol{p}}_3)_j(\hat{\boldsymbol{p}}_3)_l\right).
$$

$$
(3.189)
$$

This time we have the identical three pole contributions from $p_i \sim k_{\rm IR}$. Note that if $p_1 \sim k_{\rm IR} \ll k_{\rm CMB}$ and $k_1, k_2, k_3 \simeq k_{\rm CMB}$, the delta functions require that $\boldsymbol{p}_2 \simeq \boldsymbol{k}_2$ and $\boldsymbol{p}_3 \simeq \boldsymbol{k}_3$. For example the pole contribution from $p_1 \sim k_{\rm IR}$ is given by

$$
\text{(r.h.s of eq. (3.189))} \quad (3.190)
$$

$$
\supset \delta(\boldsymbol{k}_1 + \boldsymbol{k}_2 + \boldsymbol{k}_3)\, 4 \times 10^{-20}{\rm Mpc}^{-3} k_2^{-4} k_3^{-4}
$$

$$
\times \left(\delta_{ij} - (\hat{\boldsymbol{k}}_2)_i(\hat{\boldsymbol{k}}_2)_j\right)\left(\delta_{jl} - (\hat{\boldsymbol{k}}_3)_j(\hat{\boldsymbol{k}}_3)_l\right)\int_{k_{\rm IR}}\frac{d^3p_1}{p_1^4}\left(\delta_{li} - (\hat{\boldsymbol{p}}_1)_l(\hat{\boldsymbol{p}}_1)_i\right)
$$

$$
= \delta(\boldsymbol{k}_1 + \boldsymbol{k}_2 + \boldsymbol{k}_3)\, 4 \times 10^{-20}{\rm Mpc}^{-3} \frac{8\pi}{3k_{\rm IR}}\frac{1 + \left(\hat{\boldsymbol{k}}_2 \cdot \hat{\boldsymbol{k}}_3\right)^2}{k_2^4 k_3^4}, \quad (3.191)
$$

where we use $\int d\Omega_{\boldsymbol{k}} \hat{k}_i \hat{k}_j = \frac{4\pi}{3}\delta_{ij}$ to perform the p_1 integral. The other pole contributions have similar forms. Then we obtain

$$
\langle \zeta^{\rm em}(\boldsymbol{k}_1)\zeta^{\rm em}(\boldsymbol{k}_2)\zeta^{\rm em}(\boldsymbol{k}_3)\rangle (t_{\rm reh}) \gtrsim
$$

$$
\delta(\boldsymbol{k}_1 + \boldsymbol{k}_2 + \boldsymbol{k}_3)\frac{32\pi}{3}10^{-20}\frac{{\rm Mpc}^{-3}}{k_{\rm IR}k_{\rm CMB}^2}\left[\frac{1 + (\hat{\boldsymbol{k}}_1 \cdot \hat{\boldsymbol{k}}_2)^2}{(k_1 k_2)^3} + 2\ {\rm perms}\right], \quad (3.192)
$$

where the approximation, $k_i \simeq k_{\rm CMB}$, are used in the denominator. Comparing this result to eq. (3.54), one obtains the induced $f_{\rm NL}^{\rm local}$ as

$$
f_{\rm NL}^{\rm em} \gtrsim 2 \times 10^5 \left(\frac{0.002{\rm Mpc}^{-1}}{k_{\rm CMB}}\right)^2 \left(\frac{10^{-6}{\rm Mpc}^{-1}}{k_{\rm IR}}\right)\left(\frac{2.2 \times 10^{-9}}{\mathcal{P}_\zeta}\right)^2. \quad (3.193)
$$

Here, in order to evaluate the generated non-linearity as the local $f_{\rm NL}$, we approximate $\left(\frac{1+(\hat{\boldsymbol{k}}_1 \cdot \hat{\boldsymbol{k}}_2)^2}{(k_1 k_2)^3} + 2 \text{ perms} \right) \simeq \frac{4}{3} \sum_{i=1}^{3} k_i^3 / \prod_{i=1}^{3} k_i^3$ because if the angular average is taken, $(\hat{\boldsymbol{k}}_1 \cdot \hat{\boldsymbol{k}}_2)^2$ yields 1/3. In light of the Planck upper bound on $f_{\rm NL}^{\rm local}$ eq. (3.66), this result, eq. (3.193), excludes Kobayashi's model with his parameter choice.

3.4.4 Summary of the section

In this subsection, we review the post-inflationary amplification mechanism of the primordial magnetic field in the kinetic coupling model proposed in ref. [35] and then we investigate the curvature perturbation problem. In the model, the magnetic field grows between the end of inflation and reheating. Nevertheless, since the curvature perturbation can be sourced by isocurvature perturbations even after inflation and the electric energy accounts for as large as 10% of the total energy density of the universe, the non-gaussianity of the induced curvature perturbation on CMB scale far exceeds the observational upper bound in this model. With the model parameters proposed given in eq.(3.166) which are provided by the author as the preferred parameters in ref. [35], we calculate the power spectrum and the non-linear parameter $f_{\rm NL}$ of the induced curvature perturbation as

$$\mathcal{P}_\zeta^{\rm em}(k_{\rm CMB}) \gtrsim 4 \times 10^{-7}, \qquad f_{\rm NL}^{\rm em}(k_{\rm CMB}) \gtrsim 2 \times 10^5. \tag{3.194}$$

Since these results are far greater than the observed value or the upper bound, the model is under pressure and at least that parameter choice is excluded.

In this model, even though the magnetic field is amplified after inflation, the curvature perturbation problem is still relevant. This is because the amplification mechanism due to the kinetic function I inevitably leads to much stronger electric fields than magnetic fields (see eq. (3.159)). Then the electric energy density induces curvature perturbation to an unacceptable level. This is exactly same as the kinetic coupling model without a post-inflationary magnetogenesis. Therefore Kobayashi's model suffers from the problem which excludes original Ratra's model.

In addition, even if the kinetic function I continues to vary, magnetic fields cannot be amplified after reheating because the electric conductivity works as a *friction* for magnetic fields and the mode function $\mathcal{A}_k$ are forced to be constant after reheating [65]. Therefore in Kobayashi's model, the amplification mechanism cannot work during the subsequent radiation dominated era and its effect has to be limited. Thus the reheating temperature was set to be quite low ($T_{\rm reh} \approx 50 {\rm MeV}$ with the proposed parameters) to minimize the decay of magnetic field during the radiation dominated era.

Contents

4.1   Gravitational Waves from Vacuum Fluctuation

In this section, we review the generation of gravitational waves from vacuum fluctuation during inflation and discuss the significance of the detection of primordial GW. It is widely believed that detecting primordial GW straightforwardly implies the determination of the inflation energy scale. However, it is not necessarily true because GW with an alternative origin dominates the observed primordial GW, in principle.

4.1.1 Quantization and mode function

Let us derive the basic prediction of inflation for gravitational waves. Tensor perturbations h_{ij} on the FRW metric are introduced as

$$\mathrm{d}s^2 = a^2(\eta) \left[\mathrm{d}\eta^2 - (\delta_{ij} + h_{ij}) \mathrm{d}x^i \mathrm{d}x^j \right], \tag{4.1}$$

where h_{ij} satisfies the traceless and transverse (T.T.) condition;

$$h_{ii} = 0 \text{ (traceless)}, \quad \partial_i h_{ij} = 0 \text{ (transverse)}. \tag{4.2}$$

These two condition guarantee that h_{ij} only has tensor component. Since h_{ij} is a symmetric tensor and the transverse and traceless condition kill one and three degrees of freedom, respectively, two degrees of freedom remain in h_{ij}. Thus gravitational wave or graviton has two polarizations and they are often called the plus (+) mode and the cross (×) mode.

Substituting eq. (4.1) into the Einstein-Hilbert action,

$$S_{\mathrm{GR}} = -\frac{M_{\mathrm{Pl}}^2}{2} \int \mathrm{d}^4 x \sqrt{-g} R, \tag{4.3}$$

one can show the action reads

$$S_h = \frac{M_{\mathrm{Pl}}^2}{8} \int \mathrm{d}\eta \mathrm{d}^3 x \, a^2(\eta) \left[h_{ij}'^2 - (\partial_l h_{ij})^2 \right]. \tag{4.4}$$

To obtain a canonical field, one redefines the field as

$$v_{ij}(\eta, \boldsymbol{x}) \equiv \frac{a M_{\mathrm{Pl}}}{2} h_{ij}(\eta, \boldsymbol{x}). \tag{4.5}$$

With this new variable, the action is rewritten as

$$S_v = \frac{1}{2} \int \mathrm{d}\eta \mathrm{d}^3 x \left[v_{ij}'^2 - (\partial_l v_{ij})^2 + \frac{a''}{a} v_{ij}^2 \right]. \tag{4.6}$$

This action coincides with the action of a massless scalar field except for the tensor leg "ij". Here we decompose v_{ij} into two independent modes in Fourier space as

$$v_{ij}(\eta.\boldsymbol{x}) = \int \frac{\mathrm{d}^3 k}{(2\pi)^3} e^{i\boldsymbol{k}\cdot\boldsymbol{x}} \sum_{\lambda=\pm} \left[\hat{a}_{\boldsymbol{k}}^{\lambda} v_k^{\lambda}(\eta) e_{ij}^{\lambda}(\boldsymbol{k}) + \hat{a}_{-\boldsymbol{k}}^{\lambda\dagger} v_k^{\lambda*}(\eta) e_{ij}^{\lambda*}(-\boldsymbol{k}) \right] \tag{4.7}$$

where we introduce the polarization tensors $e_{ij}^{\pm}(\boldsymbol{k})$ which satisfy the symmetric, transverse, traceless, orthogonal conditions,

$$e_{ij}^{\lambda}(\boldsymbol{k}) = e_{ji}^{\lambda}(\boldsymbol{k}), \quad k_i e_{ij}^{\lambda}(\boldsymbol{k}) = 0, \quad e_{ii}^{\lambda}(\boldsymbol{k}) = 0, \quad e_{ij}^{\lambda}(\boldsymbol{k}) e_{ij}^{\lambda'}(\boldsymbol{k}) = \delta^{\lambda\lambda'}. \tag{4.8}$$

If one adopts the linear polarization tensors, they are written with the linear polarization vectors $e_i(\boldsymbol{k})$ and $\bar{e}_i(\boldsymbol{k})$ as

$$e_{ij}^+(\boldsymbol{k}) = \frac{1}{\sqrt{2}}\left[e_i(\boldsymbol{k})e_j(\boldsymbol{k}) - \bar{e}_i(\boldsymbol{k})\bar{e}_j(\boldsymbol{k})\right],$$

$$e_{ij}^-(\boldsymbol{k}) = \frac{1}{\sqrt{2}}\left[e_i(\boldsymbol{k})\bar{e}_j(\boldsymbol{k}) + \bar{e}_i(\boldsymbol{k})e_j(\boldsymbol{k})\right]. \tag{4.9}$$

$e_i(\boldsymbol{k})$ and $\bar{e}_i(\boldsymbol{k})$ are two basis vectors which are orthogonal to each other and $\boldsymbol{k}$. For example, when $\boldsymbol{k}$ is parallel to the z-axis, these polarization vectors and tensors are explicitly given by

$$e_i = \begin{pmatrix} 1 \\ 0 \\ 0 \end{pmatrix}, \quad \bar{e}_i = \begin{pmatrix} 0 \\ 1 \\ 0 \end{pmatrix}, \quad e_{ij}^+ = \frac{1}{\sqrt{2}}\begin{pmatrix} 1 & 0 & 0 \\ 0 & -1 & 0 \\ 0 & 0 & 0 \end{pmatrix}, \quad e_{ij}^- = \frac{1}{\sqrt{2}}\begin{pmatrix} 0 & 1 & 0 \\ 1 & 0 & 0 \\ 0 & 0 & 0 \end{pmatrix}. \tag{4.10}$$

The quantization of each polarization mode of gravitational waves can be done in the same way as the scalar field case. The usual commutation relation is imposed on the creation and annihilation operators $\hat{a}_{\boldsymbol{k}}^\lambda, \hat{a}_{\boldsymbol{k}}^{\lambda,\dagger}$ in eq. (4.7),

$$\left[\hat{a}_{\boldsymbol{k}}^\lambda, \hat{a}_{\boldsymbol{k}'}^{\lambda'\dagger}\right] = (2\pi)^3\delta^{\lambda\lambda'}\delta(\boldsymbol{k}-\boldsymbol{k}'), \quad \left[\hat{a}_{\boldsymbol{k}}^\lambda, \hat{a}_{\boldsymbol{k}'}^{\lambda'}\right] = 0, \quad \left[\hat{a}_{\boldsymbol{k}}^{\lambda\dagger}, \hat{a}_{\boldsymbol{k}'}^{\lambda'\dagger}\right] = 0. \tag{4.11}$$

The normalization condition of the mode function $v_k(\eta)$ is given by

$$v_k^{\lambda*}\partial_\eta v_k^\lambda - v_k^\lambda\partial_\eta v_k^{\lambda*} = i. \tag{4.12}$$

From the action eq. (4.6), one finds that the euqation of motion of the mode function is

$$v_k'' + \left(k^2 - \frac{a''}{a}\right)v_k = 0. \tag{4.13}$$

Here we suppress the polarization label λ of the mode function because the two modes are identical. In de Sitter universe, $a(\eta) = -1/H\eta$, the above equation reads

$$v_k'' + \left(k^2 - \frac{2}{\eta^2}\right)v_k = 0. \tag{4.14}$$

With Bunch-Davies initial condition,

$$v_k(\eta) = \frac{1}{\sqrt{2k}}e^{-ik\eta}, \tag{4.15}$$

the solution of the mode function is obtained as

$$v_k(\eta) = \frac{1}{\sqrt{2k}}\left(1 - \frac{i}{k\eta}\right)e^{-ik\eta}. \tag{4.16}$$

In the super-horizon limit, it reads

$$v_k(\eta) \simeq \frac{1}{\sqrt{2k}k\eta}, \quad (|k\eta| \ll 1), \tag{4.17}$$

where we have neglected the constant phase factor.

4.1.2   Power spectrum and observations

Let us consider the power spectrum of GW which is directly connected to observations. The power spectrum of the tensor perturbation is defined as

$$\langle h_{ij}(\eta, \boldsymbol{x}) h_{ij}(\eta, \boldsymbol{x}) \rangle \equiv \int \frac{\mathrm{d}^3 k}{(2\pi)^3} P_h(\eta, k) = \int \frac{\mathrm{d}k}{k} \mathcal{P}_h(\eta, k), \tag{4.18}$$

with $\mathcal{P}_h = k^3 P_h / 2\pi^2$. Substituting eq. (4.7) into eq. (4.18), one obtains

$$\mathcal{P}_h(\eta, k) = \frac{2k^3}{a^2 M_{\mathrm{Pl}}^2 \pi^2} \left(|v_k^+(\eta)|^2 + |v_k^-(\eta)|^2 \right). \tag{4.19}$$

Therefore on the super-horizon scales in de Sitter universe, the GW power spectrum is given by [36]

$$\mathcal{P}_h(\eta, k) = \frac{2H^2}{\pi^2 M_{\mathrm{Pl}}^2}, \quad (|k\eta| \ll 1). \tag{4.20}$$

This is the famous result as the basic prediction of GW in the inflation paradigm. The inflationary GW in eq. (4.20) shows the scale invariant spectrum $\mathcal{P}_h \propto k^0$, and its amplitude depends only on the energy scale of inflation, $\mathcal{P}_h \propto H^2 \propto \rho_{\mathrm{inf}}$.

The ratio between the power spectrum of GW and the curvature perturbation ζ is called the *tensor-to-scalar ratio r*;

$$r \equiv \frac{\mathcal{P}_h}{\mathcal{P}_\zeta}. \tag{4.21}$$

It is a useful quantity to compare the predictions of models and observations. In standard slow-roll inflation, the curvature power spectrum on super-horizon scales is computed as (see eq. (2.61))

$$\mathcal{P}_\zeta = \frac{\rho_{\mathrm{inf}}}{24\pi^2 \varepsilon M_{\mathrm{Pl}}^4} = \frac{H^2}{8\pi^2 \varepsilon M_{\mathrm{Pl}}^2}, \tag{4.22}$$

where ε is the slow-roll parameter. Then we obtain

$$r = 16\varepsilon. \tag{4.23}$$

The tensor-to-scalar ratio is simply given by the slow-roll parameter. This is the basic prediction of slow-roll inflation models. It should be also noted that the curvature power spectrum has been already observed as $\mathcal{P}_\zeta \approx 2.2 \times 10^{-9}$. Since we know the denominator of r, $\mathcal{P}_h$ and r are basically equivalent.

Currently, the observational constraint of the Planck satellite on r is [40]

$$r < 0.11, \quad (95\% \, C.L., \; \mathrm{Planck} + \mathrm{WP} + \mathrm{high}{-}\ell), \tag{4.24}$$

where the pivot scale is $0.002 \mathrm{Mpc}^{-1}$, and the running of the scalar spectrum index $\mathrm{d}n_s / \mathrm{d}\ln k$ and higher order quantities (e.g. running of running) are set to zero. Taking into account of the running n_s', the constraint on r is relaxed to $r < 0.23$ [40]. On the

other hand, the BICEP2 experiment reported to detect the CMB B-mode polarization and it implies the primordial GW with the amplitude [80]

$$r \approx 0.16^{+0.06}_{-0.05}, \tag{4.25}$$

with their subtraction scheme of the foreground dust emission. The BICEP2 team claim that $r = 0$ is disfavored at 5.9σ in their analysis. Nevertheless

We should also refer to the so-called consistency relation between the tensor-to-scalar ratio r and the spectrum index of the GW power spectrum n_T. The GW spectrum index (or the tensor tilt) is defined as

$$n_T \equiv \frac{d \ln \mathcal{P}_h}{d \ln k}. \tag{4.26}$$

One can show that n_T is computed as

$$n_T = \frac{d \ln H^2}{H dt} = \frac{2\dot{H}}{H^2} = -2\varepsilon. \tag{4.27}$$

Eliminating ε from eq. (4.23) and eq. (4.27), we obtain the *consistency relation* as

$$r = -8n_T. \tag{4.28}$$

This relation is also considered as the basic prediction of single slow-roll inflation models.

4.1.3 Estimate inflation energy scale from GW

Provided that GWs generated from vacuum fluctuation druing inflation are detected, we can know the energy density of inflation $\rho_{\rm inf}$. Substituting eq. (4.20) into eq. (4.21), one finds

$$r = \frac{2H_{\rm inf}^2}{\pi^2 M_{\rm Pl}^2 \mathcal{P}_\zeta} = \frac{2\rho_{\rm inf}}{3\pi^2 M_{\rm Pl}^4 \mathcal{P}_\zeta} \tag{4.29}$$

Solving this equation in term of $\rho_{\rm inf}$ and using the observational result $\mathcal{P}_\zeta \approx 2.2 \times 10^{-9}$ [4], one obtains

$$\rho_{\rm inf}^{1/4} = 7.5 \times 10^{-3} M_{\rm Pl} \left(\frac{r}{0.1}\right)^{1/4} = 1.8 \times 10^{16} {\rm GeV} \left(\frac{r}{0.1}\right)^{1/4}. \tag{4.30}$$

Note that eq. (4.30) indicates $\rho_{\rm inf}$ at the time of the horizon crossing of the mode on the CMB scale if r is detected by a CMB observation. In the same way, we can also estimate the Hubble parameter as

$$H_{\rm inf} = 3.3 \times 10^{-5} M_{\rm Pl} \sqrt{\frac{r}{0.1}} = 8 \times 10^{13} {\rm GeV} \sqrt{\frac{r}{0.1}}. \tag{4.31}$$

The detection of primordial GW from vacuum fluctuation during inflation has the following three major impacts. First, since it is the basic prediction of inflation, it can

be crucial evidence of the inflation paradigm. Furthermore, if confirmed, its gaussianity indicates that it comes from vacuum fluctuation and support the quantum origin of fluctuations. Second, the tensor-to-scalar ratio is a excellent discriminator of inflation models. For example, if $r \sim 0.1$, only large-field models survive. The consistency relation also distinguishes single slow-roll inflation models from other more complicated models [88]. Finally, the discovered $\rho_{\rm inf}$ implies that there exists unknown new physics on the energy scale. It is indispensable clue to construct the high energy theory because particle accelerators are unlikely to reach $\rho_{\rm inf}$. Then it would strongly motivates particle theorist who work on physics beyond the standard model of particle physics. Therefore the detection of primordial GW is important and meaningful.

However, when one claims that $\rho_{\rm inf}$ is determined by detecting r, a big assumption is made. The assumption is that the GW coming from vacuum fluctuation, eq. (4.20), dominates the detected primordial GW and any GWs from other sources are subdominant. Nevertheless no theoretical or observational argument excludes the possibility that the main contribution to the primordial GW is different from GW of vacuum fluctuation, eq.(4.20). Therefore it is also quite important to investigate the alternative possibility that GW of another source dominates the primordial GW. In the following sections, we explore the cases where the second order perturbations induce GW. The key question is whether such an alternative GW can be larger than the conventional GW from vacuum fluctuation.

4.2 GW Induced by Second Order Scalar Perturbation

In the previous section, we derive the gravitational wave generated from the vacuum fluctuation during inflation, eq. (4.20). However, that is just one source of primordial GWs. In this section, we consider the GWs induced by second order perturbations of a spectator scalar field.

4.2.1 Alternative generation mechanism

It is well known that scalar, vector and tensor perturbations are decoupled at the linear order of the perturbative expansion in the isotropic universe. However, they are coupled at the second order. Thus the second order perturbations can produce tensor perturbations. One can easily see that the anisotropic component of the energy momentum tensor of a scalar perturbation $\propto \partial_i \delta\sigma \partial_j \delta\sigma$ (or a vector perturbation $\propto \delta V_i \delta V_j$) induces gravitational waves h_{ij}, according to the Einstein equation. Note that these second order perturbations must exist if there are light scalar fields (or vector fields with a coupling which breaks the conformal symmetry). Since known high energy theories (e.g. supergravity or superstring theory) typically predict many scalar degrees of freedom, it is natural to expect some of them acquire fluctuations during inflation. In fig. 4.1, the two different generation mechanisms are sketched.

This alternative generation mechanism is totally different from the conventional one in which the tensor modes are generated from the vacuum fluctuation as we review in the previous section. If the primordial GW is dominated by the GW generated by the alternative mechanism, the interpretation of the GW observation should be modified. It is because the relation between the observational quantities associated with the primordial GW (e.g. the power spectrum, the spectrum index) and the parameters of inflation (e.g. the energy density $\rho_{\rm inf}$, the slow-roll parameter ε) can be drastically changed. For example, provided the power spectrum of the alternative GW has a different dependence on the Hubble parameter during inflation, $\mathcal{P}_h^{\rm alt} \propto H_{\rm inf}^4$, from the conventional one, $\mathcal{P}_h^{\rm vac} \propto H_{\rm inf}^2$, the estimation of $H_{\rm inf}$ from the observed GW changes in general. Therefore it is important to investigate the possibility that GWs are generated from alternative mechanisms and examine whether such a GW can dominate over the conventional GW.

4.2.2 Previous works

In this subsection, we briefly review previous works in which the generation of GW from second order perturbations is studied.

In ref. [89, 90, 91, 92, 93, 94, 95, 96], GWs induced by the second order scalar perturbations *after inflation* are explored. Some of them have reported the induced GW may be detectable by the future interferometer with very high sensitivities (e.g. LISA, BBO and DECIGO). However, none of them found induced GW which is large enough for CMB B-mode observations.
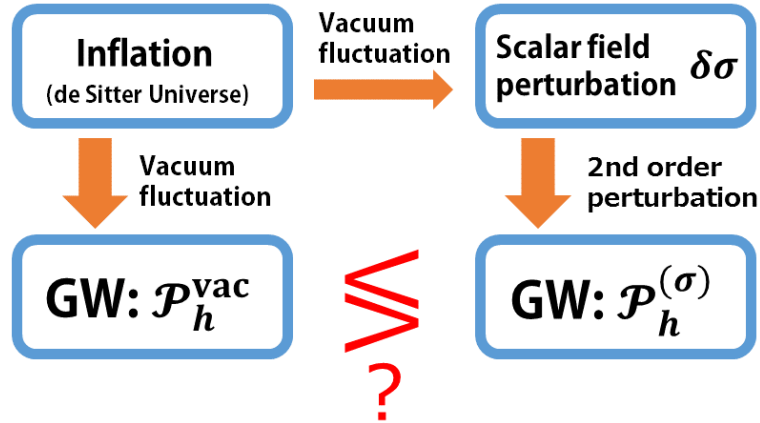
Figure 4.1 : A sketch of two different generation mechanism of gravitational waves. $\mathcal{P}_h^{\text{vac}}$ denotes GW which is directly generated from the vacuum fluctuation during inflation (bottom-left box). On the other hand, if there exists a light scalar field σ during inflation, σ also acquires the perturbation $\delta\sigma$ from the vacuum fluctuation (top-right box). Then its second order perturbation $\mathcal{O}(\delta\sigma^2)$ induces another GW, $\mathcal{P}_h^{(\sigma)}$ (bottom-right box). The important question is which is dominant.

On the other hand, many works investigated the possibility the gauge field produced during inflation via the axial coupling induces detectable GWs [27, 81, 83, 82, 84, 85, 86, 87, 97]. Since the Planck satellite puts the tight constraint on the axial coupling model, the induced tensor modes on the CMB scale must be subdominant in the case where the pseudo-scalar is the inflaton. If the pseudo-scalar field coupled to the gauge field is not inflaton, the generation of detectable GW on the CMB scale is not completely excluded while it seems that a dedicated model building is necessary to avoid the constraint [81, 97].

In ref. [37], GWs induced by the second order perturbation of a spectator scalar field is investigated. The authors claimed that if the sound speed of the spectator field is sufficiently small, the induced GW can be larger than the GW from the vacuum fluctuation, and be detectable by CMB B-mode observations. If it is true, this possibility would be very interesting. In the next subsection, we review the paper.

4.2.3   Review on Biagetti et al.(2013)

In this subsection, we quickly review ref. [37] in which the authors claims that the dominant and observable GW can be generated by the second order perturbation of a spectator scalar field during inflation. Here we skip most calculations, while they are explained in detail in the next section with a more robust setup.

In ref. [37], the authors consider a spectator field which has a speed of sound, c_s, smaller than unity. Their calculation begins with the following action for the scalar

perturbation [1]:

$$S_{\delta\sigma} = \int \mathrm{d}\eta \mathrm{d}^3x \, a^4 \left[\frac{1}{2a^2} \left(\delta\sigma'^2 - c_s^2 (\partial_i \delta\sigma)^2 \right) - \partial_\sigma^2 V \right]. \tag{4.32}$$

If the sound speed c_s is constant, one can easily find the mode function of $\delta\sigma$ as

$$\delta\sigma_k(\eta) = \frac{H_{\mathrm{inf}}}{\sqrt{2}(c_s k)^{3/2}} (1 + ic_s k\eta) e^{-ic_s k\eta}. \tag{4.33}$$

The power spectrum of the spectator field on super-horizon scales is given by

$$\mathcal{P}_{\delta\sigma} = \frac{1}{c_s^3} \left(\frac{H_{\mathrm{inf}}}{2\pi} \right)^2. \tag{4.34}$$

Thus the small sound speed amplifies the power spectrum by the factor of c_s^{-3}.

Next, let us calculate the tensor mode induced by this spectator scalar field. In the paper, the equation of motion for the tensor mode is written as [37]

$$h_{ij}'' + 2aHh_{ij}' - \partial_l^2 h_{ij} = -4 \frac{c_s^2}{M_{\mathrm{Pl}}^2} \tilde{T}_{ij}^{lm} \partial_l \delta\sigma \partial_m \delta\sigma, \tag{4.35}$$

where $\tilde{T}_{ij}^{lm}$ is the projection tensor into the T.T. component. Nevertheless, it should be noted that the source term in r.h.s. of this equation cannot be derived from the action eq. (4.32) because the action does not respect the general covariance and the expression of the energy momentum tensor in the general relativity is not applicable. However, the authors somehow write down this equation. This equation indicates that the tensor mode is induced by the second order perturbation of the spectator scalar field.

Eq. (4.35) can be solved by the Green function method in Fourier space. With the Green function $g_k(\eta, \tau)$ (see eq. (4.76) for its expression), the inhomogeneous solution of eq. (4.35) is written as

$$h_k^{(\sigma)}(\eta) = \frac{1}{a(\eta)} \int \mathrm{d}\tau a(\tau) g_k(\eta, \tau) S_{\boldsymbol{k}}(\tau), \tag{4.36}$$

where the superscript "(σ)" denotes quantities induced by the scalar, and $S_{\boldsymbol{k}}(\tau)$ is the Fourier transform of the source term. In principle, by substituting the solution into the tensor power spectrum

$$\mathcal{P}_h^{(\sigma)} = \frac{k^3}{\pi^2} |h_k^{(\sigma)}|^2, \tag{4.37}$$

where the contributions of the two polarization are summed, one obtains the amplitude of the induced GW. However, since the calculation is technically difficult to be done, they

---

[1]Since this action explicitly violates the Lorentz symmetry and the general covariance, we consider another action in the next section.

perform the numerical calculation. [2] The numerical result is fitted to a ansatz for the tensor power spectrum,

$$\mathcal{P}_h^{(\sigma)} = \mathcal{C} \, \frac{H_{\text{inf}}^4}{c_s^n M_{\text{Pl}}^4} \tag{4.38}$$

and the parameters $\mathcal{C}$ and n are found as

$$\mathcal{C} \approx 3, \qquad n \approx \frac{18}{5}. \tag{4.39}$$

This result implies that the induced GW is larger than the GW from the vacuum fluctuation eq. (4.20), if the sound speed is sufficiently small as

$$c_s^{18/5} < \frac{3\pi^2}{2} \frac{H_{\text{inf}}^2}{M_{\text{Pl}}^2}, \quad \implies \quad c_s < 8 \times 10^{-3} \left(\frac{H_{\text{inf}}}{10^{14} \text{GeV}} \right)^{5/9}. \tag{4.40}$$

Nevertheless, as we show in the next section, it cannot happen. It is because the spectator scalar field simultaneously induces the curvature perturbation and the lower bound on the sound speed derived from the CMB observation restricts the induced GW from being dominant.

---

[2]In fact, this calculation can be analytically performed with several good approximations. See the next section.

4.3 No-go result for single spectator scalar field

In this section, [3] we consider the possibility of enhancing the inflationary tensor mode by introducing a spectator scalar field with a small sound speed which induces gravitational waves as a second order effect. We analytically obtain the power spectra of gravitational waves and curvature perturbation induced by the spectator scalar field. We found that the small sound speed amplifies the curvature perturbation much more than the tensor mode and the current observational constraint forces the induced gravitational waves to be negligible compared with those from the vacuum fluctuation during inflation.

This section is organized as follows. In sec. 4.3.1, we perturb the action and obtain the power spectrum of the spectator field perturbation. In sec. 4.3.2, the power spectra of the induced GWs and the curvature perturbation are derived and their constraints are discussed. In sec. 4.3.3, we develop the understanding of the reason why such a stringent constraint on the induced GWs is obtained. In sec. 4.3.4, the extended action of the spectator field is briefly argued. We summarize this section in sec. 4.3.5.

4.3.1 Perturbed action

We consider the following Lagrangian:

$$\mathcal{L} = \frac{1}{2}M_{\mathrm{Pl}}^2 R + \frac{1}{2}\partial_\mu\phi\partial^\mu\phi - V(\phi) + P(X, \sigma), \tag{4.41}$$

where ϕ is the inflaton, $V(\phi)$ is its potential, σ is a spectator field, and $X \equiv \frac{1}{2}\partial_\mu\sigma\partial^\mu\sigma$. In this section, the inflaton ϕ is assumed to be responsible for both the occurrence of inflation and the generation of the scalar perturbations imprinted in CMB [40, 31]. On the other hand, the σ field is supposed to generate gravitational waves through its second order perturbations. For the moment, we assume that the Lagrangian of σ is an arbitrary function of X and σ, $P(X, \sigma)$, while we further extend it in sec. 4.3.4. In this subsection, we perturb the action and derive the equations of motion for the perturbed fields.

In the (3+1) decomposition, the metric is given by

$$\mathrm{d}s^2 = N^2\mathrm{d}t^2 - \gamma_{ij}(\mathrm{d}x^i + N^i\mathrm{d}t)(\mathrm{d}x^j + N^j\mathrm{d}t), \tag{4.42}$$

where we incorporate metric perturbations around the flat FLRW metric as,

$$N = 1 + \delta N, \quad N_i = \partial_i\psi, \quad \gamma_{ij} = a^2\left(\delta_{ij} + h_{ij} + \frac{1}{2}h_{ik}h_j^k\right), \tag{4.43}$$

working in the flat gauge for the scalar perturbations and the transverse-traceless (T.T.) gauge for the tensor perturbations. One can show that the gravity sector of the perturbed

---

[3]This section is based on my work [38].

action up to the second order is given by

$$
S_g^{(1,2)} = \int \mathrm{d}t \mathrm{d}^3 x \, a^3 \Big[\; 3 M_{\mathrm{Pl}}^2 H^2 \delta N \quad \text{(1st order)}
$$

$$
- 3 M_{\mathrm{Pl}}^2 H^2 (\delta N)^2 - 2 M_{\mathrm{Pl}}^2 H \delta N a^{-2} \partial_i^2 \psi + \frac{M_{\mathrm{Pl}}^2}{8} \left(\dot{h}_{ij} \dot{h}_{ij} - a^{-2} \partial_k h_{ij} \partial_k h_{ij} \right) \quad \text{(2nd order)} \Big].
$$

$$(4.44)$$

Here we ignore the third and higher order terms in the gravity sector. Although they include $\mathcal{O}(h\delta\sigma^2)$ coupling terms, these terms are slow-roll suppressed compared to similar terms in the matter sector and hence they are sub-leading [98].

We now consider the matter sector of the action. The two scalar fields are decomposed into the background part and the perturbation,

$$
\phi(t, \boldsymbol{x}) = \phi_0(t) + \delta\phi(t, \boldsymbol{x}), \quad \sigma(t, \boldsymbol{x}) = \sigma_0(t) + \delta\sigma(t, \boldsymbol{x}). \tag{4.45}
$$

The calculation of the perturbed matter action is straightforward. First, let us compute the perturbed Lagrangian of the σ field. The perturbation expansion of $X \equiv \frac{1}{2} \partial_\mu \sigma \partial^\mu \sigma$ is given by

$$
X = \frac{1}{2}\dot{\sigma}_0^2 \quad \text{(0th order)} \; + \dot{\sigma}_0 \dot{\delta\sigma} - \dot{\sigma}_0^2 \delta N \quad \text{(1st order)}
$$

$$
+ \frac{1}{2}\dot{\delta\sigma}^2 - \dot{\sigma}_0 a^{-2} \partial_i \psi \partial_i \delta\sigma - 2\delta N \dot{\sigma}_0 \dot{\delta\sigma} + \frac{3}{2}\dot{\sigma}_0^2 \delta N^2 - \frac{1}{2}a^{-2}(\partial_i \delta\sigma)^2 \quad \text{(2nd order)}
$$

$$
- \dot{\delta\sigma} a^{-2} \partial_i \psi \partial_i \delta\sigma - \delta N \left(\dot{\delta\sigma}^2 - 2\dot{\sigma}_0 a^{-2} \partial_i \psi \partial_i \delta\sigma \right) + 3\dot{\sigma}_0 \dot{\delta\sigma} \delta N^2
$$

$$
- 2\dot{\sigma}_0^2 \delta N^3 + \frac{1}{2}a^{-2} h_{ij} \partial_i \delta\sigma \partial_j \delta\sigma \quad \text{(3rd order)} \quad + \mathcal{O}(\delta\sigma^4). \tag{4.46}
$$

Then one finds

$$
NP(X,\sigma) = (1 + \delta N) P(X, \sigma)
$$

$$
= P^{(0)} \quad \text{(0th order)}
$$

$$
+ P^{(0)} \delta N + P_X^{(0)} \left(\dot{\sigma}_0 \dot{\delta\sigma} - \dot{\sigma}_0^2 \delta N \right) + P_\sigma^{(0)} \delta\sigma \quad \text{(1st order)}
$$

$$
+ \frac{1}{2}P_X^{(0)} \left[\dot{\delta\sigma}^2 - 2\dot{\sigma}_0 a^{-2} \partial_i \psi \partial_i \delta\sigma - 2\dot{\sigma}_0 \dot{\delta\sigma} \delta N + \dot{\sigma}_0^2 (\delta N)^2 - a^{-2}(\partial_i \delta\sigma)^2 \right]
$$

$$
+ \frac{1}{2}P_{XX}^{(0)} \left(\dot{\sigma}_0 \dot{\delta\sigma} - \dot{\sigma}_0^2 \delta N \right)^2 + \frac{1}{2}P_{\sigma\sigma}^{(0)} (\delta\sigma)^2 + P_\sigma^{(0)} \delta\sigma \delta N \quad \text{(2nd order)}
$$

$$
+ \frac{1}{2}P_{XX}^{(0)} \dot{\sigma}_0 (\dot{\delta\sigma})^3 - \left(\frac{1}{2}P_X^{(0)} - 2P_{XX}^{(0)} \dot{\sigma}_0^2 \right) (\dot{\delta\sigma})^2 \delta N + \left(P_X^{(0)} + \frac{5}{2}P_{XX}^{(0)} \dot{\sigma}_0^2 \right) \dot{\sigma}_0 \dot{\delta\sigma} \delta N^2
$$

$$
- \left(\frac{1}{2}P_X^{(0)} + P_{XX}^{(0)} \dot{\sigma}_0^2 \right) \dot{\sigma}_0^2 (\delta N)^3 + \left(P_X^{(0)} + P_{XX}^{(0)} \dot{\sigma}_0^2 \right) \left(\dot{\sigma}_0 \delta N - \dot{\delta\sigma} \right) a^{-2} \partial_i \psi \partial_i \delta\sigma
$$

$$
- \frac{1}{2}P_{XX}^{(0)} \dot{\sigma}_0 \dot{\delta\sigma} a^{-2} (\partial_i \delta\sigma)^2 - \frac{1}{2} \left(P_X^{(0)} - P_{XX}^{(0)} \dot{\sigma}_0^2 \right) \delta N a^{-2} (\partial_i \delta\sigma)^2
$$

$$
+ \frac{1}{2}P_{\sigma\sigma}^{(0)} (\delta\sigma)^2 \delta N + \frac{1}{2}P_X^{(0)} h_{ij} a^{-2} \partial_i \delta\sigma \partial_j \delta\sigma \quad \text{(3rd order)} \quad + \mathcal{O}(\delta\sigma^4), \tag{4.47}
$$

where $P_{X^n}^{(0)} \equiv \partial^n P / \partial X^n |_{X=\dot\sigma_0^2/2, \sigma=\sigma_0}$. Note that we suppress the terms in proportion to $P_{X\sigma}^{(0)}, P_{\sigma\sigma\sigma}^{(0)}$ and other higher derivatives which do not yield the $h\delta\sigma^2$ coupling. A general multi-field perturbed action can be found in ref. [99] while it does not include the tensor perturbations. One can easily obtain the perturbed lagrangian of the ϕ sector by making replacements, $\delta\sigma \to \delta\phi, P_X^{(0)} \to 1, P_{XX}^{(0)} \to 0, P_\sigma^{(0)} \to -V_\phi^{(0)}$ and $P^{(0)} \to \dot\phi_0^2/2 + V^{(0)}$ in eq. (4.47).

Now we have the perturbed action with the four scalar perturbation quantities, $\delta N, \psi, \delta\phi$ and $\delta\sigma$. However, the Hamiltonian and momentum constraints of the second order action eliminates the two of them,

$$2M_{\rm Pl}^2 H \delta N = \dot\phi_0 \delta\phi + P_X^{(0)} \dot\sigma_0 \delta\sigma, \tag{4.48}$$

$$-2M_{\rm Pl}^2 H a^{-2} \partial_i^2 \psi = \left(6M_{\rm Pl}^2 H^2 - \dot\phi_0^2 - K\dot\sigma_0^2\right) \delta N + \dot\phi_0 \dot{\delta\phi} + V_\phi^{(0)} \delta\phi + K\dot\sigma_0 \dot{\delta\sigma} - P_\sigma^{(0)} \delta\sigma, \tag{4.49}$$

with $K \equiv P_X + P_{XX}\dot\sigma_0^2$. Using these constraint equations and eliminating δN and ψ, we obtain the second order action of $\delta\phi$ and $\delta\sigma$ as [99]

$$S^{(2)} = \frac{1}{2} \int {\rm dt d}^3 x a^3 \Big[(\dot{\delta\phi})^2 + K(\dot{\delta\sigma})^2 - a^{-2}(\partial_i \delta\phi)^2 - P_X a^{-2}(\partial_i \delta\sigma)^2$$
$$- \mu_\phi^2(\delta\phi)^2 - \mu_\sigma^2(\delta\sigma)^2 - \Omega\delta\phi\delta\sigma - \tilde\Omega\delta\phi\dot{\delta\sigma} \Big], \tag{4.50}$$

where

$$\mu_\phi^2 \equiv V_{\phi\phi} + \frac{3\dot\phi_0^2}{2M_{\rm Pl}^2} + \frac{\dot\phi_0 V_\phi}{M_{\rm Pl}^2 H} - \frac{\dot\phi_0^2}{4M_{\rm Pl}^4 H^2}\left(\dot\phi_0^2 + K\dot\sigma_0^2\right) - \frac{\partial_t(a^3\dot\phi_0^2/H)}{2M_{\rm Pl}^2 a^3}, \tag{4.51}$$

$$\mu_\sigma^2 \equiv -P_{\sigma\sigma} + \frac{3P_X^2\dot\sigma_0^2}{M_{\rm Pl}^2} - \frac{P_\sigma P_X \dot\sigma_0}{M_{\rm Pl}^2 H} - \frac{P_X^2\dot\sigma_0^2}{4M_{\rm Pl}^4 H^2}\left(\dot\phi_0^2 + K\dot\sigma_0^2\right) - \frac{\partial_t(a^3 K P_X \dot\sigma_0^2/H)}{2M_{\rm Pl}^2 a^3}, \tag{4.52}$$

$$\Omega \equiv 3\frac{\dot\phi_0 P_X \dot\sigma_0}{M_{\rm Pl}^2} - \frac{P_\sigma \dot\phi_0}{M_{\rm Pl}^2 H} + \frac{V_\phi P_X \dot\sigma_0}{M_{\rm Pl}^2 H} - \frac{\dot\phi_0 P_X \dot\sigma_0}{2M_{\rm Pl}^4 H^2}\left(\dot\phi_0^2 + K\dot\sigma_0^2\right) - \frac{\partial_t(a^3\dot\phi_0 P_X \dot\sigma_0/H)}{M_{\rm Pl}^2 a^3}, \tag{4.53}$$

$$\tilde\Omega \equiv \frac{\dot\phi_0 K \dot\sigma_0}{M_{\rm Pl}^2 H} + \frac{\dot\phi_0 P_{XX} \dot\sigma_0^3}{M_{\rm Pl}^2 H}. \tag{4.54}$$

Note we omit the superscript "(0)" hereafter. To canonically normalize the fields, we redefine

$$\chi \equiv a\delta\phi, \qquad \Sigma \equiv a\sqrt{K}\delta\sigma. \tag{4.55}$$

With these new variables, the second-order action reads

$$S^{(2)} = \frac{1}{2} \int {\rm d}\eta {\rm d}^3 x \Big[\chi'^2 - (\partial_i\chi)^2 + \left(\frac{a''}{a} - a^2\mu_\phi^2\right)\chi^2$$
$$+ \Sigma'^2 - c_s^2(\partial_i\Sigma)^2 + \left(\frac{(a\sqrt{K})''}{a\sqrt{K}} - a^2\mu_\sigma^2\right)\Sigma^2$$
$$+ \frac{a}{\sqrt{K}}\left(\tilde\Omega\frac{(a\sqrt{K})'}{a\sqrt{K}} - a\Omega\right)\chi\Sigma - \frac{a}{\sqrt{K}}\tilde\Omega\chi\Sigma' \Big], \tag{4.56}$$

where the prime denotes the derivative with respect to the conformal time η and we introduce the sound speed of the canonical field Σ,

$$c_s^2 \equiv \frac{P_X}{K} = \frac{P_X}{P_X + P_{XX}\dot{\sigma}_0^2}. \tag{4.57}$$

The equations of motion of the two canonical fields are given by

$$\chi'' - \partial_i^2 \chi + \left(a^2 \mu_\phi^2 - \frac{a''}{a} \right) \chi = \frac{a}{\sqrt{K}} \left[\left(\tilde{\Omega} \frac{(a\sqrt{K})'}{a\sqrt{K}} - a\Omega \right) \Sigma - \tilde{\Omega}\Sigma' \right], \tag{4.58}$$

$$\Sigma'' - c_s^2 \partial_i^2 \Sigma + \left[a^2 \mu_\sigma^2 - \frac{(a\sqrt{K})''}{a\sqrt{K}} \right] \Sigma = \frac{a}{\sqrt{K}} \left(\tilde{\Omega} \frac{(a\sqrt{K})'}{a\sqrt{K}} - a\Omega \right) \chi + \left(\frac{a}{\sqrt{K}}\tilde{\Omega}\chi \right)'. \tag{4.59}$$

Since these equations are coupled to each other due to the mixing terms (see the third line in eq. (4.56)), it is hard to solve them if the mixing is significantly strong. Moreover, if the masses, μ_ϕ^2 and μ_σ^2, are not much less than H^2, their fluctuations are not generated during inflation. Thus we explore the condition in which both the mixing and their mass are negligible and we focus on these cases in the following subsections.

The inflaton mass, μ_ϕ^2, is evaluated as

$$\frac{\mu_\phi^2}{H^2} \simeq 3\eta_\phi - 6\varepsilon_H + 6\sqrt{\varepsilon_\phi \varepsilon_H} - P_X \frac{\varepsilon_H^2 \dot{\sigma}_0^2}{c_s^2 \dot{\phi}_0^2} + \mathcal{O}(\varepsilon^2), \tag{4.60}$$

where $\varepsilon_H \equiv -\dot{H}/H^2$, $\varepsilon_\phi \equiv M_{\rm Pl}^2 V_\phi^2 / 2V^2$, $\eta_\phi \equiv M_{\rm Pl}^2 V_{\phi\phi}/V$ as usual. We also use the background equation, $-2M_{\rm Pl}^2 \dot{H} = \dot{\phi}_0^2 + P_X \dot{\sigma}_0^2$. In eq. (4.60), only the last term can be large for a very small c_s. It requires a condition,

$$c_s^2 \gg \left| \varepsilon_H^2 \frac{P_X \dot{\sigma}_0^2}{\dot{\phi}_0^2} \right|, \tag{4.61}$$

for the inflaton mass to be negligibly small. Provided $P_{\sigma\sigma} \lesssim V_{\phi\phi}$, $P_\sigma \lesssim V_\phi$ and $P_X \dot{\sigma}_0 \lesssim \dot{\phi}_0$ which are natural conditions for a spectator field, one can show that eq. (4.61) guarantees $\mu_\sigma^2 \ll H^2$ and $\Omega \ll H^2$. However, for a small c_s, one finds

$$\frac{\tilde{\Omega}}{H} \simeq 4 \frac{\varepsilon_H}{c_s^2} \frac{P_X \dot{\sigma}_0}{\dot{\phi}_0}. \tag{4.62}$$

To ignore the mixing, we need an additional condition;

$$c_s^2 \gg \left| \varepsilon_H \frac{P_X \dot{\sigma}_0}{\dot{\phi}_0} \right|. \tag{4.63}$$

and they do not appear if σ has a usual kinetic term.

When the two conditions, eqs. (4.61) and (4.63), are satisfied and the slow-roll parameters are sufficiently small, the mass terms and the mixing terms are safely ignored. Then we obtain the mode functions of the two fields as

$$\chi_k \simeq \frac{e^{-ik\eta}}{\sqrt{2k}}\left(1 - \frac{i}{k\eta}\right), \qquad \Sigma_k \simeq \frac{e^{-ic_s k\eta}}{\sqrt{2c_s k}}\left(1 - \frac{i}{c_s k\eta}\right), \tag{4.64}$$

where the time variation of K is assumed to be negligible compared with a. The power spectrum of the original fields on super-horizon scales are given by

$$\mathcal{P}_{\delta\phi} \simeq \frac{H^2}{4\pi^2}, \qquad \mathcal{P}_{\delta\sigma} \simeq \frac{1}{c_s^3 K}\frac{H^2}{4\pi^2} = \frac{1}{c_s P_X}\frac{H^2}{4\pi^2}. \tag{4.65}$$

Note that the power spectrum of the σ field is amplified by the factor of $(c_s P_X)^{-1}$.

4.3.2 Induced curvature and graviton perturbations

In this subsection, we calculate the curvature perturbations and gravitational waves induced by the σ field through the third-order terms in the perturbed action. The third-order action contains many terms,

$$S^{(3)} \supset \int \mathrm{dt}\mathrm{d}^3 x a^3 \left[\frac{1}{2}P_X h_{ij} a^{-2}\partial_i \delta\sigma \partial_j \delta\sigma - \frac{1}{2}\left(P_X - P_{XX}\dot{\sigma}_0^2\right) a^{-2}(\partial_i \delta\sigma)^2 \delta N \right.$$
$$\left. - \left(\frac{1}{2}P_X - 2P_{XX}\dot{\sigma}_0^2\right)(\dot{\delta\sigma})^2 \delta N + \frac{1}{2}P_{\sigma\sigma}(\delta\sigma)^2 \delta N + \cdots\right], \tag{4.66}$$

where we have shown only a few terms. Remember δN can be written by $\delta\phi$ and $\delta\sigma$ using eq. (4.48). Actually, there is only one $h(\delta\sigma)^2$ coupling term (the first term in eq. (4.66)), except for the slow-roll suppressed terms in the gravity sector. However, there are many $\delta\phi(\delta\sigma)^2$ coupling terms and it is not transparent which one is most significant. Then we focus on the term with $\delta N(\partial_i \delta\sigma)^2$ (the second term in eq. (4.66)) because it has a similar form to the graviton coupling term and it is easy to compare them. As we see later, the curvature perturbation induced only by this term excludes the dominant production of gravitational waves via the spectator field. Thus this treatment is conservative and sufficient.

Since σ is a spectator field, the comoving curvature perturbation is determined by the inflaton as

$$\mathcal{R} \simeq -\frac{H}{\dot{\phi}_0}\delta\phi \simeq -\frac{2M_{\mathrm{Pl}}H^2}{\dot{\phi}_0^2}\delta N \simeq -\frac{\delta N}{\varepsilon_H}. \tag{4.67}$$

As we see later, to produce the induced gravitons significantly, c_s should be much smaller than unity. Thus one can approximate

$$c_s^2 = \frac{P_X}{P_X + P_{XX}\dot{\sigma}_0^2} \ll 1 \quad \Longrightarrow \quad K \equiv P_X + P_{XX}\dot{\sigma}_0^2 \simeq P_{XX}\dot{\sigma}_0^2. \tag{4.68}$$

Then the first line in eq. (4.66) reads

$$S_{\text{calc}}^{(3)} = \int d\eta d^3x \, a^2 \left[\frac{1}{2} P_X h_{ij} \partial_i \delta\sigma \partial_j \delta\sigma - \frac{1}{2} \varepsilon_H K \mathcal{R} \partial_i \delta\sigma \partial_i \delta\sigma \right]. \tag{4.69}$$

On the other hand, substituting eq. (4.67) into eq. (4.50), we obtain the relevant second order action as

$$S_{\mathcal{R},h}^{(2)} = \int d\eta d^3x \left[a^2 \varepsilon M_{\text{Pl}}^2 \left(\mathcal{R}'^2 - (\partial_i \mathcal{R})^2 \right) + \frac{a^2 M_{\text{Pl}}^2}{8} \left(h'_{ij} h'_{ij} - \partial_k h_{ij} \partial_k h_{ij} \right) \right]. \tag{4.70}$$

Note that all sub-leading terms are dropped and h_{ij} terms come from eq. (4.44). Combining it with eq. (4.69), one obtains the equations of motion as

$$\mathcal{R}'' + 2\mathcal{H}\mathcal{R}' - \partial_i^2 \mathcal{R} = -\frac{K}{4M_{\text{Pl}}^2} \partial_i \delta\sigma \partial_i \delta\sigma, \tag{4.71}$$

$$h''_{ij} + 2\mathcal{H} h'_{ij} - \partial_k^2 h_{ij} = \frac{2P_X}{M_{\text{Pl}}^2} \tilde{T}_{ij}^{lm} \partial_l \delta\sigma \partial_m \delta\sigma. \tag{4.72}$$

Here $\tilde{T}_{ij}^{lm}$ is the projection tensor into the T.T. component defined by

$$\tilde{T}_{ij}^{lm}(\boldsymbol{x}) \equiv \int \frac{d^3k}{(2\pi)^3} e^{i\boldsymbol{k}\cdot\boldsymbol{x}} \left[e_{ij}^+(\boldsymbol{k}) e_{lm}^+(\boldsymbol{k}) + e_{ij}^-(\boldsymbol{k}) e_{lm}^-(\boldsymbol{k}) \right]. \tag{4.73}$$

Here $e_{ij}^{\pm}$ are the linear polarization tensors which are written in terms of the linear polarization vectors $e_i(\boldsymbol{k})$ and $\bar{e}_i(\boldsymbol{k})$ as

$$e_{ij}^+(\boldsymbol{k}) = \frac{1}{\sqrt{2}} \left[e_i(\boldsymbol{k}) e_j(\boldsymbol{k}) - \bar{e}_i(\boldsymbol{k}) \bar{e}_j(\boldsymbol{k}) \right], \quad e_{ij}^-(\boldsymbol{k}) = \frac{1}{\sqrt{2}} \left[e_i(\boldsymbol{k}) \bar{e}_j(\boldsymbol{k}) + \bar{e}_i(\boldsymbol{k}) e_j(\boldsymbol{k}) \right], \tag{4.74}$$

where $e_i(\boldsymbol{k})$ and $\bar{e}_i(\boldsymbol{k})$ are two basis vectors which are orthogonal to each other and $\boldsymbol{k}$. The only differences between the source terms of $\mathcal{R}$ and h_{ij} are the coefficients and the projection tensor. In what follows, we focus on the calculation of h_{ij}. One can solve the equation of $\mathcal{R}$ in a similar manner.

Equation (4.72) can be solved by the Green function method. The Green function $g_k(\eta, \tau)$ which satisfies

$$g_k'' + 2\mathcal{H} g_k' + k^2 g_k = \delta(\eta - \tau), \tag{4.75}$$

is given by

$$g_k(\eta, \tau) = \frac{\theta(\eta - \tau)}{k^3 \tau^2} \Re e \left[e^{ik(\eta-\tau)}(1 - ik\eta)(-i + k\tau) \right], \tag{4.76}$$

where $\theta(\eta)$ is the step function and $\Re e[\cdots]$ represents the real part of $[\cdots]$. Using this Green function, one finds the inhomogeneous solutions of eq. (4.72) as

$$h_{\boldsymbol{k}}^{\pm}(\eta) = \frac{2P_X}{M_{\text{Pl}}^2} \int \frac{d^3p d^3q}{(2\pi)^3} \delta(\boldsymbol{p} + \boldsymbol{q} - \boldsymbol{k}) e_{ij}^{\pm}(\boldsymbol{k}) p_i q_j \int_{-\infty}^{\infty} d\tau \, g_k(\eta, \tau) \sigma_{\boldsymbol{p}}(\tau) \sigma_{\boldsymbol{q}}(\tau). \tag{4.77}$$

Substituting them into the definitions of the power spectrum,

$$\langle h^{\pm}_{\boldsymbol{k}}(\eta) h^{\pm}_{\boldsymbol{k}'}(\eta) \rangle = \frac{2\pi^2}{k^3} \delta(\boldsymbol{k} + \boldsymbol{k}') \mathcal{P}^{\pm}_h(k, \eta), \tag{4.78}$$

one obtains

$$\frac{2\pi^2}{k^3} \delta(\boldsymbol{k} + \boldsymbol{k}') \mathcal{P}^{\pm}_h(k, \eta) =$$
$$\frac{4P_X^2}{M_{\text{Pl}}^4} \int \frac{\mathrm{d}^3 p \, \mathrm{d}^3 q \, \mathrm{d}^3 p' \, \mathrm{d}^3 q'}{(2\pi)^6} \delta(\boldsymbol{p} + \boldsymbol{q} - \boldsymbol{k}) \delta(\boldsymbol{p}' + \boldsymbol{q}' - \boldsymbol{k}') e^{\pm}_{ij}(\boldsymbol{k}) e^{\pm}_{ml}(\boldsymbol{k}') p_i q_j p'_m q'_l$$
$$\times \int_{-\infty}^{\infty} \mathrm{d}\tau \mathrm{d}\tau' g_k(\eta, \tau) g_{k'}(\eta, \tau') \langle \sigma_{\boldsymbol{p}}(\tau) \sigma_{\boldsymbol{q}}(\tau) \sigma_{\boldsymbol{p}'}(\tau') \sigma_{\boldsymbol{q}'}(\tau') \rangle. \tag{4.79}$$

Since we are treating the source terms of $\mathcal{R}$ and h_{ij} due to the spectator field σ in eqs. (4.71) and (4.72) as classical stochastic quantities, momentum integrations in eqs. (4.77) and (4.79) are performed only in the domain where the quantum operator $\sigma_{\boldsymbol{p}}$ behaves as a classical stochastic variable. Specifically we introduce a parameter γ smaller than unity such that one can approximate

$$\sigma_{\boldsymbol{p}}(\eta) \cong \frac{H}{\sqrt{2 c_s P_X} p^{3/2}} \left(\hat{a}_{\boldsymbol{p}} + \hat{a}^{\dagger}_{-\boldsymbol{p}} \right), \tag{4.80}$$

for $|c_s p \eta| < \gamma$, where $\hat{a}_{\boldsymbol{k}}$ and $\hat{a}^{\dagger}_{\boldsymbol{k}}$ are creation and annihilation operators which satisfy the usual commutation relation, $\left[\hat{a}_{\boldsymbol{k}}, \hat{a}^{\dagger}_{-\boldsymbol{k}'} \right] = (2\pi)^3 \delta(\boldsymbol{k} + \boldsymbol{k}')$. Then both $\sigma_{\boldsymbol{p}}(\eta)$ and its canonically conjugate momentum variable have the same operator dependence proportional to $\hat{a}_{\boldsymbol{p}} + \hat{a}^{\dagger}_{-\boldsymbol{p}}$ and commute with each other.

Thus replacing $\sigma_{\boldsymbol{p}}$ in eq. (4.79) by

$$\sigma_{\boldsymbol{p}}(\eta) \cong \frac{H}{\sqrt{2 c_s P_X} p^{3/2}} \theta(\gamma + c_s p \eta) \left(\hat{a}_{\boldsymbol{p}} + \hat{a}^{\dagger}_{-\boldsymbol{p}} \right), \tag{4.81}$$

one finds

$$\langle \sigma_{\boldsymbol{p}}(\tau) \sigma_{\boldsymbol{q}}(\tau) \sigma_{\boldsymbol{p}'}(\tau') \sigma_{\boldsymbol{q}'}(\tau') \rangle$$
$$= \frac{H^4}{4 P_X^2 c_s^2} (pqp'q')^{-\frac{3}{2}} \theta(\gamma + c_s p \tau) \theta(\gamma + c_s q \tau) \theta(\gamma + c_s p' \tau') \theta(\gamma + c_s q' \tau')$$
$$\times (2\pi)^6 \left[\delta(\boldsymbol{p} + \boldsymbol{q}') \delta(\boldsymbol{q} + \boldsymbol{p}') + \delta(\boldsymbol{p} + \boldsymbol{p}') \delta(\boldsymbol{q} + \boldsymbol{q}') \right]. \tag{4.82}$$

Substituting it into eq. (4.79), and using the symmetry $\boldsymbol{p}' \leftrightarrow \boldsymbol{q}'$, we obtain

$$\mathcal{P}^{\pm}_h(\eta, k) = \pm \frac{k^3}{\pi^2 c_s^2} \frac{H^4}{M_{\text{Pl}}^4} \int \mathrm{d}^3 p \, \mathrm{d}^3 p' \delta(\boldsymbol{p} - \boldsymbol{p}' - \boldsymbol{k}) e^{\pm}_{ij}(\boldsymbol{k}) e^{\pm}_{ml}(\boldsymbol{k}) \frac{p_i p'_j p'_m p_l}{(pp')^3}$$
$$\times \left[\int_{-\infty}^{\infty} \mathrm{d}\tau g_k(\eta, \tau) \theta(\gamma + c_s p \tau) \theta(\gamma + c_s p' \tau) \right]^2, \tag{4.83}$$

where the property of the linear tensor polarization, $e_{ij}^{\pm}(-\boldsymbol{k}) = \pm e_{ij}^{\pm}(\boldsymbol{k})$, is used. The time integration can be analytically performed as

$$k^2 \int_{-\infty}^{\infty} \mathrm{d}\tau g_k(\eta, \tau)\theta(\gamma + c_s p\tau)\theta(\gamma + c_s p'\tau)$$

$$= 1 + \frac{\sin[k(\eta - \tilde{\eta}_p)]}{k\tilde{\eta}_p} - \frac{\eta}{\tilde{\eta}_p} \cos[k(\eta - \tilde{\eta}_p)], \tag{4.84}$$

with

$$\tilde{\eta}_p \equiv -\frac{\gamma}{c_s \max[p, p']}, \tag{4.85}$$

which is the sound horizon crossing time of either p or p' mode, whichever exits the horizon later. Finally, in the p integration, one can show that the contribution from $p \sim \gamma k/c_s$ is dominant. Then eq. (4.84) can be approximated by $1 - x\sin(x^{-1})$ for $c_s \ll \gamma$, where $x \equiv c_s p/\gamma k$. After the angular integration, one finds

$$\mathcal{P}_h^{\pm}(\eta, k) \simeq \pm\frac{8\gamma}{15\pi c_s^3} \frac{H^4}{M_{\mathrm{Pl}}^4} \int_{\varepsilon}^{\xi} \mathrm{d}x \left[1 - x\sin\left(x^{-1}\right)\right]^2, \tag{4.86}$$

where $\xi \gg 1$ and $\varepsilon \ll 1$ are introduced to define the integration interval. Although the x integration cannot be performed analytically, a numerical calculation shows that it converges to $\approx 1/2$ for a sufficiently large ξ and small ε. Since $\mathcal{P}_h = \mathcal{P}_h^+ - \mathcal{P}_h^-$ as we show in the next subsection, one obtains

$$\mathcal{P}_h^{(\sigma)}(\eta, k) \simeq \frac{8\gamma}{15\pi c_s^3} \frac{H^4}{M_{\mathrm{Pl}}^4}, \tag{4.87}$$

where the superscript "(σ)" denotes that this $\mathcal{P}_h$ is induced by the σ field. In the same way as $\mathcal{P}_h^{(\sigma)}$, one can show the induced power spectrum of the curvature perturbation is given by

$$\mathcal{P}_{\mathcal{R}}^{(\sigma)}(\eta, k) \simeq \frac{\gamma}{32\pi c_s^7} \frac{H^4}{M_{\mathrm{Pl}}^4}. \tag{4.88}$$

Thus a spectator field which induces the gravitational waves of eq. (4.87) inevitably produces the curvature perturbation of eq. (4.88) as well.

Since $H \ll M_{\mathrm{Pl}}$, the induced $\mathcal{P}_h$, eq. (4.87), is negligible compared to the one coming from the vacuum fluctuation, eq. (4.20), unless the sound speed c_s takes a tiny value satisfying $c_s^3 < 4\pi\gamma H^2/15 M_{\mathrm{Pl}}^2$. In that case, however, the tensor-to-scalar ratio induced by the spectator field,

$$r_\sigma \equiv \frac{\mathcal{P}_h^{(\sigma)}}{\mathcal{P}_{\mathcal{R}}^{(\sigma)}} \simeq \frac{256}{15} c_s^4, \tag{4.89}$$

becomes very small. As a result, the requirement that the induced curvature perturbation must not exceed the observed value, $\mathcal{P}_{\mathcal{R}}^{(\sigma)} \leq \mathcal{P}_{\mathcal{R}}^{\mathrm{obs}} \approx 2.2 \times 10^{-9}$, puts a lower bound on c_s and consequently constrains $\mathcal{P}_h^{(\sigma)}$ as

$$\frac{\mathcal{P}_h^{(\sigma)}}{\mathcal{P}_h^{\mathrm{vac}}} \leq 2 \times 10^{-5} \, \gamma^{\frac{4}{7}} \left(\frac{H}{10^{14}\mathrm{GeV}}\right)^{\frac{2}{7}}, \tag{4.90}$$

where $\mathcal{P}_h^{\text{vac}}$ denotes the GW from the vacuum fluctuation, eq. (4.20). As mentioned above, we expect $\gamma \lesssim 1$ and it is known $H \lesssim 10^{14}\text{GeV}$ from the CMB observations [40, 31, 80]. Therefore the induced GW cannot dominate the GW from the vacuum fluctuation.

4.3.2.1 The minus sign in the linear polarization tensor

In this subsection, we briefly comment on the sign of the tensor power spectrum which depends on the choice of polarization tensor. The power spectrum of the tensor perturbation is defined as

$$\langle h_{ij}(\eta.\boldsymbol{x}) h_{ij}(\eta.\boldsymbol{x}) \rangle = \int \frac{\mathrm{d}^3 k}{(2\pi)^3} P_h(\eta, k) \tag{4.91}$$

and $h_{ij}(\eta.\boldsymbol{x})$ is decomposed as

$$h_{ij}(\eta.\boldsymbol{x}) = \int \frac{\mathrm{d}^3 k}{(2\pi)^3} e^{i\boldsymbol{k}\cdot\boldsymbol{x}} \sum_{\lambda=\pm} \left[\hat{a}_{\boldsymbol{k}}^\lambda v_k^\lambda(\eta) e_{ij}^\lambda(\boldsymbol{k}) + \hat{a}_{-\boldsymbol{k}}^{\lambda\dagger} v_k^{\lambda*}(\eta) e_{ij}^{\lambda*}(-\boldsymbol{k}) \right] \tag{4.92}$$

where $\hat{a}_{\boldsymbol{k}}$ and $\hat{a}_{\boldsymbol{k}}^\dagger$ are creation/annihilation operators, $v_k^\pm(\eta)$ is the mode function and e_{ij}^λ is the polarization tensor. Substituting eq. (4.92) into eq. (4.91), one obtains the usual result,

$$P_h(\eta, k) = |v_k^+|^2 + |v_k^-|^2, \tag{4.93}$$

However, in the case of the linear polarization tensor eq. (4.74), it can be found

$$e_{ij}^+(-\boldsymbol{k}) = e_{ij}^+(\boldsymbol{k}), \quad e_{ij}^-(-\boldsymbol{k}) = -e_{ij}^-(\boldsymbol{k}). \tag{4.94}$$

This is because either of the linear polarization vectors, $e_i(\boldsymbol{k})$ or $\bar{e}_i(\boldsymbol{k})$, is odd for the transformation $\boldsymbol{k} \to -\boldsymbol{k}$. Using this property and comparing (4.92) and the standard polarization decomposition,

$$h_{ij}(\eta, \boldsymbol{x}) = \int \frac{\mathrm{d}^3 k}{(2\pi)^3} e^{i\boldsymbol{k}\cdot\boldsymbol{x}} \left[e_{ij}^+(\boldsymbol{k}) h_{\boldsymbol{k}}^+ + e_{ij}^-(\boldsymbol{k}) h_{\boldsymbol{k}}^- \right]. \tag{4.95}$$

one finds

$$h_{\boldsymbol{k}}^+(\eta) = \hat{a}_{\boldsymbol{k}}^+ v_k^+(\eta) + \hat{a}_{-\boldsymbol{k}}^{+\dagger} v_k^{+*}(\eta), \quad h_{\boldsymbol{k}}^-(\eta) = \hat{a}_{\boldsymbol{k}}^- v_k^-(\eta) - \hat{a}_{-\boldsymbol{k}}^{-\dagger} v_k^{-*}(\eta). \tag{4.96}$$

Using eq. (4.78), one can show

$$P_h^+(\eta, k) = |v_k^+|^2, \quad P_h^-(\eta, k) = -|v_k^-|^2. \tag{4.97}$$

Therefore we see that $P_h = P_h^+ - P_h^-$, or equivalently $\mathcal{P}_h = \mathcal{P}_h^+ - \mathcal{P}_h^-$. Note that if one adopt the L and R polarization tensor, $e_{ij}^{L,R}(\boldsymbol{k}) = e_{ij}^+(\boldsymbol{k}) \pm i e_{ij}^-(\boldsymbol{k})$, this weird minus sign does not appear.

4.3.3   Interpretation

In the previous subsection, it was shown that the spectator field with a tiny sound speed produces the curvature perturbation $\mathcal{P}_{\mathcal{R}}^{(\sigma)} \propto c_s^{-7}$ larger than the gravitational waves, $\mathcal{P}_h^{(\sigma)} \propto c_s^{-3}$. This contrast originates in the difference of coupling constants. One can see in the right hand side of eqs. (4.71) and (4.72) that the ratio of the coupling constants is given by

$$\left| \frac{h\delta\sigma^2 \text{ coupling}}{\mathcal{R}\delta\sigma^2 \text{ coupling}} \right| \simeq \frac{8P_X}{K} = 8c_s^2. \tag{4.98}$$

Hence the $h(\delta\sigma^2)$ coupling is highly suppressed compared to the $\mathcal{R}(\delta\sigma)^2$ coupling for $c_s \ll 1$. Now let us take a closer look at what makes these two couplings so different.

The difference stems from the perturbative expansion of the action, $P(X,\sigma) = P + P_X \delta X + \frac{1}{2} P_{XX} (\delta X)^2 + \cdots$. The $h(\delta\sigma)^2$ coupling appears in the perturbation of X, (see eq. (4.46))

$$\delta X \supset \frac{1}{2} a^{-2} h_{ij} \partial_i \delta\sigma \partial_j \delta\sigma. \tag{4.99}$$

Since this is already the third order, no other perturbation can be multiplied to this term. Thus only $P_X \delta X$ carries the $h\delta\sigma^2$ coupling. On the other hand, δX also has the following terms:

$$\delta X \supset \dot{\sigma}_0^2 \delta N - \frac{1}{2} a^{-2} (\partial_i \delta\sigma)^2, \tag{4.100}$$

where the first term in the right hand side is the first order of perturbation and includes $\delta\phi$ (or $\mathcal{R}$), while the second term is the second order. This time, $P_{XX}(\delta X)^2$ can carry the $\mathcal{R}(\delta\sigma)^2$ coupling terms. Therefore although the coefficient of the $h(\delta\sigma)^2$ coupling is only P_X, the $\mathcal{R}(\delta\sigma)^2$ coupling has $P_{XX}\dot{\sigma}_0^2$ in its coefficient. Meanwhile, since the sound speed is given by

$$c_s^2 = \frac{P_X}{P_X + P_{XX}\dot{\sigma}_0^2}, \tag{4.101}$$

$P_{XX}\dot{\sigma}_0^2 \gg P_X$ is necessary to make c_s tiny to boost $\mathcal{P}_h^{(\sigma)}$. However, it results in suppression of the P_X terms in comparison to the $P_{XX}\dot{\sigma}_0^2$ terms. Thus the $h(\delta\sigma)^2$ coupling is suppressed compared to the $\mathcal{R}(\delta\sigma)^2$ coupling.

This feature can also be understood as follows. A small sound speed means that the coefficient of the spacial kinetic term is smaller than that of the time kinetic term. Nevertheless, gravitational wave is induced by the spacial kinetic term of the σ field since the quadrupole component in the energy momentum tensor of a scalar field is given only by its spacial kinetic energy. On the other hand, the adiabatic perturbation is sensitive to both the time and spacial kinetic energy. Therefore the suppression of the GW production in comparison with the curvature perturbation is a generic consequence of a small sound speed of a scalar field.

In summary, if the sound speed of the spectator field is much smaller than unity, its perturbation is amplified. As a result, both the gravitational waves and the curvature perturbation induced by its second order perturbation are boosted. However, the sound

speed also controls the coupling constants of the $h(\delta\sigma)^2$ and $\mathcal{R}(\delta\sigma)^2$ coupling terms (see eq. (4.98)). As c_s becomes smaller, the $h(\delta\sigma)^2$ coupling is more suppressed compared to the $\mathcal{R}(\delta\sigma)^2$ coupling. Therefore, since a spectator field with a small sound speed induces the curvature perturbation much more than the gravitational waves, it cannot produce the dominant GW in a way that is consistent with the CMB observation.

4.3.4 Extension to the Galileon theory

So far the Lagrangian of the spectator field has been assumed to take a function of σ and X only. In this subsection, we show that the result obtained in the previous subsection does not change even if the action is extended to a more general form. Specifically we consider the Galileon-like theory [100, 101, 102, 103],

$$\mathcal{L}_\sigma = P(X, \sigma) - G(X, \sigma)\Box\sigma, \tag{4.102}$$

where $G(X, \sigma)$ is an arbitrary function of X and σ and the other pert of action is same as eq. (4.41). With this action, the sound speed of $\delta\sigma$ is given by [104]

$$c_s^2 = \frac{P_X + 2G_X(\ddot\sigma_0 + 2H\dot\sigma_0) - 2G_\sigma + G_{X\sigma}\dot\sigma_0^2 + G_{XX}\dot\sigma_0^2\ddot\sigma_0}{P_X + 6HG_X\dot\sigma_0 - 2G_\sigma - G_{X\sigma}\dot\sigma_0^2 + P_{XX}\dot\sigma_0^2 + 3HG_{XX}\dot\sigma_0^3}. \tag{4.103}$$

To make the sound speed small, terms proportional to P_{XX} or G_{XX} in the denominator have to be much larger than the other terms. As we discuss in the previous subsection, however, that leads to the suppression of the $h(\delta\sigma)^2$ coupling compared to the $\mathcal{R}(\delta\sigma)^2$ coupling because the $h(\delta\sigma)^2$ coupling does not include P_{XX} nor G_{XX} in the coupling constant while the $\mathcal{R}(\delta\sigma)^2$ coupling does. Indeed, the Galileon term additionally carries the following coupling terms:

$$- NG(X, \sigma)\Box\sigma \supset a^{-2}\left(G_\sigma - \frac{3}{2}H\dot\sigma_0 G_X\right) h_{ij}\partial_i\delta\sigma\partial_j\delta\sigma + \frac{3}{2}a^{-2}G_{XX}H\dot\sigma_0^3\delta N(\partial_i\delta\sigma)^2, \tag{4.104}$$

where we show only the leading terms. It is obvious that the discussion in sec. 4.3.3 holds even in this Galileon case. Therefore we conclude that a spectator field with a small sound speed cannot produce the dominant GW even if its action is extended to the Galileon theory. This result implies that it is impossible for *a single scalar field with a small sound speed* to generate GW which is larger than the GW comes from the vacuum fluctuation.

4.3.5 Summary of the section

It is important to explore an alternative source of primordial GWs other than GWs from the vacuum fluctuation because it can contribute the observed GWs and change the consequence on the inflation mechanism. We consider a spectator scalar field with the a generalized kinetic function and/or the Galileon-like action which gives it a small

sound speed. The scalar field induces both GWs and curvature perturbation which are analytically obtained as eq. (4.87) and eq. (4.88), respectively. Since a small sound speed makes the $\mathcal{R}(\delta\sigma)^2$ coupling much stronger than the $h(\delta\sigma)^2$ coupling, the induced curvature perturbation is considerably larger than the induced GWs. Then the CMB observation put the lower limit on the sound speed, and the stringent constraint on the induced GWs is derived. Consequently, we conclude that the GWs induced by the single spectator scalar field cannot exceed $\mathcal{P}_h^{\mathrm{vac}}$. [4]

---

[4]Recently, Biagetti et al [105] discussing the same topic showed up in the arXiv. Their conclusion is basically consistent with ours.

CONCLUSION

Inflation is widely studied as the theory describing the very early universe and now it is considered as an indispensable component of the standard model of cosmology. During inflation, cosmological perturbations are generated from the quantum fluctuations and subsequently become the seed of the cosmic structures which are currently observed. The prediction of inflation, the scale invariant spectrum of the curvature perturbation, is tested various observation, especially by the cosmic microwave background radiation (CMB) observations with great accuracy and is confirmed to be consistent. Nevertheless, the mechanism of inflation is still unclear. The scalar perturbation which has been observed by the CMB observations puts strong constraints on a number of inflation models. But it is not sufficient to determine the correct model. Thus in the next generation of cosmology, the perturbations other than the scalar one, namely vector perturbation and tensor perturbation become increasingly important.

Although primordial vector perturbation is not intensively investigated so far, it acquires a strong motivation from recent observations. It is known for a long time that galaxies and galaxy clusters have their own magnetic fields. However, the magnetic field even in void regions is detected in 2010 by blazar observations. The observational lower bound still has a few order of uncertainty depending on the method and assumptions, and roughly given by $B_{\text{obs}} \gtrsim \mathcal{O}(10^{-20} - 10^{-15})$G. There is also the report that the helical magnetic field with the strength $\sim 10^{-14}$G which can support magnetogenesis models with parity violation.

The study on inflationary magnetogenesis was pioneered by Turner and Widrow in 1988, and many models have been proposed so far. However, recently, it is pointed out that the models of inflationary magnetogenesis suffer from two serious problems, namely the backreaction problem and the curvature perturbation problem. In this paper, we first investigate the kinetic coupling model (Ratra's model). We calculate the energy density of the electromagnetic fields and the induced curvature perturbation in the model and derive the constrains using the Planck observation. Furthermore, since these problems are universal in inflationary magnetogenesis, a model-independent constraint can be derived. The model-independent argument of the backreaction put the constraint $\rho_{\text{inf}}^{1/4} \lesssim 10^{11}$GeV. The model-independent constraint from the curvature perturbation is much more stringent, $\rho_{\text{inf}}^{1/4} \lesssim 30$GeV. Therefore it is very difficult to achieve viable inflation magnetogenesis, if the magnetic field just decays after inflation as a usual radiation component, $B^2 \propto a^{-4}$. We also consider the case where the kinetic function $I(\phi)$ in the IFF model varies even after inflation and the magnetic field is amplified during the

inflaton oscillating phase. However, it is found that the induced curvature perturbation is abundantly produced again and the model is under pressure.

The tensor perturbation with a primordial origin has been investigated as the primordial gravitational wave (GW) in the theoretical and observational context. However, previous works have focused on the tensor mode generated from the vacuum fluctuation and ignore the other possibilities. In this paper, we consider not only that the conventional GW but also GW produced by an alternative mechanism during inflation. That is the second order perturbation of a scalar field. Although the scalar perturbation and the tensor perturbation are decoupled at the first order of the cosmological perturbation, they are coupled at the second order. If GWs from alternative sources dominate the observed primordial GW, the relation between the observation of the primordial GW and the properties of inflation can be drastically changed. For example, it is known that the tensor-to-scalar ratio r is proportional to the energy density of inflation ρ_{inf} if the conventional GW is dominant. However, if the GW induced by the second order perturbation, it is changed into $r \propto \rho_{\mathrm{inf}}^2$. Therefore it is important to investigate the alternative scenario of the GW generation. In this paper, we discuss the possibility that the second order perturbation of a spectator scalar field induces GW during inflation. We assume the very general action of the spectator scalar field that is the k-essence and the Galileon term. We perturb the action and calculate the induced GW as well as the induced curvature perturbation. As a result, contrary to the previous work [37], we show that the induced GW cannot be larger than the conventional GW because the curvature perturbation is much more produced than the induced GW and the model becomes inconsistent with the CMB observation. Since our setup is very general, our result can be interpreted that a single spectator field cannot enhance the inflationary tensor mode.

Bibliography

[1] A. A. Starobinsky, Phys. Lett. B **91**, 99 (1980). (Cited on pages 1 and 5.)

[2] K. Sato, Mon. Not. Roy. Astron. Soc. **195**, 467 (1981). (Cited on pages 1 and 5.)

[3] A. H. Guth, Phys. Rev. D **23**, 347 (1981). (Cited on pages 1 and 5.)

[4] P. A. R. Ade *et al.* [Planck Collaboration], Astron. Astrophys. **571**, A16 (2014) [arXiv:1303.5076 [astro-ph.CO]]. (Cited on pages 1, 7, 15, 36 and 79.)

[5] J. Martin, C. Ringeval and V. Vennin, Phys. Dark Univ. (2014) [arXiv:1303.3787 [astro-ph.CO]]. (Cited on pages 1 and 16.)

[6] J. Martin, C. Ringeval, R. Trotta and V. Vennin, JCAP **1403**, 039 (2014) [arXiv:1312.3529 [astro-ph.CO]]. (Cited on pages 1 and 16.)

[7] R. Wielebinski, "Magnetic fields in the milky way, derived from radio continuum observations and faraday rotation studies." Cosmic Magnetic Fields. Springer Berlin Heidelberg, Lecture Notes in Physics Volume 664, 2005, pp 89-112. (Cited on pages 1 and 18.)

[8] M. L. Bernet, F. Miniati, S. J. Lilly, P. P. Kronberg and M. Dessauges-Zavadsky, Nature **454**, 302 (2008) [arXiv:0807.3347 [astro-ph]]. (Cited on pages 1 and 18.)

[9] A. Bonafede, L. Feretti, M. Murgia, F. Govoni, G. Giovannini, D. Dallacasa, K. Dolag and G. B. Taylor, Astron. Astrophys. **513**, A30 (2010) [arXiv:1002.0594 [astro-ph.CO]]. (Cited on pages 1 and 18.)

[10] R. Beck, "Magnetic fields in galaxies." Space Science Reviews, May 2012, Volume 166, Issue 1-4, pp 215-230. (Cited on pages 1 and 18.)

[11] A. Neronov and I. Vovk, Science **328**, 73 (2010) [arXiv:1006.3504 [astro-ph.HE]]. (Cited on pages 1, 19 and 20.)

[12] F. Tavecchio, G. Ghisellini, L. Foschini, G. Bonnoli, G. Ghirlanda and P. Coppi, Mon. Not. Roy. Astron. Soc. **406**, L70 (2010) [arXiv:1004.1329 [astro-ph.CO]]. (Cited on pages 1, 19 and 20.)

[13] K. Dolag, M. Kachelriess, S. Ostapchenko and R. Tomas, Astrophys. J. **727**, L4 (2011) [arXiv:1009.1782 [astro-ph.HE]]. (Cited on pages 1, 19 and 20.)

[14] C. D. Dermer, M. Cavadini, S. Razzaque, J. D. Finke and B. Lott, Astrophys. J. **733**, L21 (2011) [arXiv:1011.6660 [astro-ph.HE]]. (Cited on pages 1, 19 and 20.)

[15] H. Huan, T. Weisgarber, T. Arlen and S. P. Wakely, Astrophys. J. **735**, L28 (2011) [arXiv:1106.1218 [astro-ph.HE]]. (Cited on pages 1, 19, 20 and 22.)

[16] W. Essey, S. Ando and A. Kusenko, Astropart. Phys. **35**, 135 (2011) [arXiv:1012.5313 [astro-ph.HE]]. (Cited on pages 1, 19, 21 and 53.)

[17] A. M. Taylor, I. Vovk and A. Neronov, Astron. Astrophys. **529**, A144 (2011) [arXiv:1101.0932 [astro-ph.HE]]. (Cited on pages 1, 19, 20 and 53.)

[18] K. Takahashi, M. Mori, K. Ichiki, S. Inoue and H. Takami, Astrophys. J. **771**, L42 (2013). (Cited on pages 1, 19 and 21.)

[19] J. Finke *et al.* [Fermi-LAT Collaboration], eConf C **121028**, 365 (2012) [arXiv:1303.5093 [astro-ph.HE]]. (Cited on pages 1 and 19.)

[20] B. Ratra, Astrophys. J. **391**, L1 (1992). (Cited on pages 2, 25, 26 and 45.)

[21] M. S. Turner and L. M. Widrow, Phys. Rev. D **37**, 2743 (1988). (Cited on pages 2, 25, 28, 47 and 50.)

[22] W. D. Garretson, G. B. Field and S. M. Carroll, Phys. Rev. D **46**, 5346 (1992) [hep-ph/9209238]. (Cited on pages 2, 25 and 50.)

[23] F. Finelli and A. Gruppuso, Phys. Lett. B **502**, 216 (2001) [hep-ph/0001231]. (Cited on pages 2, 25 and 63.)

[24] A. C. Davis, K. Dimopoulos, T. Prokopec and O. Tornkvist, Phys. Lett. B **501**, 165 (2001) [Phys. Rev. Focus **10**, STORY9 (2002)] [astro-ph/0007214]. (Cited on pages 2 and 25.)

[25] M. M. Anber and L. Sorbo, JCAP **0610**, 018 (2006) [astro-ph/0606534]. (Cited on pages 2, 25 and 50.)

[26] R. Durrer, L. Hollenstein and R. K. Jain, JCAP **1103**, 037 (2011) [arXiv:1005.5322 [astro-ph.CO]]. (Cited on pages 2, 25 and 55.)

[27] C. Caprini and L. Sorbo, JCAP **1410**, no. 10, 056 (2014) [arXiv:1407.2809 [astro-ph.CO]]. (Cited on pages 2, 25 and 82.)

[28] V. Demozzi, V. Mukhanov and H. Rubinstein, JCAP **0908**, 025 (2009) [arXiv:0907.1030 [astro-ph.CO]]. (Cited on pages 2, 26, 29, 41, 45, 50 and 63.)

[29] N. Barnaby, R. Namba and M. Peloso, Phys. Rev. D **85**, 123523 (2012) [arXiv:1202.1469 [astro-ph.CO]]. (Cited on pages 2, 30, 33, 34 and 35.)

[30] T. Suyama and J. Yokoyama, Phys. Rev. D **86**, 023512 (2012) [arXiv:1204.3976 [astro-ph.CO]]. (Cited on pages 2, 31, 32 and 55.)

[31] P. A. R. Ade *et al.* [Planck Collaboration], Astron. Astrophys. **571**, A24 (2014) [arXiv:1303.5084 [astro-ph.CO]]. (Cited on pages 2, 16, 34, 36, 85 and 93.)

[32] T. Fujita and S. Yokoyama, JCAP **1309**, 009 (2013) [arXiv:1306.2992 [astro-ph.CO]]. (Cited on pages 2, 25, 36 and 56.)

[33] T. Fujita and S. Mukohyama, JCAP **1210**, 034 (2012) [arXiv:1205.5031 [astro-ph.CO]]. (Cited on pages 2, 44 and 45.)

[34] T. Fujita and S. Yokoyama, JCAP **1403**, 013 (2014) [Erratum-ibid. **1405**, E02 (2014)] [arXiv:1402.0596 [astro-ph.CO]]. (Cited on pages 2, 44, 52 and 53.)

[35] T. Kobayashi, JCAP **1405**, 040 (2014) [arXiv:1403.5168 [astro-ph.CO]]. (Cited on pages 2, 3, 64, 67, 68, 71 and 73.)

[36] A. A. Starobinsky, JETP Lett. **30**, 682 (1979) [Pisma Zh. Eksp. Teor. Fiz. **30**, 719 (1979)]. (Cited on pages 2 and 78.)

[37] M. Biagetti, M. Fasiello and A. Riotto, Phys. Rev. D **88**, no. 10, 103518 (2013) [arXiv:1305.7241 [astro-ph.CO]]. (Cited on pages 3, 82, 83 and 98.)

[38] T. Fujita, J. Yokoyama and S. Yokoyama, arXiv:1411.3658 [astro-ph.CO]. (Cited on pages 3 and 85.)

[39] S. Weinberg, "*Gravitation and Cosmology: Principles and Applications of the General Theory of Relativity*", John Wiley & Sons, Inc. (1972) (Cited on page 6.)

[40] P. A. R. Ade *et al.* [Planck Collaboration], Astron. Astrophys. **571**, A22 (2014) [arXiv:1303.5082 [astro-ph.CO]]. (Cited on pages 16, 59, 71, 78, 85 and 93.)

[41] K. T. Chyzy and R. Beck, Astron. Astrophys. **417**, 541 (2004) [astro-ph/0401157]. (Cited on page 18.)

[42] R. Beck, "Galactic and extragalactic magnetic fields - a concise review," Astrophysics and Space Sciences Transactions, 2009, 5, 43-47 (Cited on page 18.)

[43] K. T. Chyzy, R. Beck, S. Kohle, U. Klein and M. Urbanik, "Regular magnetic fields in the dwarf irregular galaxy NGC 4449," aap, 2000, 355, 128-137 [astro-ph/0001205]. (Cited on page 18.)

[44] A. Brandenburg, in Magnetic fields in diffuse media, ed. E. de Gouveia Dal Pino A. Lazarian, Astrophys. Space Sci. Lib., Vol. 407, Springer, pp. 529-555 (2015) [arXiv:1402.0212 [astro-ph.GA]]. (Cited on page 18.)

[45] M. Giovannini, Int. J. Mod. Phys. D **13**, 391 (2004) [astro-ph/0312614]. (Cited on page 18.)

[46] A. Kandus, K. E. Kunze and C. G. Tsagas, Phys. Rept. **505**, 1 (2011) [arXiv:1007.3891 [astro-ph.CO]]. (Cited on page 18.)

[47] R. Durrer and A. Neronov, Astron. Astrophys. Rev. **21**, 62 (2013) [arXiv:1303.7121 [astro-ph.CO]]. (Cited on page 18.)

[48] R. Pakmor, F. Marinacci and V. Springel, Astrophys. J. **783**, L20 (2014) [arXiv:1312.2620 [astro-ph.GA]]. (Cited on page 18.)

[49] A. Neronov and D. V. Semikoz, Phys. Rev. D **80**, 123012 (2009) [arXiv:0910.1920 [astro-ph.CO]]. (Cited on page 19.)

[50] D. G. Yamazaki, T. Kajino, G. J. Mathew and K. Ichiki, Phys. Rept. **517**, 141 (2012) [arXiv:1204.3669 [astro-ph.CO]]. (Cited on page 21.)

[51] J. R. Shaw and A. Lewis, Phys. Rev. D **86**, 043510 (2012) [arXiv:1006.4242 [astro-ph.CO]]. (Cited on page 21.)

[52] M. Kawasaki and M. Kusakabe, Phys. Rev. D **86**, 063003 (2012) [arXiv:1204.6164 [astro-ph.CO]]. (Cited on page 21.)

[53] H. Tashiro and T. Vachaspati, Phys. Rev. D **87**, no. 12, 123527 (2013) [arXiv:1305.0181 [astro-ph.CO]]. (Cited on page 21.)

[54] H. Tashiro, W. Chen, F. Ferrer and T. Vachaspati, Monthly Notices of the Royal Astronomical Society: Letters 2014 445 (1): L41-L45 [arXiv:1310.4826 [astro-ph.CO]]. (Cited on page 21.)

[55] H. Tashiro and T. Vachaspati, arXiv:1409.3627 [astro-ph.CO]. (Cited on page 21.)

[56] W. Chen, B. D. Chowdhury, F. Ferrer, H. Tashiro and T. Vachaspati, arXiv:1412.3171 [astro-ph.CO]. (Cited on page 21.)

[57] R. Durrer and C. Caprini, JCAP **0311**, 010 (2003) [astro-ph/0305059]. (Cited on page 23.)

[58] D. Grasso and H. R. Rubinstein, Phys. Rept. **348**, 163 (2001) [astro-ph/0009061]. (Cited on pages 23 and 58.)

[59] B. Himmetoglu, C. R. Contaldi and M. Peloso, Phys. Rev. Lett. **102**, 111301 (2009) [arXiv:0809.2779 [astro-ph]]. (Cited on pages 25 and 50.)

[60] D. Lemoine and M. Lemoine, Phys. Rev. D **52**, 1955 (1995). (Cited on page 25.)

[61] M. Gasperini, M. Giovannini and G. Veneziano, Phys. Rev. Lett. **75**, 3796 (1995) [hep-th/9504083]. (Cited on pages 25 and 45.)

[62] K. Bamba and J. Yokoyama, Phys. Rev. D **69**, 043507 (2004) [astro-ph/0310824]. (Cited on pages 25, 26 and 45.)

[63] K. Bamba and J. Yokoyama, Phys. Rev. D **70**, 083508 (2004) [hep-ph/0409237]. (Cited on page 25.)

[64] M. A. Ganjali, JHEP **0509**, 004 (2005) [hep-th/0509032]. (Cited on page 25.)

[65] J. Martin and J. Yokoyama, JCAP **0801**, 025 (2008) [arXiv:0711.4307 [astro-ph]]. (Cited on pages 25, 28, 47 and 73.)

[66] S. Kanno, J. Soda and M. a. Watanabe, JCAP **0912**, 009 (2009) [arXiv:0908.3509 [astro-ph.CO]]. (Cited on pages 26 and 29.)

[67] J. Ahonen and K. Enqvist, Phys. Lett. B **382**, 40 (1996) [hep-ph/9602357]. (Cited on page 28.)

[68] G. Baym and H. Heiselberg, Phys. Rev. D **56**, 5254 (1997) [astro-ph/9704214]. (Cited on page 28.)

[69] P. B. Arnold, G. D. Moore and L. G. Yaffe, JHEP **0011**, 001 (2000) [hep-ph/0010177]. (Cited on page 28.)

[70] P. B. Arnold, G. D. Moore and L. G. Yaffe, JHEP **0305**, 051 (2003) [hep-ph/0302165]. (Cited on page 28.)

[71] M. Shiraishi, E. Komatsu, M. Peloso and N. Barnaby, JCAP **1305**, 002 (2013) [arXiv:1302.3056 [astro-ph.CO]]. (Cited on pages 30 and 34.)

[72] D. H. Lyth, K. A. Malik and M. Sasaki, JCAP **0505**, 004 (2005) [astro-ph/0411220]. (Cited on page 30.)

[73] N. Kogo and E. Komatsu, Phys. Rev. D **73**, 083007 (2006) [astro-ph/0602099]. (Cited on page 43.)

[74] B. Himmetoglu, C. R. Contaldi and M. Peloso, Phys. Rev. D **80**, 123530 (2009) [arXiv:0909.3524 [astro-ph.CO]]. (Cited on page 50.)

[75] R. J. Z. Ferreira, R. K. Jain and M. S. Sloth, JCAP **1310**, 004 (2013) [arXiv:1305.7151 [astro-ph.CO]]. (Cited on page 59.)

[76] R. J. Z. Ferreira, R. K. Jain and M. S. Sloth, JCAP **1406**, 053 (2014) [arXiv:1403.5516 [astro-ph.CO]]. (Cited on pages 59 and 63.)

[77] J. Martin and C. Ringeval, JCAP **0608**, 009 (2006) [astro-ph/0605367]. (Cited on page 61.)

[78] J. Martin and C. Ringeval, Phys. Rev. D **82**, 023511 (2010) [arXiv:1004.5525 [astro-ph.CO]]. (Cited on page 61.)

[79] S. Hannestad, Phys. Rev. D **70**, 043506 (2004) [astro-ph/0403291]. (Cited on page 62.)

[80] P. A. R. Ade *et al.* [BICEP2 Collaboration], Phys. Rev. Lett. **112**, no. 24, 241101 (2014) [arXiv:1403.3985 [astro-ph.CO]]. (Cited on pages 63, 79 and 93.)

[81] R. Z. Ferreira and M. S. Sloth, JHEP **1412**, 139 (2014) [arXiv:1409.5799 [hep-ph]]. (Cited on page 82.)

[82] N. Barnaby, R. Namba and M. Peloso, JCAP **1104**, 009 (2011) [arXiv:1102.4333 [astro-ph.CO]]. (Cited on page 82.)

[83] N. Barnaby and M. Peloso, Phys. Rev. Lett. **106**, 181301 (2011) [arXiv:1011.1500 [hep-ph]]. (Cited on page 82.)

[84] L. Sorbo, JCAP **1106**, 003 (2011) [arXiv:1101.1525 [astro-ph.CO]]. (Cited on page 82.)

[85] J. L. Cook and L. Sorbo, Phys. Rev. D **85**, 023534 (2012) [Erratum-ibid. D **86**, 069901 (2012)] [arXiv:1109.0022 [astro-ph.CO]]. (Cited on page 82.)

[86] P. D. Meerburg and E. Pajer, JCAP **1302**, 017 (2013) [arXiv:1203.6076 [astro-ph.CO]]. (Cited on page 82.)

[87] S. G. Crowder, R. Namba, V. Mandic, S. Mukohyama and M. Peloso, Phys. Lett. B **726**, 66 (2013) [arXiv:1212.4165 [astro-ph.CO]]. (Cited on page 82.)

[88] T. Fujita, M. Kawasaki and S. Yokoyama, JCAP **1409**, 015 (2014) [arXiv:1404.0951 [astro-ph.CO]]. (Cited on page 80.)

[89] K. N. Ananda, C. Clarkson and D. Wands, Phys. Rev. D **75**, 123518 (2007) [gr-qc/0612013]. (Cited on page 81.)

[90] D. Baumann, P. J. Steinhardt, K. Takahashi and K. Ichiki, Phys. Rev. D **76**, 084019 (2007) [hep-th/0703290]. (Cited on page 81.)

[91] N. Bartolo, S. Matarrese, A. Riotto and A. Vaihkonen, Phys. Rev. D **76**, 061302 (2007) [arXiv:0705.4240 [astro-ph]]. (Cited on page 81.)

[92] H. Assadullahi and D. Wands, Phys. Rev. D **81**, 023527 (2010) [arXiv:0907.4073 [astro-ph.CO]]. (Cited on page 81.)

[93] R. Saito and J. Yokoyama, Prog. Theor. Phys. **123**, 867 (2010) [Erratum-ibid. **126**, 351 (2011)] [arXiv:0912.5317 [astro-ph.CO]]. (Cited on page 81.)

[94] L. Alabidi, K. Kohri, M. Sasaki and Y. Sendouda, JCAP **1209**, 017 (2012) [arXiv:1203.4663 [astro-ph.CO]]. (Cited on page 81.)

[95] L. Alabidi, K. Kohri, M. Sasaki and Y. Sendouda, JCAP **1305**, 033 (2013) [arXiv:1303.4519 [astro-ph.CO]]. (Cited on page 81.)

[96] M. Kawasaki, N. Kitajima and S. Yokoyama, JCAP **1308**, 042 (2013) [arXiv:1305.4464 [astro-ph.CO]]. (Cited on page 81.)

[97] S. Mukohyama, R. Namba, M. Peloso and G. Shiu, JCAP **1408**, 036 (2014) [arXiv:1405.0346 [astro-ph.CO]]. (Cited on page 82.)

[98] J. M. Maldacena, JHEP **0305**, 013 (2003) [astro-ph/0210603]. (Cited on page 86.)

[99] D. Langlois, S. Renaux-Petel, D. A. Steer and T. Tanaka, Phys. Rev. D **78**, 063523 (2008) [arXiv:0806.0336 [hep-th]]. (Cited on page 87.)

[100] A. Nicolis, R. Rattazzi and E. Trincherini, Phys. Rev. D **79**, 064036 (2009) [arXiv:0811.2197 [hep-th]]. (Cited on page 95.)

[101] C. Deffayet, G. Esposito-Farese and A. Vikman, Phys. Rev. D **79**, 084003 (2009) [arXiv:0901.1314 [hep-th]]. (Cited on page 95.)

[102] C. Deffayet, O. Pujolas, I. Sawicki and A. Vikman, JCAP **1010**, 026 (2010) [arXiv:1008.0048 [hep-th]]. (Cited on page 95.)

[103] T. Kobayashi, M. Yamaguchi and J. Yokoyama, Phys. Rev. Lett. **105**, 231302 (2010) [arXiv:1008.0603 [hep-th]]. (Cited on page 95.)

[104] H. Wang, T. Qiu and Y. S. Piao, Phys. Lett. B **707**, 11 (2012) [arXiv:1110.1795 [hep-ph]]. (Cited on page 95.)

[105] M. Biagetti, E. Dimastrogiovanni, M. Fasiello and M. Peloso, arXiv:1411.3029 [astro-ph.CO]. (Cited on page 96.)